The application of Friction Stir Welding Processes to new materials and new material combinations.

By

William Todd Evans

Dissertation
Submitted to the Faculty of the
Graduate School of Vanderbilt University
in partial fulfillment of the requirements
For the degree of
DOCTOR OF PHILOSOPHY
in
Mechanical Engineering
May 11, 2018
Nashville, Tennessee

Professor Alvin M. Strauss
Professor George E. Cook
Professor Kenneth Frampton
Professor Haoxiang Luo
Professor Kenneth R. Pence

ACKNOWLEDGEMENTS

I would like to thank Dr. Alvin Strauss and Dr. George Cook for their support and guidance in navigating school, life and research. Their insights in all these areas have enriched my studies and my life.

Thank you to the Tennessee Space Grant Consortium and the Department of Mechanical Engineering for funding and financial support to conduct this research.

I would also like to thank all the numerous people that helped in the many aspects involved in to completing this degree. Bob Patchin, John Fellenstein, and Phil Davis provided expert advice in materials and tool design. Dr. Ken Frampton, Dr. Haoxiang Luo, and Dr. Ken Pence all helped provide guidance in aspects of my dissertation. I am very grateful for their service on my dissertation committee.

I have been blessed to be a part of an academic community that pursues excellence in teaching and cares for their students. I have gained great insights into how to be a better professor from the example of so many excellent professors here.

I especially want to thank all of my family who has been supportive and believed in me every step of the way. Your prayers, patience, encouragement, and love has kept me going.

LIST OF FIGURES

LIST OF TABLES

LIST OF ABBREVIATIONS

AM	Additively Manufactured
ARM	Asteroid Redirect Mission
DMLS	Direct Metal Laser Sintering
EBF3	Electron Beam Free Form Fabrication
EDS	Energy-dispersive X-ray spectroscopy
FSBR	Friction Stir Blind Riveting
FSE	Friction Stir Extrusion
FSP	Friction Stir Processing
FSR	Friction Stir Riveting
FSSW	Friction Stir Spot Welding
FSW	Friction Stir Welding
HAZ	Heat Affected Zone
IMCs	Intermetallic Compounds
LWD	Linear Weld Density
MEK	Methyl Ethyl Ketone
PCBN	Polycrystalline Cubic Boron Nitride
RAFSSW	Rotating Anvil Friction Stir Spot Welding
SEM	Scanning Electron Microscope
SLS	Selective Laser Sintering
SZ	Stir Zone
TMAZ	Thermomechanically Affected Zone
TWI	The Welding Institute
UAM	Ultrasonic Additive Manufacturing
UTS	Ultimate Tensile Strength
WC	Tungsten Carbide

TABLE OF CONTENTS

Chapter I

INTRODUCTION

Friction Stir Welding(FSW) is a solid-state joining process that uses a non-consumable, rotating tool with a shoulder and attached probe to heat and plasticize a material by stirring it. The setup involves clamping the material onto a backing plate to keep it from moving and to provide a rigid surface to withstand the high force applied along the central axis of the tool. The tool advances along the length of the weld, shearing small amounts of the material and stirring it to the backside of the probe. There, the stirred material is reconsolidated under the force of the shoulder where it cools to leave a solid joint. FSW has opened up the possibilities of welding and joining new materials and is being used in some capacity in most every industry.

Though many models and theories have been presented to describe FSW, we still do not have a full understanding of all the aspects of the welding process and experimental work is needed to determine the weldability and weld characteristics of new materials. This research aims to contribute to field of FSW by accomplishing three major goals: (1) Determine the effectiveness of using Friction Stir

Welding to weld additively manufactured aluminum alloys, (2) Explore the ability to use Friction Stir Welding processes to join an iron meteorite to itself for in-space manufacture, and (3) Apply Friction Stir Welding and its related processes to join dissimilar materials.

The first goal of this research is to determine the effectiveness of using Friction Stir Welding to join additively manufactured aluminum alloys. Specifically, 6061 aluminum formed by Ultrasonic Additive Manufacturing(UAM) was used for this study. Optimized parameters from current research were used for welding so that easy comparison could be made between the standard material and the UAM material. Chapter 3 covers the results and analysis of this research and is currently under review for publication.

The second objective of the research was to explore the ability to use Friction Stir Welding processes to join an iron meteorite to itself for application to in-space welding. Welding by traditional means has proven to be difficult due to impurities in the meteorite that create solidification cracking. Since FSW is a solid-state process, these impurities present less of a problem for producing quality welds using FSW. A related process, Friction Stir Spot Welding(FSSW), was used to determine the feasibility of using Friction Stir processes to weld meteoric materials. Results of this study are presented in Chapter 4.

The final area of research addresses the need within many industries to join dissimilar materials. Weight savings can be achieved by using stronger, light-weight material such as high strength aluminum, but many key components still need the strength of steel or similar materials. This leads to a mixture of materials in the design that requires a way to join them at their interfaces. Other joining processes such as adhesives, rivets, bolts, etc... have been used but they have limitations in their use, application and/or strength. Aluminum and steel are common components that are used together and represent the challenges of joining as most current welding methods do not work because of the disparate properties of the materials. Two new processes utilizing Friction Stir Welding techniques were developed to provide new ways for joining dissimilar materials. Chapters 6 and 7 will present the application of the Friction Stir Extrusion(FSE) process to two dissimilar material combinations. Chapter 8 will present a related process called Two-sided Friction Stir Riveting by Extrusion which uses Friction Stir Spot Welding to create a dissimilar weld of aluminum-steel-aluminum.

While these three objectives are varied, they each contribute to extending our capabilities of using Friction Stir Welding and its related processes. A better understanding of how Friction Stir Welding can be used and optimized on additively manufactured aluminum alloys and

the iron meteorite will open new possibilities for using the process in industry and in space. The joining of dissimilar materials will allow for material combinations that have previously been challenging or impossible.

Chapter II

BACKGROUND OF FRICTION STIR WELDING

Overview

Friction Stir Welding(FSW) and its related processes have been around since 1991 when they were first patented by The Welding Institute in Cambridge, UK (TWI).(Thomas 1995) Traditional FSW is characterized by a rotating tool with a shoulder and pin that is plunged into two adjoining metal plates. The rotating tool heats and plasticizes the material from the combination of frictional forces from the shoulder and pin and the through the shear forces exerted within the material as the tool passes through it. Downward force is maintained on the rotating tool while it is moved along the length of the material to keep the tool fully engaged within the material. The shoulder of the FSW tool serves as a constraint to force all the material to stay within the weld zone. As the tool advances, material is plasticized and stirred together to form a solid joint as seen in Figure 2.1.

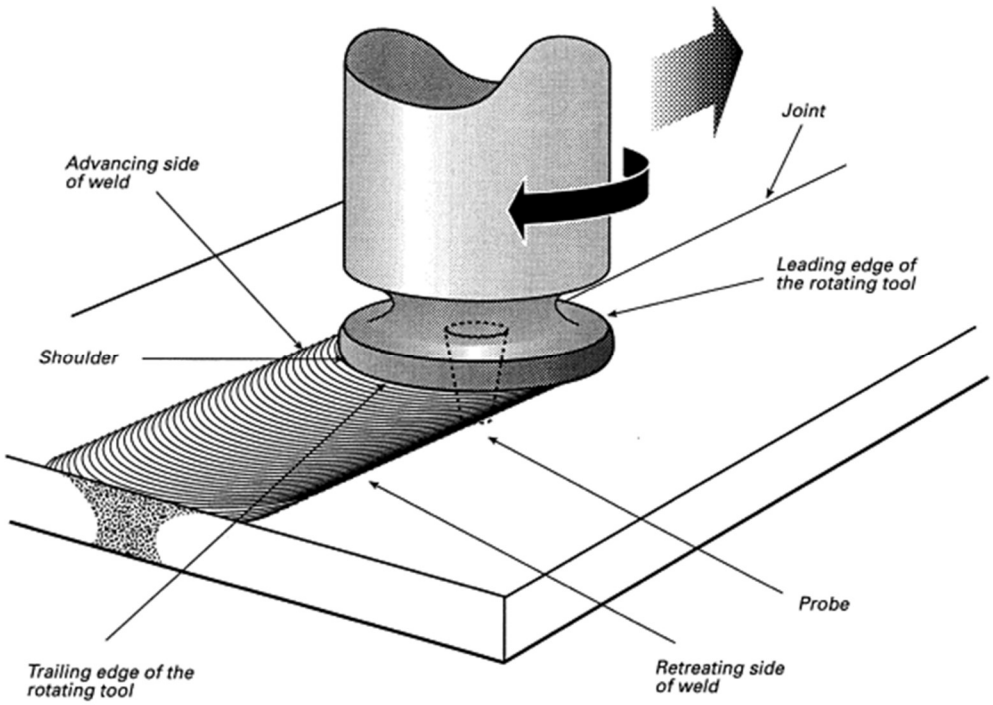

Figure 2.1 Friction Stir Welding process(Thomas and Nicholas 1997)

Basic Weld Terminology

While the original FSW patent and subsequent papers initially expressed some new terminology for the field, many other terms were introduced in various parts of the world as research emerged. In an effort to standardize the existing terminology and understanding of the process at the time, Threadgill published a paper that has been used as the first standard for the field. Key aspects of the paper have been summarized here to provide a basic overview of the process and establish terms used throughout the research.

According to Threadgill, a weld contains four distinct zones known as the parent material, the heat affected zone (HAZ), the

thermomechanically affected zone(TMAZ) and the weld nugget. The parent material zone represents material that has not been changed in any way from the original. The HAZ refers to the area beside the weld that shows minor microstructural changes due to the heat of the process. The TMAZ is the area of material that has been affected by both heating and mechanical deformation induced by the tool. The nugget region is the area confined within or near where the pin moved through the material and represents the most stirred area that has been forced to reconsolidate and recrystallize. FSW is an asymmetric process and it is therefore necessary to distinguish the two sides of the weld. The side that is affected by the tool turning in the same direction as the traversing of the tool across the weld is known as the advancing side and the other side is called the retreating side.(Threadgill 2007) Later studies noted the difference in material properties at the top of the weld and designated this region as the flow arm. The flow arm is composed of the material from the trailing side of the shoulder of the FSW tool. These zones can be seen in Figure 2.2.

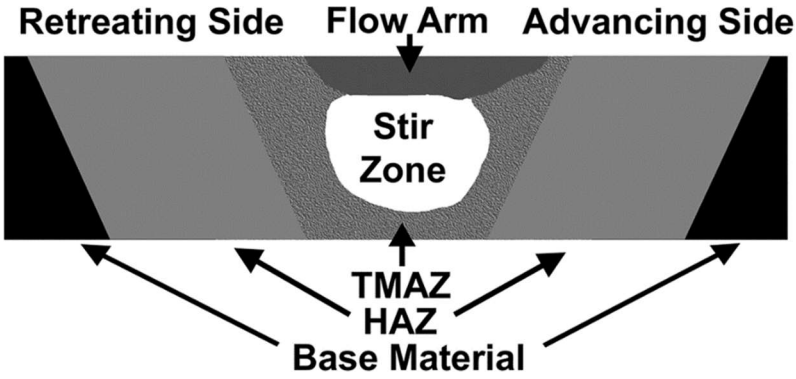

Figure 2.2 Regions of the weld zone created by a tool rotating in a clockwise direction.(Misak et al. 2014)

Joint Geometry

While there have been many advances and variations in joint geometry, basic geometries of an FSW weld are T-joints, butt joints, and lap joints which are also common configurations used in traditional welding. Due to the rigid setup needed for FSW welds and the nature of the rotating tool, it is difficult to design other configurations other than these without modification of the setup or tooling. Figure 2.3 shows the most common joint configurations along with some basic variations on them.

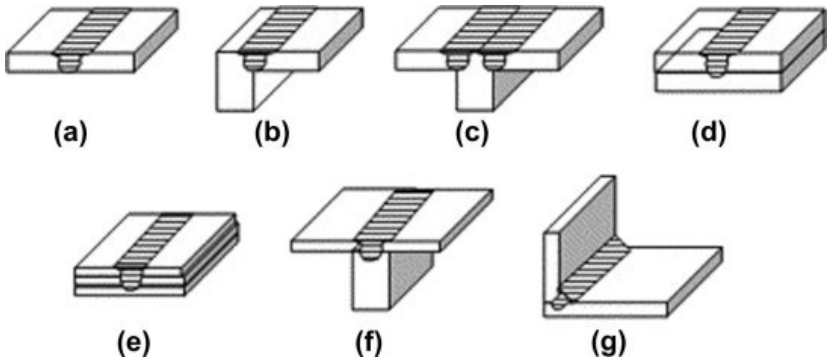

Figure 2.3 Joint configurations in FSW a) square butt, b) edge butt, c) T butt, d: lap joint, e) multiple lap joint, f) T lap joint, g) fillet joint(Mishra and Ma 2005)

Key Parameters

The specific process by which FSW joints are formed is still hotly debated with many theories proposed to describe it, but the key parameters that affect the formation of the weld are generally agreed upon. These parameters include tool material, shoulder width, shoulder geometry(concave or convex), shoulder features(scrolls or other features), probe width, probe geometry(such as tapered, square, triflute, etc…), probe features(such as threads), plunge depth, tilt angle, rotation speed, and welding speed. These parameters can be easily divided into variables that affect the weld based on the design of the features of the tool which were optimized prior to welding, and those that can be adjusted during the welding such as RPM, plunge depth and welding speed. Some materials such as Al 6061 are very forgiving and can be welded with large variations in any of these parameters, while other materials such as Al 2219 are more difficult to

weld and tool design and welding parameters must be carefully planned and optimized to produce quality welds.

Figure 2.4 and Figure 2.5 show the results of a study on the effects of probe shape on the strength of Al 2219 welds conducted by Elangovan. Just the simple change in pin geometry can lead to more than double the strength of the weld.

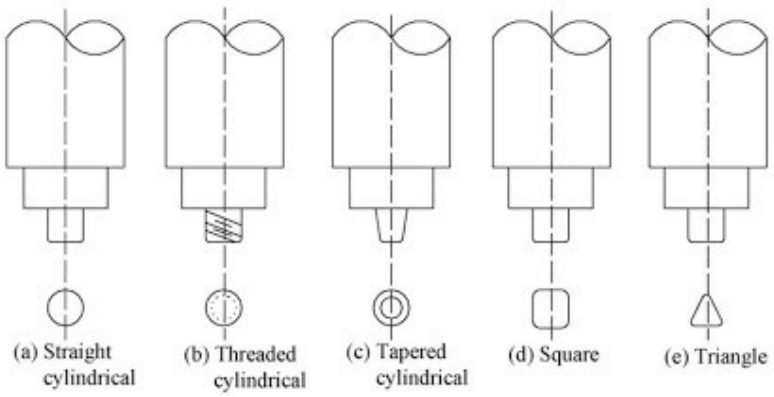

Figure 2.4 Simple probe shapes used in Friction Stir Welding(Elangovan and Balasubramanian 2007)

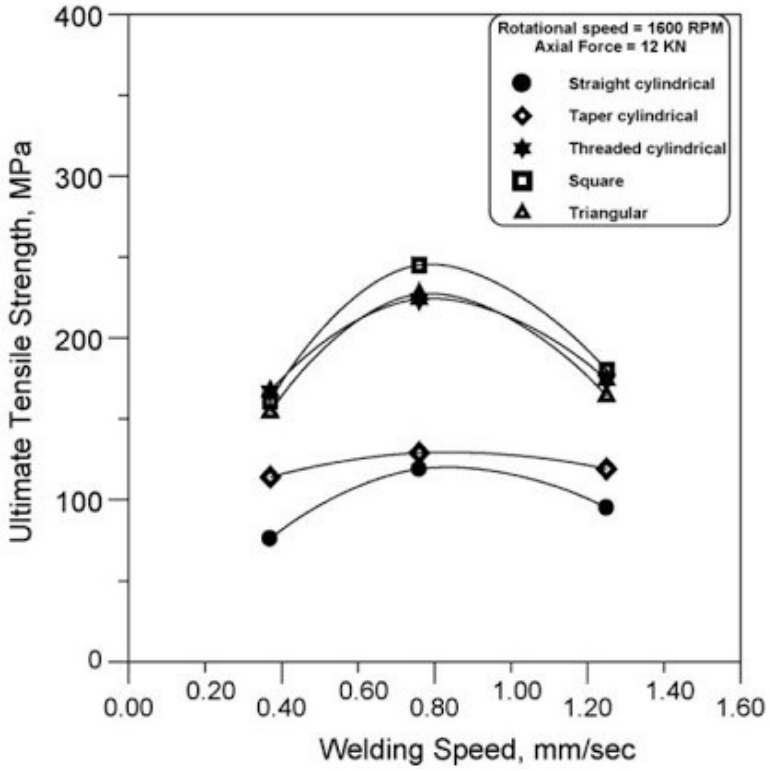

Figure 2.5 Ultimate Tensile Strength of Al 2219 butt welds for each pin shape(Elangovan and Balasubramanian 2007)

Similar effects can be seen based on shoulder design such as adding scrolls or other features that increase the amount of stirring that occurs during the weld.

The variables that can be adjusted during the weld mainly impact the energy that is directed into the weld in the form of heat. Heat generation is the primary mechanism for welding as the material must be heated enough to plasticize it and create a flow around the tool. There is a relationship between energy input into the weld and weld quality as was noted by Cox who showed that optimal tensile strengths could be achieved by controlling the overall energy input into

the FSSW weld. Too little heat and the welds were weakened because there was not enough energy put into the weld facilitate sufficient stirring and reconsolidation. Too much heat and they also experienced reduced tensile strengths because of excessive heat treatment that created unfavorable microstructural changes. (Cox, Gibson, Strauss, et al. 2014)

The influence of the rotation rate and welding speed as primary variables can be better understood given their relation to power. While there are losses in the system the weld power can be calculated by multiplying torque (Nm) by rotation rate (rad/s). It can also be estimated by multiplying the downward force exerted by the tool (N) by its welding speed (m/s). It should be noted that the downward force exerted by the machine through the tool is not a directly adjustable parameter. The downward force has a direct relationship to the plunge depth as the percentage of the tool engaged within the weld dictates the overall force needed to maintain it there. This force is also an outcome of the input variables and can be reduced by increasing the RPM or decreasing the welding speed. Both of these actions increase the energy of the weld and thus the overall heat in the weld zone, which decreases the viscosity of the material and thus decreases the force. This basic understanding of material flow and

heat generation are the main factors that are used in understanding and modeling the FSW process.

Modeling

A comprehensive model for FSW does not exist, but many theories and models have been presented that help us better understand the process and also provide some predictive capabilities for well-studied systems and simple geometries. The two major parts of the FSW process are the heat generation due to friction and shearing forces and the material flow created by the tool pin and shoulder. Due to the nature of the process, temperature readings in the weld zone are difficult to measure directly as any measurement device in the weld zone would be destroyed. Therefore, temperature measurements are most often taken in regions adjacent to the weld zone and estimated or modeled for the stir zone. In addition, there has not been a way to directly observe the material flow during the welding process. Many studies have used tracers and other materials to estimate material flow, but as of yet, no way has been developed to directly measure the material flow process.

Given these constraints and challenges in coupling the mechanics and heat transfer, it is difficult to provide an exact model for FSW that can be applied across materials and across welding

parameters. Many models have been proposed to explain the process of friction stir welding and most either simplify the model to a pure temperature based model, or use a coupled model that takes into account the thermal model as well as the mechanical behavior within the weld. Some popular models are Nunes' Rotating Plug Model(Nunes, Bernstein, and McClure 2000), Schmidt's Thermo Mechanical Model(Schmidt, Hattel, and Wert 2004), Gould's Heat Transfer Model(Gould and Feng 1998), Colegrove's analytical heat generation model and separate material flow model(Colegrove and Shercliff 2013)(Colegrove and Shercliff 2005), and Reynolds' solid mechanical model.(Xu et al. 2001)

Related Friction Stir Welding Processes

As research continues with FSW, new applications of the process and variants on it have been developed. These new variations on the process have become quite numerous and have greatly extended the ability to join materials. The variations most relevant to this research are Friction Stir Spot Welding(FSSW) and Friction Stir Processing(FSP).

FSSW has a very similar setup to FSW except that the tool does not advance along the weld. In FSSW, the tool engages the material and stirs the material directly under the shoulder. This process mixes

the material to leave a small joint area equal to the width of the engaged tool. A keyhole is left behind in the material from the probes penetration into the sheets of material. The effects of the keyhole can be reduced by using a probeless tool while still retaining a similar strength to that of a traditional FSSW weld with a probe.(Cox et al. 2012) The basic setup of FSSW welds can be seen in Figure 2.6.

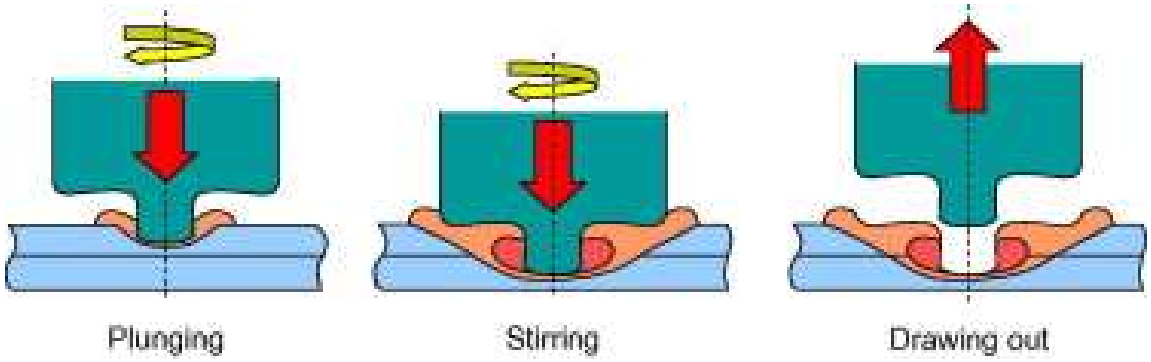

Figure 2.6 Friction Stir Spot Welding as a three-step process(Hovanski, Santella, and Grant 2007)

Friction Stir Processing(FSP) is a generic term incorporating everything from stirring a metal to produce certain microstructural properties, to stirring powder into a metal to create a composite, to using the FSW process to move material to create channels. The cross-sectional view of one such channel is shown in Figure 2.7.

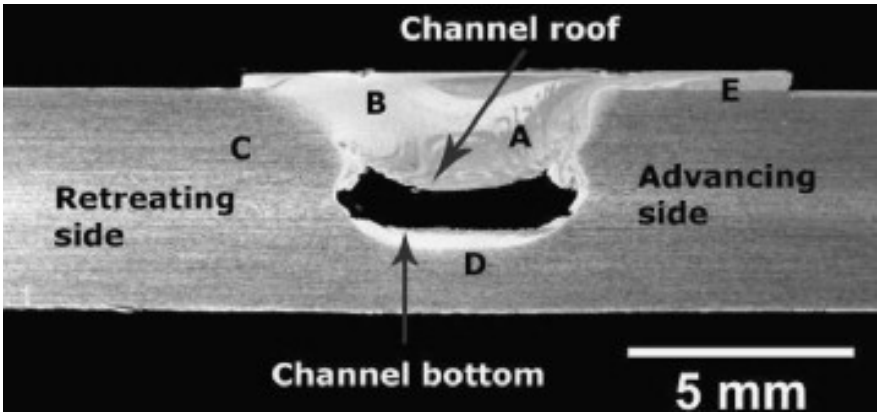

Figure 2.7 Friction Stir Channeling showing the relocation and movement of material.(Balasubramanian, Mishra, and Krishnamurthy 2009)

The key application of FSP in this research relates to the movement of material using FSW. Other authors also refer to similar process that move material in a specific way which they call Friction Stir Forming.(Lazarevic et al. 2013)(Nishihara 2003) The ability to use the FSW process to move material is the key component that will be expanded upon to join dissimilar materials.

Chapter III

NEW MATERIALS AND MATERIAL COMBINATIONS

Some of the greatest advancements in human societies have been spurred by the discovery and development of new materials. We can see the technological developments that led society to new heights as it transitioned from the Bronze Age, to the Iron Age and then the great advances in the Industrial Age due to the production of steel. Today's society is seeing widespread development in the type and use of materials that are available. These new materials allow more possibilities for us to develop innovative technologies. With the production of these new materials comes the need to advance all aspects of the related technologies including the way we use and join them. Friction Stir Welding and its related processes have the potential to play an important role in helping us advance in the fields of additive manufacturing, in-space construction and the ability to join dissimilar materials in new ways.

Additively Manufactured Aluminum Alloys

The development of additively manufactured(AM) materials represents a new era in our ability to manufacture and create parts,

structures and systems. Some say that manufacturing as we know it today will cease to exist as AM is spurring a new industrial revolution and has become one of the fastest growing industries in the world.(Gibson, Rosen, and Stucker 2015) The majority of research into the production of metal based additive manufacturing is focused on finding new ways to build and optimize the metal produced, achieving material properties that can be consistently reproduced, and optimizing the process through modeling to enhance and inform our ability to produce high quality parts that consistently perform in predictable ways when used in real world applications. There are many ways to produce additively manufactured metal parts such as Direct Metal Laser Sintering(DMLS), Selective Laser Sintering(SLS), Electron Beam Free Form Fabrication(EBF3), Ultrasonic Additive Manufacturing(UAM) and numerous others. However, all methods of production at this point are limited by the size of the build plate. As such, small parts can be additively made, but larger parts will need to be formed by joining smaller, built sections together.

To date, there is no publicly published research on the characteristics of joints formed by Friction Stir Welding on additively manufactured materials. This research helps develop a better understanding of the application of Friction Stir Welding to Ultrasonically Additively Manufactured Aluminum 6061 which is formed

by ultrasonically welding thin sheets of aluminum to each other as shown in Figure 3.1.

Figure 3.1 Ultrasonic Additively Manufactured Aluminum showing consolidated region created from individual thin sheets.(Graff, Short, and Norfolk)

Meteoric Material

The interest in space ventures has grown significantly in the past decade as private companies have entered the space market and government agencies such as NASA are seeking ways to make longer voyages which require more in-space support. The reduced cost of reaching space and traveling makes this frontier more appealing, but one major challenge is the cost of sending materials into orbit for use in construction.

NASA has recognized the importance of in-space material and has started initiatives such as the Asteroid Redirect Mission (ARM), which was scheduled to capture a boulder off of an asteroid and

bringing it into orbit around the moon for testing and for evaluation of use of elements such as oxygen and hydrogen.(Wilson 2015) These elements can be used for fueling travel in space, but asteroids can also serve as a source of raw material for in-space construction due to the large iron and nickel content of some asteroids. Based on meteorite studies, which are asteroids that have impacted the earth, the makeup of these iron asteroids is mostly iron and nickel, but there are also inclusions of other materials such as phosphorous, which make it difficult to weld together for structural components without further processing.(Elmer et al. 2014) The chemical composition of one iron nickel meteorite can be seen below in Table 3.1.

Table 3.1 Bulk chemical composition of iron meteorite Javorje.(Miler and Gosar 2011)

		Method			
Element	Unit	FUS-ICP/MS	FUS-ICP/OES	INAA	FA-ICP/MS
Fe	wt%	91.7	n.a.	n.a.	n.a.
Ni	wt%	n.a.	7.83	n.a.	n.a.
Co	wt%	n.a.	0.48	n.a.	n.a.
P	wt%	0.12	n.a.	n.a.	n.a.
V	µg/g	16	n.a.	n.a.	n.a.
Cr	µg/g	n.a.	n.a.	110	n.a.
Cu	µg/g	n.a.	110	n.a.	n.a.
Ga	µg/g	25	n.a.	n.a.	n.a.
Ge	µg/g	47	n.a.	n.a.	n.a.
As	µg/g	n.a.	n.a.	5.8	n.a.
Mo	µg/g	9	n.a.	n.a.	n.a.
Pd	µg/g	n.a.	n.a.	n.a.	2.01

Sb	µg/g	n.a.	n.a.	1.6	n.a.
La	µg/g	204	n.a.	n.a.	n.a.
Ce	µg/g	327	n.a.	n.a.	n.a.
Pr	µg/g	30.5	n.a.	n.a.	n.a.
Nd	µg/g	88	n.a.	n.a.	n.a.
Sm	µg/g	9.3	n.a.	n.a.	n.a.
Eu	µg/g	2.13	n.a.	n.a.	n.a.
Gd	µg/g	5.7	n.a.	n.a.	n.a.
Dy	µg/g	2.1	n.a.	n.a.	n.a.
Er	µg/g	1	n.a.	n.a.	n.a.
W	µg/g	2	n.a.	n.a.	n.a.
Ir	µg/g	n.a.	n.a.	7.6	n.a.
Pt	µg/g	n.a.	n.a.	n.a.	13.4
Au	µg/g	n.a.	n.a.	0.47	n.a.
Pb	µg/g	13	n.a.	n.a.	n.a.
Th	µg/g	2.3	n.a.	n.a.	n.a.

n.a. = not analyzed; FUS-ICP / MS = fusion inductively coupled plasma mass spectrometry; FUS-ICP / OES = fusion inductively coupled plasma optical emission spectrometry; INAA =instrumental neutron activation analysis; FA-ICP / MS = fire assay inductively coupled plasma mass spectrometry.

One attempt was made to weld an iron meteorite by electron beam welding, but the fast cooling in the presence of phosphorous, sulfur and carbon created extensive cracking in the welds. The conclusion was that "innovative welding approaches will be required to create sound welds in meteorites…"(Elmer et al. 2014) Friction Stir Welding and Friction Stir Spot Welding are viable, innovative alternatives to other welding technologies as the process joins the material without ever melting it. This research will test the ability to successfully join meteoritic material using FSSW.

Joining of Dissimilar Metals

While additive materials and meteoric material represent exciting opportunities for welding new materials, another challenging area for welding has been the ability to weld dissimilar materials. The term "dissimilar materials" can refer to a wide range of applications from two similar alloys of aluminum such as 2024 joined to 7075, to joining two very disparate materials such as aluminum and steel which have vastly different material properties. The term dissimilar materials will be used in this paper to refer to the second combination of materials that involve very different material properties.

Numerous joining techniques have been proposed to join dissimilar materials such as diffusion bonding(Jiangwei, Yajiang, and Tao 2002)(Miyagawa et al. 2009)(Wilden and Bergmann 2004), laser welding(Anawa, Olabi, and Elshukri 2009), friction welding(Fuji 2002)(Fuji, Ameyama, and North 1995), friction stir welding(Chen and Nakata 2009)(Aonuma and Nakata 2011), and ultrasonic welding(Zhang, Robson, and Prangnell 2016) to name a few. Each of these methods provides a way to join dissimilar materials and can be used for different geometries and thicknesses, but each has its limitations. The limited success of these joining techniques means that industry has relied on more traditional joining methods such as adhesives, rivets, clinching, bolts, etc… These more traditional

methods are stronger than most new ways of joining dissimilar materials, but they take time, add weight and often introduce other issues such as crevice corrosion and areas of weakness due to holes created in the materials.

FSW and FSSW of dissimilar materials has been suggested as an alternative to traditional joining and welding methods. However, three major obstacles make the FSW of dissimilar materials challenging. The first is the difference in melting temperatures. FSW is a solid-state process, but it uses friction and shearing to significantly raise the temperature of the material. With a material such as steel the melting point is 1,400 degrees C, while aluminum 6061 is 600 degrees C. To heat the steel up to the temperature needed to plasticize it takes the joint above the melting temperature of the 6061 and consequently causes melting in the aluminum which leads to poor joint quality.

The second major obstacle is the formation of intermetallic compounds(IMCs) which occur at the interface of the materials. This IMC layer is quickly formed when the materials are joined at an elevated temperature. The creation of a thick, intermetallic bond layer weakens the weld because of its brittle nature(Liyanage et al. 2009)(Bozzi et al. 2008). A good overview of the challenges associated with traditional FSW and FSSW for dissimilar welding of aluminum and

steel can be found in Haghshenas(Haghshenas, M. Sahraeinejad et al. 2013).

The third major obstacle is the wear of the tool as it interacts with a hard material such as steel or aluminum. Common tool materials used for joining aluminum wear out very quickly and more robust tool materials are expensive and much more difficult to machine.(Gibson et al. 2014) One way of avoiding wear is through the use of pinless tools that contact only the aluminum, or tools with short pins along with position control that keep the pin within the aluminum only.(Watanabe et al. 2011)(Chen and Nakata 2008)(Lee et al. 2009)

Traditional FSW and FSSW of these dissimilar materials has produced joints that are weaker than the parent material as only limited mixing of the materials can be achieved. In fact, most of the current studies attribute the majority of the strength of the weld to factors other than welding of steel to aluminum. In the FSSW study by Lee where the probe only entered the aluminum, the conclusion was that the strength of the bond was entirely attributed to the formation of IMCs and that no mixing of the aluminum and steel occurred.(Lee et al. 2009) In another study of FSSW that penetrated into the steel layer, it was concluded that the strength of the joint was due mainly to a mechanical interlocking produced by a "hanging" section of displaced steel similar to a hook and the greatest tensile

strength reached was 407 kgf.(Bozzi et al. 2008) Other experiments in FSW have found that the use of a zinc coated steel helps to form a stronger bond because of the better bonding between the zinc and Al due to a brazing effect of the melted zinc.(Miyagawa et al. 2009)(Choi et al. 2010)(Chen and Nakata 2008)

Building on this understanding that little mixing can occur during the process, researchers have attempted to use FSW and FSSW to create dissimilar joints using prefabricated geometrical configurations such as holes or other features(Nishihara 2003),(Balakrishnan, Kang, and Mallick 2007)(Lazarevic et al. 2013). These methods have had good success in producing better welds, but these joints still lack the structural integrity to withstand strong forces. Other alternatives have been proposed such as the introduction of a third material and using a combination of FSW and riveting. Two main processes following this research have emerged called Friction Stir Blind Riveting (FSBR) as proposed by Gao(Gao et al. 2009), Min(Min et al. 2015), and Lathabai(Lathabai et al. 2011) and Friction-Stir Riveting as presented by Ma and Durbin(Ma and Durbin 2012). These processes use Friction Stir Welding to plasticize the material to be joined so that an actual rivet made of a different material can be driven into and left behind in the materials to be joined.

There have been advances in the field such as the use of FSW to join dissimilar cast aluminum to steel in the frame of the 2013 Honda Accord in an effort to lightweight the vehicle. This setup produced a strong joint sufficient for use in production of the vehicles as pictured in Figure 3.2. This success shows the value in developing the ability to join other material combinations.

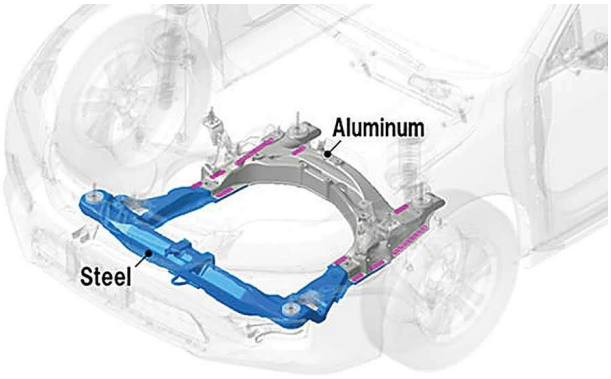

Figure 3.2 Honda Accord frame using FSW to join the frame pieces made of aluminum and steel. (Honda Worldwide, 2012)

The joining of dissimilar materials has long been a challenge in all industries and the need for joining them is increasing. This increase is attributable to the need to incorporate lighter weight materials into production to reduce the overall weight without sacrificing strength and the development of innovative materials that open new possibilities for design. New methods for joining dissimilar materials are needed to meet current industry demands.

Chapter IV

FRICTION STIR WELDING OF ULTRASONIC ADDITIVELY MANUFACTURED ALUMINUM: AN INVESTIGATION OF 3-D PRINTED ALUMINUM ALLOY

Authors

William Todd Evans, Jay T. Reynolds, George E. Cook, Alvin M. Strauss

Abstract

Additive manufacturing(AM) of metallic materials represents an important emerging technology in the aerospace sector due to its ability to reduce part counts and number of welds, reduce manufacturing lead times, and accelerate iteration of the design/build/test cycle. Additively manufactured parts must eventually be integrated into larger systems, but there has been little published research on welding characterization of additively manufactured metal parts. A better understanding of the potential differences in welded properties for AM materials versus conventionally manufactured materials is needed to facilitate the integration of AM parts into larger structures.

This work focuses on characterizing the properties of ultrasonic additively manufactured 6061 Aluminum alloys butt welded using Friction Stir Welding (FSW). Samples were polished and etched to

examine the structure and mechanically tested to compare strengths to parent and conventionally manufactured materials. In all cases, the strength of the friction stir welded region is significantly greater than that of the parent additive material. This study shows that FSW is an effective way to join ultrasonic additively manufactured Aluminum 6061 material which also has the potential to improve mechanical properties.

Introduction

The development of additively manufactured(AM) materials represents a new era in our ability to manufacture and create parts, structures and systems. AM has been characterized by some as the new industrial revolution.(Gibson, Rosen, and Stucker 2015) The term additive manufacturing covers a broad portfolio of technologies, but processes are typically classified based on the form of the native feedstock (wire or powder) and the energy source. Most additive technologies have an upper limit on component size (a consequence of a spatially restrictive deposition chamber). This will necessitate joining of materials produced using the additive process into larger structures or assemblies, which may consist of a combination of conventionally manufactured materials and/or additively manufactured materials. Many traditional methods such as bolting, riveting, adhesives, etc. can

be used, but Friction Stir Welding(FSW) can offer an additional avenue for welding additively manufactured parts that have a geometry compatible with the FSW process.

Friction Stir Welding is a solid state joining processes that uses a rotating, cylindrical tool to plasticize and stir the material to form a joint as pictured in Figure 4.1.

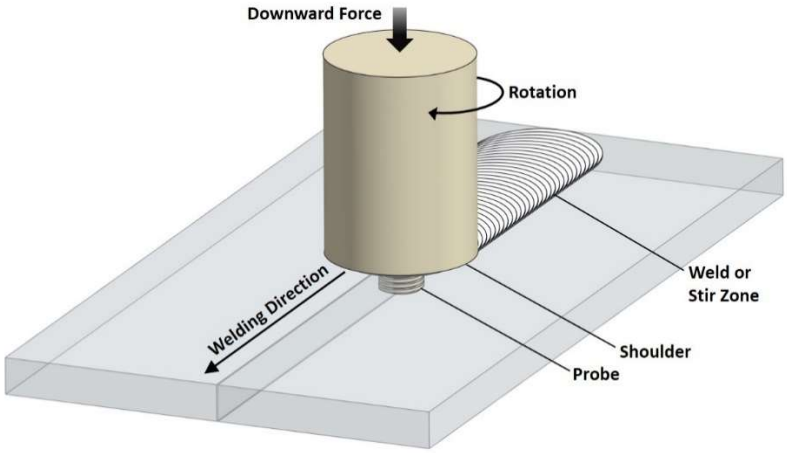

Figure 4.1 Friction Stir Welding Setup and common terms.

FSW is becoming widely used in industry because it avoids many of the common issues encountered in traditional fusion welding such as porosity, embrittlement and cracking that occur due to melting and resolidification. In addition, it requires no filler material or shielding gases. FSW is a mature process for most Aluminum alloys of the 2XXX, 6XXX, and 7XXX series. The process can also be used with steel, titanium, and other higher strength alloys.(Gibson et al. 2014)

It has gained wide acceptance in the aerospace, automotive, ship building, and railway industries. However, there is little published research on FSW of additively manufactured materials.

For this study, additively manufactured aluminum 6061 was chosen as an initial candidate given the large amount of comparative data available for the FSW of traditional aluminum 6061. The rapid oxidation of Al 6061 limits its use in additively manufactured processes, but a solid state process known as ultrasonic consolidation or Ultrasonic Additive Manufacturing(UAM) has been successful at producing AM 6061 parts.

This method was first patented as a process to bond multiple layers of material together using the frictional heat created by friction acoustic bonding using ultrasonic waves. This bonding of layers eliminated the need for adhesives and allowed layers to be joined in a solid state process.(White 2002) The UAM process has been further refined and currently involves using an ultrasonic transducer connected to a wheel shaped sonotrode to transmit the vibrations to a thin metal tape strip as shown in Figure 4.2. This process welds the topmost layer of metal to the level below it to create a solid state bond. Each successive layer is placed in an overlap configuration of the previous layer and the layers are built up to form a larger structure. In between each layer, a CNC can be used to create features or to

make sure the layer is built to the correct specifications.(Wolcott, Hehr, and Dapino 2014)

UAM has several advantages over other AM processes. The process is solid state and creates more consistent properties throughout the part. The process also allows use of different materials within the same build. While the part size produced with most metal AM processes is limited by the size of the build chamber in which the parts are fabricated, the UAM process has been extended to very large builds up to 1.8m by 1.8m.

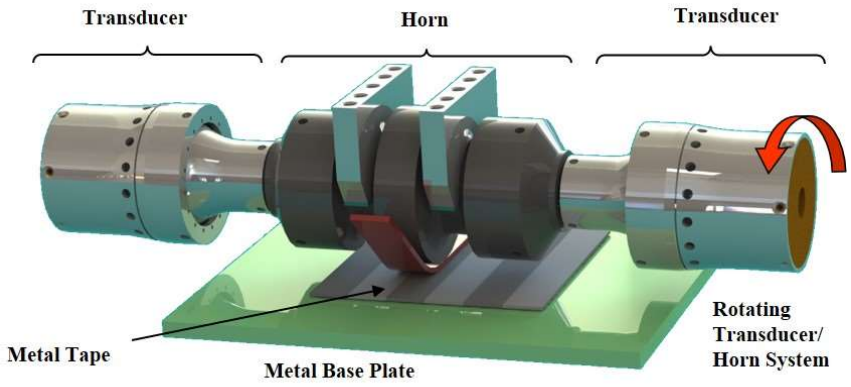

Figure 4.2 Setup for the building of Ultrasonic Additive Material(Norfolk, Laser's Today)

Research has shown that tensile properties of UAM 6061 are often lower than the bulk material. While many factors contribute to this decrease, two in particular represent the major losses in strength.

The first is related to a term known as Linear Weld Density (LWD) which is a measure of how well one layer bonded to the next. LWD can approach 100%, but is often much lower. When the layers are not bonded as well, they have a much lower strength than bulk material which has 100% bonding. The second feature of UAM that reduces strength is the gaps between the tapes used across each layer. Small misalignments in the tape strips contribute to the formation of small gaps (similar to a linear crack within a plane) which lead to reduced strength in that plane. While the tapes are staggered, this issue cannot be completely eliminated.(Gibson, Rosen, and Stucker 2015)(Schick et al. 2010)(Sridharan et al. 2016) Given that UAM creates a new structure of the base 6061 material, it is unknown how this structure will impact the welding parameters for FSW of the UAM material or any other structural outcomes that might be introduced by the process. This research seeks to characterize the post weld properties of Friction Stir Welded Ultrasonic Additively Manufactured aluminum 6061-H18 and compare these results to FSW welds of Aluminum 6061-T6.

Materials & Methods

The aluminum 6061 samples were created with the use of the Ultrasonic Additively Manufactured process. Bars were created with

dimensions of 6.35mm by 76.2mm by 305mm. The tape used for the layers was Al 6061-H18 with dimensions of 25.4 mm wide by 0.15 mm thick. Its chemical composition by percent is; Si-0.6, Fe-0.43, Cu-0.24, Mn-0.11, Mg-0.9, Cr-0.18, Zn-0.03, Ti-0.04 with the balance constituting aluminum. The bars were separated from the base plate by milling away the base plate and were then cut in half longitudinally. This allowed the two halves of the bar to be joined in a standard butt weld configuration. Similarly dimensioned 6061-H18 material is not commercially available for comparison purposes. Therefore, rolled Aluminum 6061-T6 bars of the same dimensions were used for comparison to the UAM material. While the two tempers exhibit different mechanical properties, they have many similarities and are part of the same alloy family. Differences in their properties and effects on the welds are pointed out in detail in the discussion section.

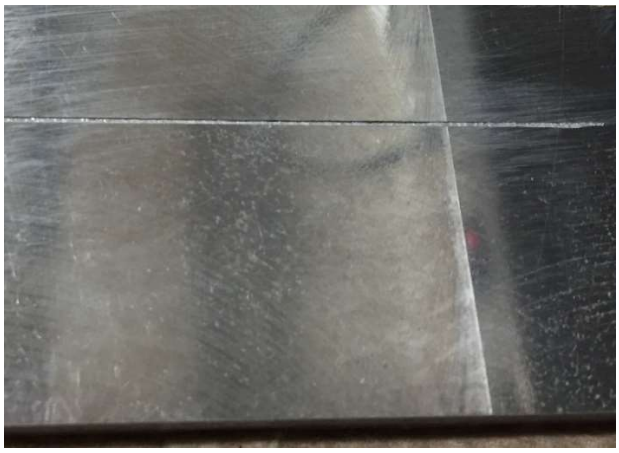

Figure 4.3- UAM 6061 as received from manufacturer, showing milled surface finish and evidence of a tape line.

Tool and weld parameters

Parameters were chosen for all welds based on previous optimization research of Al 6061 butt welds using 1,400 RPM and 2.53 mm/s traverse rate.(Longhurst et al.) The tool was made of 25.4 mm O1 hardened tool steel with a 7 degree convex shoulder with six scrolls and a 6.35 mm diameter threaded probe of 5 mm length as pictured in previous work.(Evans et al. 2015) Table 4.1 summarizes the key welding parameters used in this study.

Table 4.1 Selected Parameters for rolled 6061-T6 and UAM *6061-H18*

Material	**Process**	**Sample Direction**	**State**	**RPM**	**Traverse speed (mm)**	**Plunge depth of pin**
Al6061-H18	UAM	Longitudinal	Parent	n/a	n/a	n/a
Al6061-H18	UAM	Transverse	Parent	n/a	n/a	n/a
Al6061-H18	UAM	Longitudinal	Welded	1400	152	5 mm
Al6061-H18	UAM	Transverse	Welded	1400	152	5 mm
Al6061-T6	Rolled	Longitudinal	Parent	n/a	n/a	n/a
Al6061-T6	Rolled	Transverse	Parent	n/a	n/a	n/a
Al6061-T6	Rolled	Longitudinal	Welded	1400	152	5 mm
Al6061-T6	Rolled	Transverse	Welded	1400	152	5 mm

Testing

Tensile testing was completed on an Instru-met Model TTC-102MC tensile testing machine with a 5,000 kg capacity. Samples were tested at a rate of 5mm/min and sampled at 10 Hz. Transverse and longitudinal dogbone samples were prepared by a CNC machine to ensure that an accurate comparison of all samples could be made. In total, 32 specimens were prepared for tensile testing which represented four samples at each of the eight conditions. Dogbone samples were created with a slight modification of the ASTM E8 standards due to the shorter length of material available in the specimens in the transverse direction. This variation from the ASTM standard was consistent throughout the specimen sets. The width and length of the reduced section was prepared at the standard dimensions of 32 mm with a fillet radius of 6mm to transition to the grip section. The grip section length had to be reduced to 15 mm and the width was increased to 12.5mm to help compensate. Macroscopic analysis was performed on the fractured samples to examine fracture behavior.

Results and Discussion

Comparison of Base UAM and Rolled 6061 Material

Parent material tensile properties between the UAM and rolled materials show a drastic difference in ultimate strength as seen in Figure 4.10. This was expected due to the different tempers of the UAM vs the rolled material. The UAM parent material starts in the H18 temper which is a full-hard condition obtained by severe cold working. The H18 sheets of 6061 are ultrasonically vibrated against each other to form a bond with the layer below it as shown in Figure 4.4. This creates localized heat treatment within the layers, so the temper of the sample is a mixture of H18 and heat affected H18. The rolled material in the T6 temper which is designed for maximum strength and has undergone heat treating and artificial aging.

The Ultimate tensile strength(UTS) of the rolled material in the transverse compared with the longitudinal direction is very similar with a slightly higher strength in the rolled direction along the longitudinal length. However, the UAM material showed more variation in the transverse vs. longitudinal direction with the longitudinal direction showing a 7% higher strength. This can be explained by examining the setup of the UAM process. The thin tapes used in UAM are laid down in the longitudinal direction and therefore represent a continuous

piece of material. In addition, the tapes are rolled, which causes grain elongation and strengthening in the longitudinal direction vs the transverse one. The tape strips are 2.54 cm wide and therefore must be laid down side by side using 3 to 4 sections of tape across the transverse width of the weld. The layers are overlapped in each successive layer to increase strength, but the gaps between the tape strips weaken the material slightly in the transverse direction.

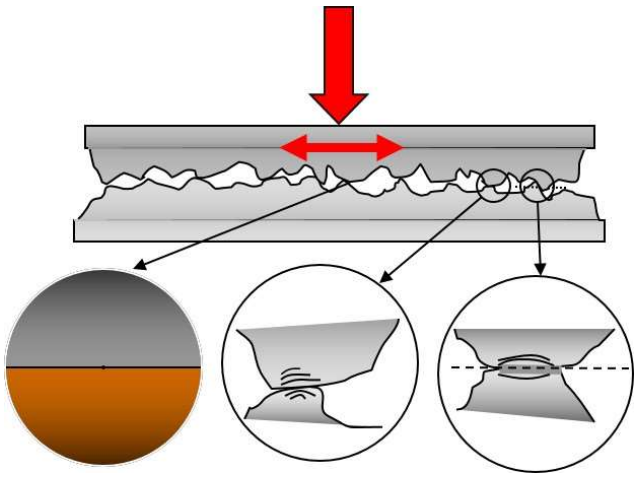

Figure 4.4 Magnified representation of bonding mechanisms in UAM. Image used by permission of Fabrisonic

While both tempers exhibited some ductility, the fracture mode of the T6 was less ductile in nature. The UAM material had slight variations in fracture modes of the longitudinal and transverse directions. The longitudinal direction shows more elongation and clear, even necking patterns at the point of fracture. Some layer lines from the 6061 tape are still visible, but have been reduced in their cross-

sectional area in the necking region as shown in Figure 6d. Each individual tape layer is pulled evenly in tension, and the necking is consistent with the tape layers that were laid in the longitudinal direction.

The transverse samples show a different fracture mode and exhibit multiple fracture patterns within the same sample as can be seen in Figure 4.5. The lower portion of the material, closest to the base plate, appears to elongate and neck. However, the portions of the UAM material closest to the surface seem to experience a great reduction in ductility. The failure mode is more brittle and occurs along each individual layer of the material as shown in Figure 4.6. This "mixed mode" results from one of the challenges of building a UAM material: the increasing energy input needed for each new layer.

Previous optimization studies have shown that more energy is needed in successively higher layers since the energy is dispersed throughout a larger volume of material. Without careful optimization, this leads to the samples closest to the surface having a lower LWD. In the lower layers of the build near the baseplate, nearly 100% LWD was achieved, so they performed in a similar fashion to the longitudinal UAM specimens and to the rolled material.

Therefore, we can understand this mixed mode of failure in the transverse direction by looking at the impact of the UAM process in

each section of the UAM material. The lower section yielded in a bulk manner since it was well joined, but the upper sections fractured in a brittle manner due to the material behaving as individual layers with sections of bonded and unbonded areas as well as gaps in the tape.(Sridharan et al. 2016)(Wolcott et al. 2014)

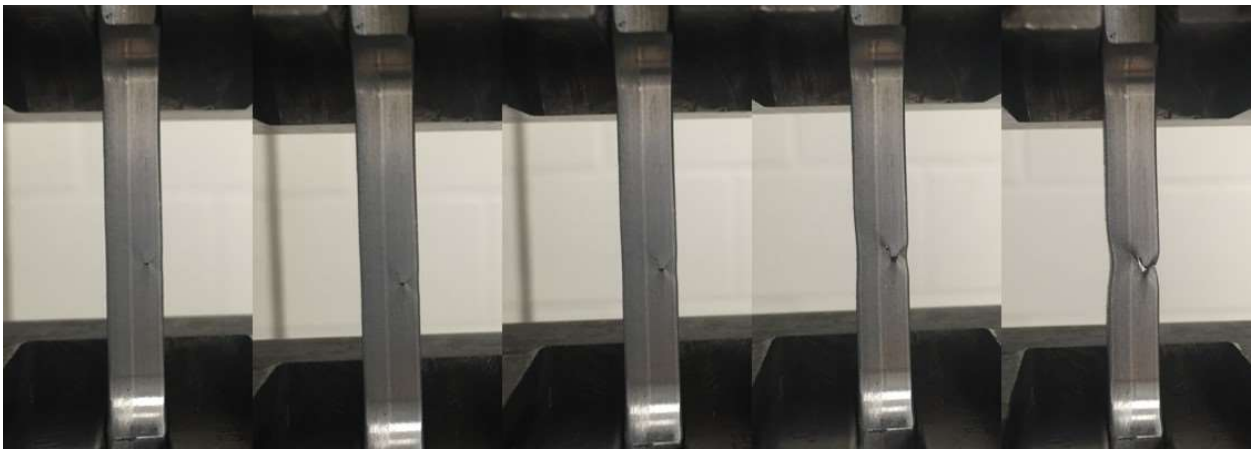

Figure 4.5 Crack initiation and progression during tensile testing of UAM 6061 in the transverse direction showing multiple fracture patterns.

Figure 4.5 shows the initiation of a crack in the upper half of the material closest to the surface of the build. This crack likely initiated from gap between layers of tape. As the tensile test progresses, the different behavior of the two sections can be clearly seen as the lower section on the left stretches in a ductile manner and the upper section on the right shows brittle fracture leaving a gap between the fractured sections. A close up of this fractured surface in Figure 4.6b shows clear evidence of individual sheets breaking in different locations on the plane of the tape layer.

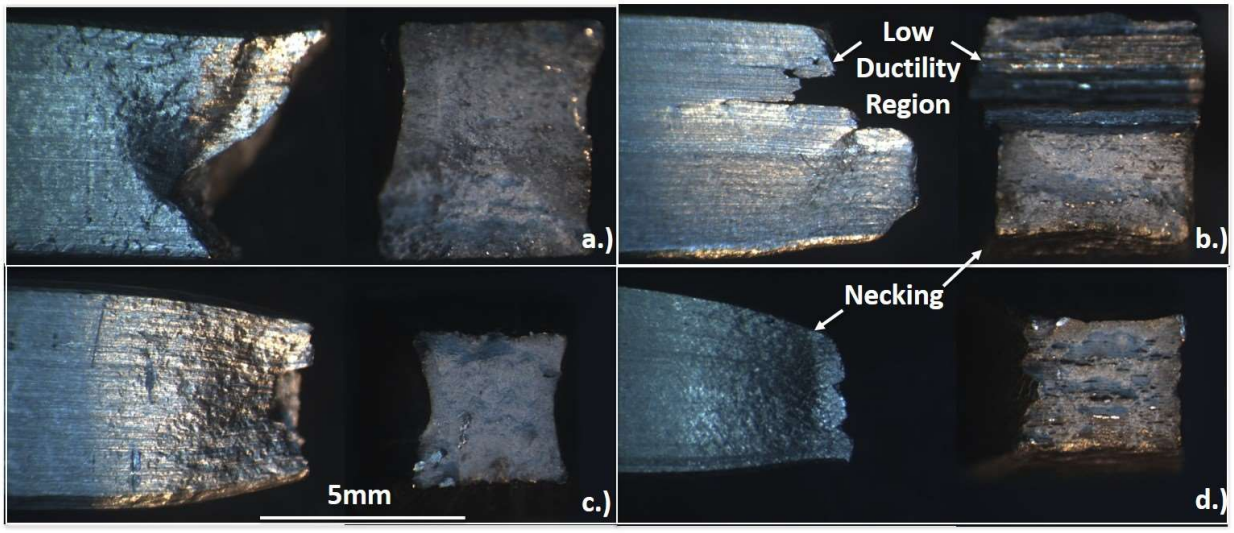

Figure 4.6 Fracture surfaces from tensile testing of parent 6061 materials. a.) Rolled parent transverse b.) UAM parent transverse c.) Rolled parent longitudinal d.) UAM parent longitudinal

Comparison of welded, transverse rolled T6 vs welded UAM

The rolled Al 6061-T6 material that was welded and tested in the transverse direction fractured at the edge of the advancing side of the weld in the heat affected zone. Failure included clear necking and ductile failure as seen in Figure 4.7a.

The UAM 6061 material that was welded and tested in the transverse direction showed failure in the parent material. The ultimate strength of the welded UAM material showed an average increase of 20 percent. The failure appears to be similar to the failure noted earlier in the parent material, transverse samples with a mixture

of necking at the bottom of the plate and a low-ductility fracture of individual sheets at the top as seen in Figure 4.7b.

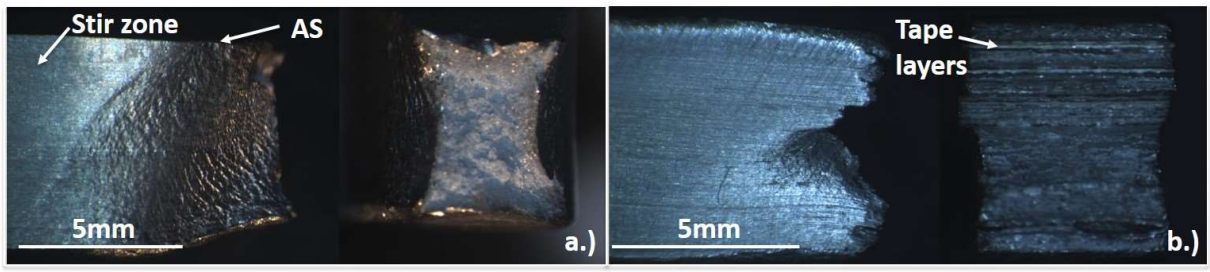

Figure 4.7 Fracture surfaces from tensile testing of transverse section of welded 6061 materials. a.) Rolled b.) UAM

The difference in the two failure modes can be explained by looking at the tensile failure process, the materials, and the welding setup. Tensile failure will occur at the location of the weakest part of the material. The T6 material is a heat treated, artificially aged material that is very strong. The stirring and heating of the material during the FSW process softens the material, meaning that the weakest part will be in or near the welded area known as the Heat affected zone (HAZ). The welding tool used in this study has features which aggressively stir the material and tends to create an asymmetric weld profile by shearing and stirring material off of the advancing side and leaving slightly more of a deposit of material on the retreating side. Therefore, the location of fracture in the T6 material is along the advancing side which is the thinnest portion of the weld where the

parent material has been softened from the FSW process. This leads to necking and ductile failure. The loss of parent material strength can be partially attributed to this thinning, however, much of the parent material strength is recoverable through heat treatment.

In comparing the overall tensile strength of the UAM welded, transverse sample, it is important to note that the UAM material has been strengthened by cold hardening, but it has not received any heat treatment to enhance its strength. This accounts for the large difference in strengths seen between the two materials.

In comparing the fracture location and the strength of the UAM welded material, the limitations discussed in the previous section influence these results. The FSW process increases the strength of the UAM material in and near the welded region by stirring the material to break it up into finer grains and create a more uniform bulk material. The FSW process does this by stirring the material to eliminate the gaps created by the adjacent tape layers and breaking up the remaining oxide layers between the pieces of tape that were not fully consolidated in the original UAM process. This processing and refinement by FSW is illustrated in Figure 4.8 which shows that there are still gaps and weaker areas in the parent material, but these are reduced in the Thermomechanically Affected Zone (TMAZ) and Heat Affected Zone (HAZ) and eliminated completely in the nugget zone.

The parent material is the weakest region and therefore tensile failure happens there, rather than in the welded region.

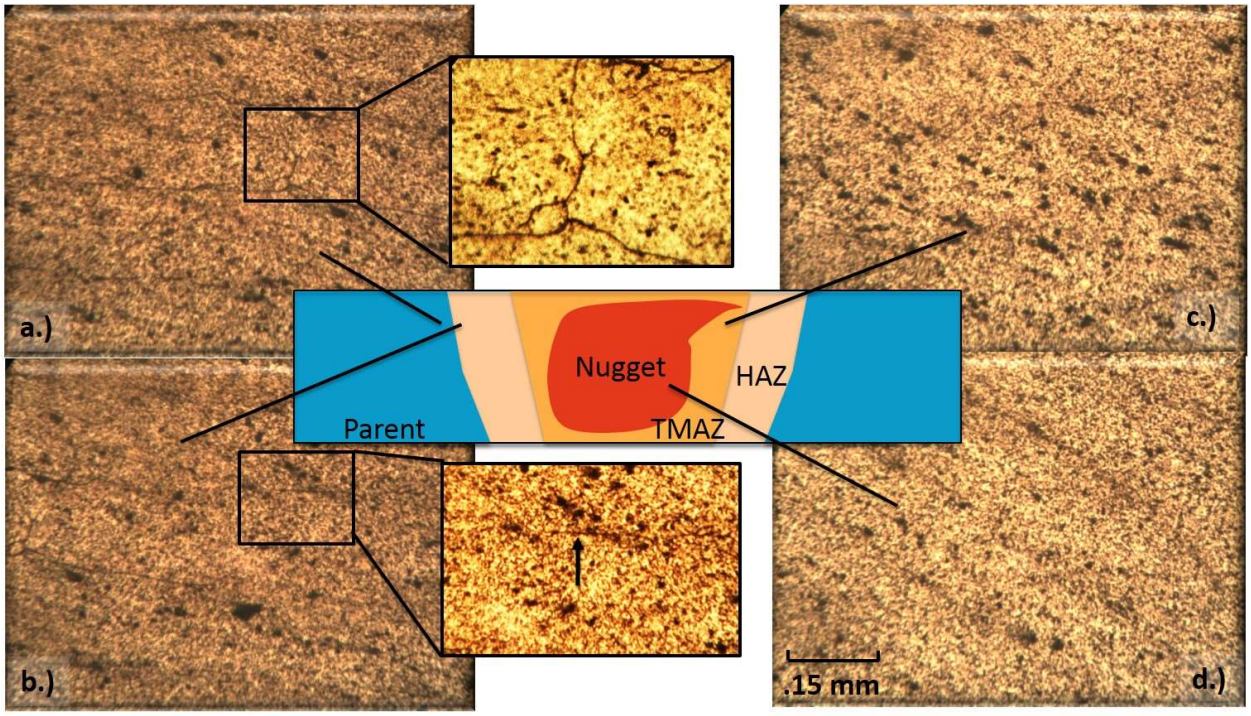

Figure 4.8 Features in Microstructure of Friction Stir Welded, Ultrasonic Additively Manufactured 6061.
a.) Parent- layer lines and tape lines evident. b.) Heat affected zone(HAZ) some layer lines still visible, but fewer in number and size. One has been shown as indicated by the arrow.
c.)Thermomechanically affected zone (TMAZ)- no visible layers. d.) Weld Nugget- all layers have been stirred and microstructure is a fine grain size.

The welded UAM, transverse specimens showed an 8% increase in strength over the parent material transverse specimens. The increase in strength of the welded UAM transverse sample can primarily be attributed to a reduction in the number of gaps and

stirring of the layers in a large portion of the reduced section of the dogbone sample. The welded region is 25 mm wide at the surface, which leaves only about 20% of the parent material on either side of the weld in the reduced section of the dogbone. Since the UAM process creates a somewhat inhomogeneous structure of gaps and solidified areas, there are localized sections that are weaker than others. Larger gaps between adjacent foils during manufacturing can lead to premature failure of the UAM material. By processing about 80% of the test region, larger gaps between layers are less likely to be present and an accompanying increase in strength of the specimen is observed. The graphs of the tensile failures of the parent and welded transverse samples shown in Figure 4.9 look very similar as expected from examination of the macrographs of the fractures.

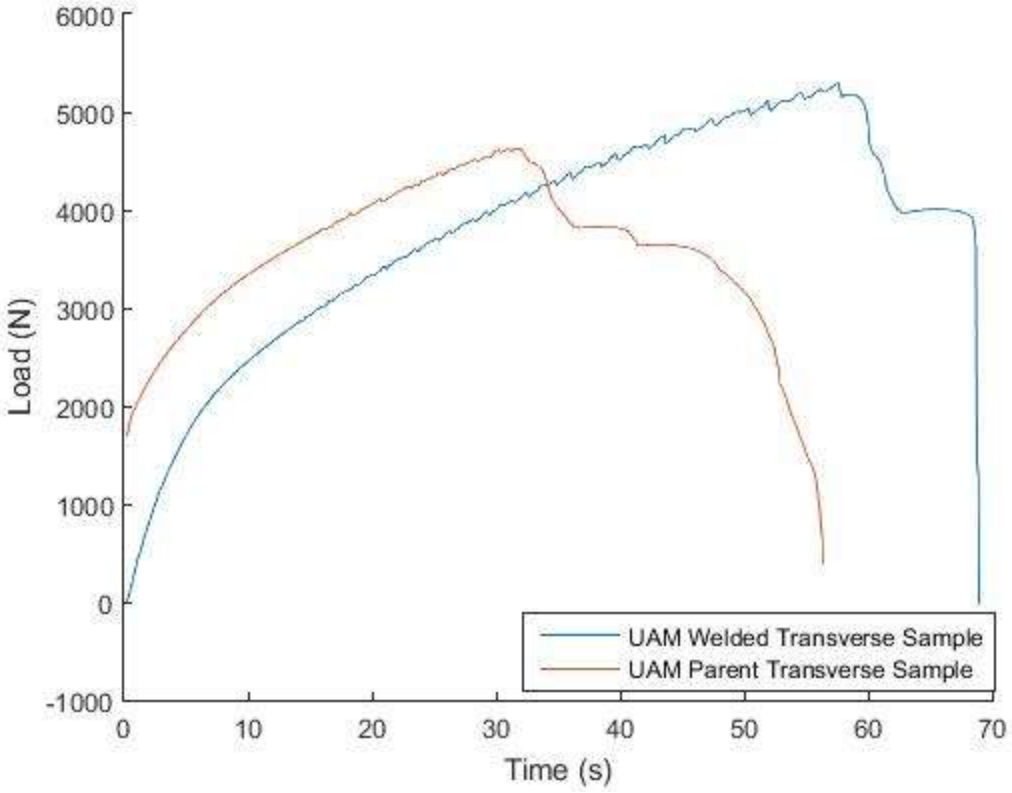

Figure 4.9 Comparison of individual UAM 6061 Transverse tensile specimens from parent and welded material

Comparison of welded, longitudinal rolled T6 vs welded, longitudinal UAM

The rolled Al 6061-T6 material that was welded and tensile tested in the longitudinal direction. Specimens exhibited ductile shear fracture behavior. There was an overall average reduction in strength of 14 percent.

The UAM 6061-H18 welded material taken in the longitudinal direction also experienced the same type of ductile shear failure as the rolled material. However, the strength of the specimen represents a

50 percent increase in strength compared to the parent UAM material as seen in Figure 4.10.

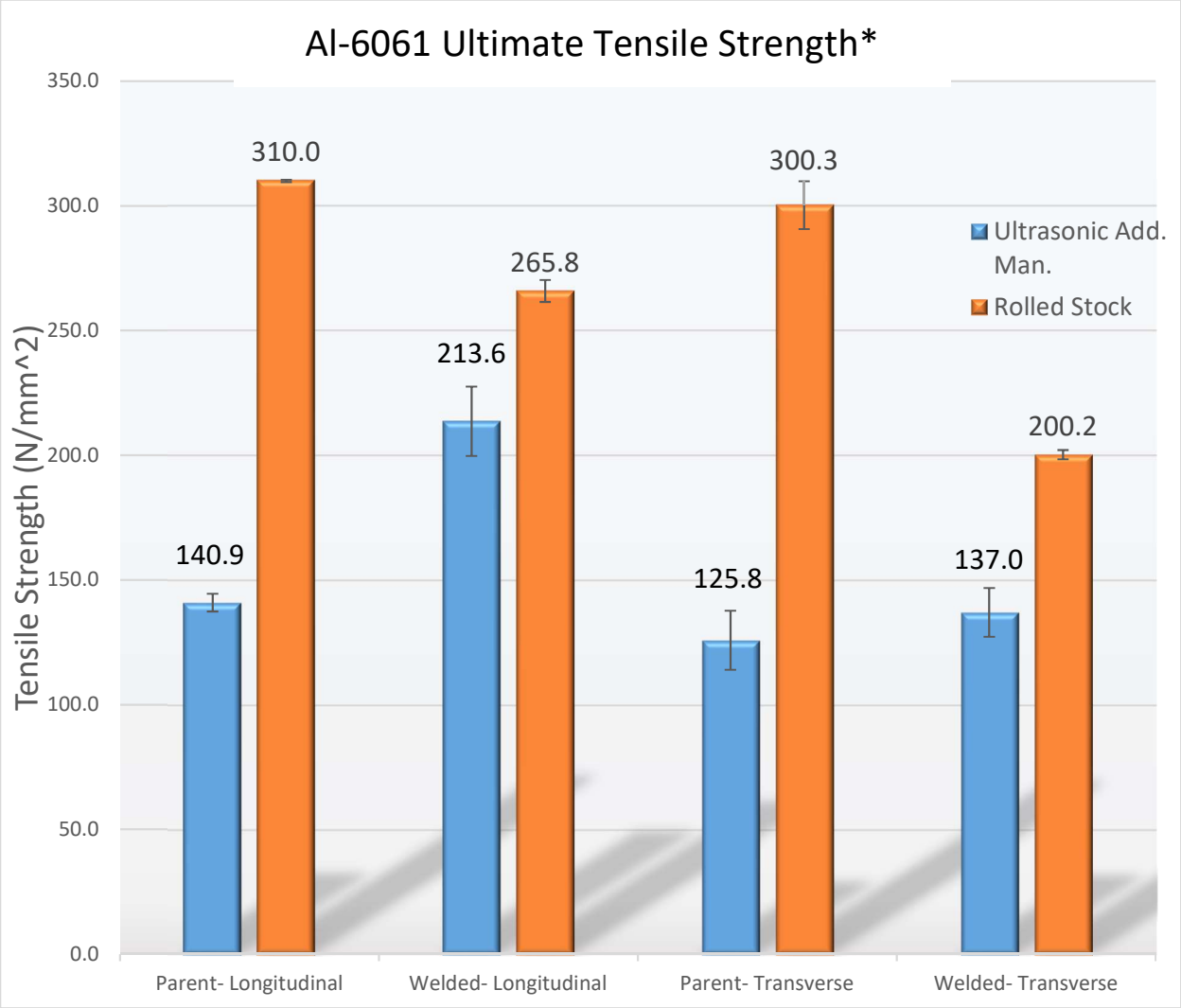

Figure 4.10 Average Ultimate Tensile Strengths(N/mm^2) for Al-6061 *Average UTS values are based on the average of four tensile specimens.

The longitudinal specimens from both materials were cut from the center line of the weld. This material is in the nugget region of the weld and represents the region of highest plastic strain and deformation. As a result, this region has the finest microstructure of

any region in the weld. As observed in the transverse sections, the welding process reduces the strength of the T6 material, but not as drastically. The finer grain microstructure produced in the T6 helps compensate for some of the losses in temper experienced during the process. For the UAM material, the refinement and heat from the FSW process enhances the material properties, creating a much stronger region in the nugget zone. The fractured specimens and the graph of the tensile results show very similar patterns as can be seen in Figure 4.11. Additional heat treatment of the material would further reduce the gap in the properties of the two specimen sets.

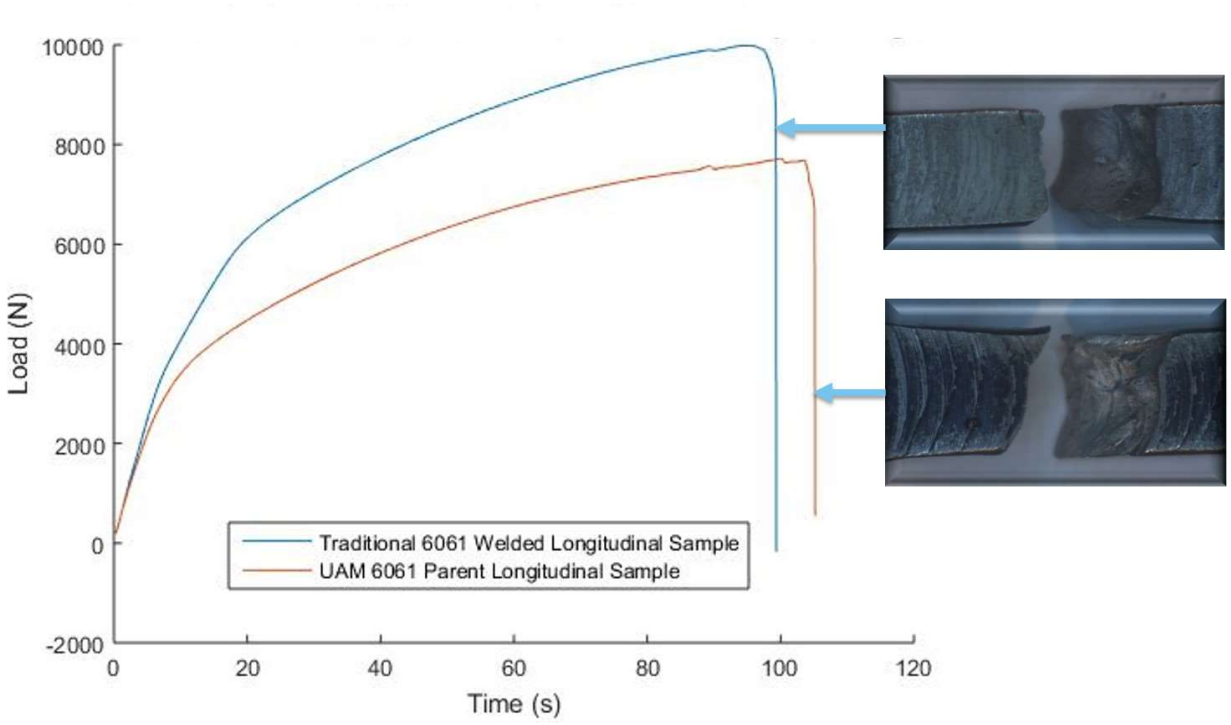

Figure 4.11 Comparison of Rolled 6061 and UAM 6061 Welded Samples- Longitudinal

Conclusions

As the field of additive manufacturing of metals continues to expand to new applications and materials, it is imperative to find ways to effectively join these AM and 3-D printed parts to larger structures. This study has shown that Friction Stir Welding is an effective way to join Ultrasonic Additively Manufactured Aluminum 6061. Results from this study indicate that FSW also has the potential to work well with other AM materials. Key results are:

- Friction Stir Welding is an effective welding solution for joining Ultrasonic Additively Manufactured Al 6061
- Despite the inherent differences in base materials and heat treatments, the welds of Al 6061-T6 and UAM 6061-H18 were similar in appearance. Fracture patterns within the nugget zone were also nearly identical. This suggests established friction stir welding parameters for Al 6061 can be generalized to use with UAM Al 6061 material.
- Friction Stir Welding improved the ultimate tensile strength of the UAM material by an average of 9% in the transverse direction and 50% in the longitudinal direction.
- Friction Stir Welding significantly enhances the material properties of the UAM material by stirring the stacked tape layers, eliminating gaps between adjacent tape layers, and

reducing the grain size which led to a significant increase in strength.

Chapter V

WELDABILITY OF AN IRON METEORITE BY FRICTION STIR SPOT WELDING: A CONTRIBUTION TO IN-SPACE MANUFACTURING

As published in Acta Astronautica November, 2017.

Authors

William Todd Evans, Kelsay E. Neely, Alvin M. Strauss, George E. Cook

Abstract

Friction Stir Welding has been proposed as an efficient and appropriate method for in space welding. It has the potential to serve as a viable option for assembling large scale space structures. These large structures will require the use of natural in space materials such as those available from iron meteorites. Impurities present in most iron meteorites limit its ability to be welded by other space welding techniques such as electron beam laser welding. This study investigates the ability to weld pieces of in situ Campo del Cielo meteorites by Friction Stir Spot Welding. Due to the rarity of the material, low carbon steel was used as a model material to determine welding parameters. Welded samples of low carbon steel, invar, and Campo del Cielo meteorite were compared and found to behave in similar ways. This study shows that meteorites can be Friction Stir

Spot Welded and that they exhibit properties analogous to that of FSSW low carbon steel welds. Thus, iron meteorites can be regarded as another viable option for in-space or Martian construction.

Introduction

The interest in space exploration has grown significantly in the past decade as private companies have entered the space market and government agencies such as NASA are seeking ways to make longer voyages which require more in space support. The reduced cost of reaching space and planetary travel makes this frontier more accessible and appealing, but one major challenge is the cost of sending materials into orbit for use in construction for human habitation or shelter.

In-space resources represent a potential solution to this issue as metals such as iron have been found in lunar regolith, in meteorites on Mars, and in asteroids.(G. A. Landis 2007)(Greicius 2015)(G. Landis 2009) Other commercial endeavors such as Deep Space Industries and Planetary Resources are both planning asteroid mining missions that involve sending prospecting technology to nearby asteroids to procure raw materials.(DeepSpaceIndustries) (PlanetaryResources) Additionally, NASA's Pysche mission will be launching in 2023 to gather and analyze compositional data of the 16 Psyche asteroid, which is

hypothesized to be primarily metallic iron and nickel similar to the composition of iron meteorites. It has a diameter of 210 kilometers and is located in the main asteroid belt. It would therefore be an excellent source of large amounts of raw materials.(Northon 2017)

It seems that space has an abundance of raw material, but issues of collection and processing will potentially limit the use of these resources. Many Earth-based methods to refine iron ore such as carbon reduction are impractical for use in space.(G. A. Landis 2007) There have been promising suggestions of using refined meteoric material on Mars for construction in situ and more methods will likely be developed.(G. Landis 2009) However, if the raw meteorite material could be used for construction it would greatly reduce the time, expense, and effort needed for in space construction.

Based on meteorite studies, the composition of iron meteorites is mostly iron and nickel, but there are also inclusions of other materials such as phosphorous and sulfur. These inclusions make the material inhomogeneous and will be difficult to weld with traditional welding techniques. One attempt was made to weld an iron meteorite by electron beam welding, but the fast cooling of the molten iron in the presence of phosphorous, sulfur and carbon created extensive cracking in the welds. The conclusion was that "innovative welding approaches will be required to create sound welds in meteorites…"(Elmer et al.

2014) Friction Stir Welding and Friction Stir Spot Welding (FSSW) are viable, off the shelf alternatives to other welding technologies that appear to be ideal candidates for use in joining iron meteorites.

Friction Stir Welding and Friction Stir Spot Welding are solid state joining processes that use a rotating, cylindrical tool to plasticize and stir the material to form a joint. Representations of the process can be seen below in Figure 5.1. Both processes have similar characteristics and avoid many common issues in traditional welding like porosity, embrittlement and cracking due to the fact the materials being joined are kept below their melting temperature. They also do not need any shielding gases or filler materials.(Gibson et al. 2014) These factors make them an ideal candidate for the welding of meteorites since the inclusions found in the meteorites will not significantly affect the process. In addition, it is not necessary to know the composition of each iron meteorite, as the FSW processes would work with any iron meteorite composition without having to adjust the welding parameters.

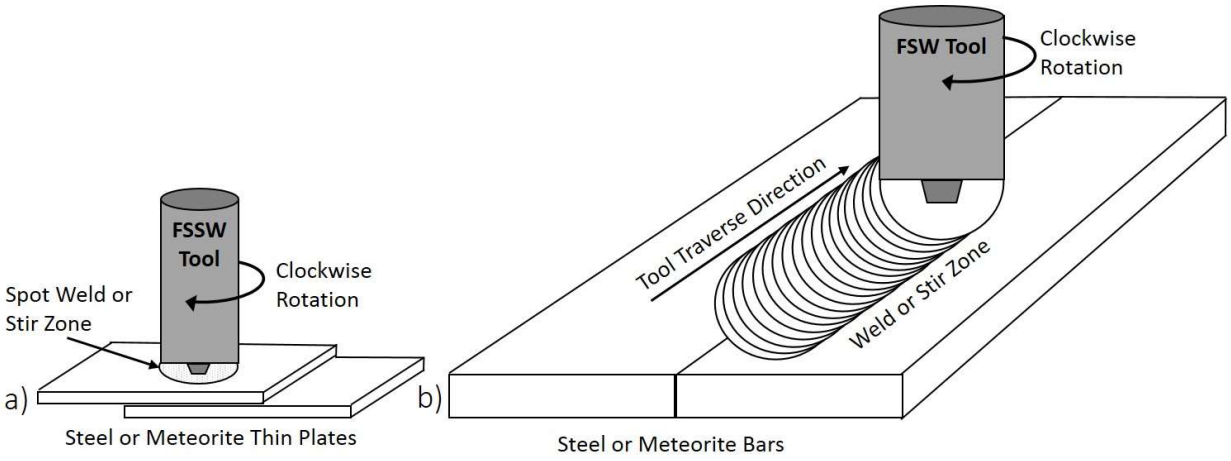

Figure 5.1- a) Friction Stir Spot Welding process(FSSW) which creates a single point spot weld. b) Friction Stir Welding (FSW) which creates a linear weld line.

Since FSSW and FSW are closely related processes, successful joints using one process on a particular material indicate a high probability of success using the other one. FSSW is performed on a lap joint with a single spot weld, while the FSW process can be utilized in numerous configurations such as butt, lap and T joints. The FSW process is performed on a linear weld line and therefore requires more raw material, more expensive tool materials, and higher forces to create the weld. By contrast, the FSSW weld is only needs a small amount of material and more common tool materials can be used. Therefore, FSSW was chosen as the process for this initial research. This research is designed to illustrate the ability to successfully join meteoritic material using FSSW.

Materials and methods

Materials

Iron meteorites are unique materials with nothing exactly like them found on earth and no way to artificially recreate them. Each iron meteorite is different in composition and structure with different distributions of trace particles, but iron meteorites are usually overall about 93% iron and 7% nickel with variations in their chemical compositions in their kamacite layer (similar to alpha phase iron) and their taenite layer (similar to gamma phase iron). Kamacite layers are defined as regions of iron with nickel percentages less than 7.5% and taenite layers contain over 25% nickel.(Buchwald 1975)

Large iron meteorites tend to be rare and are expensive. Given the cost of material and the desire to be able to compare the meteorite welds to more common materials, the testing and analysis was first performed on low carbon steel sheets and then invar which represent the two distinct layers of the meteorite. Standard rolled samples of 1 mm, general purpose low carbon steel that meet ASTM A653 standards were obtained with a yield strength of 40,000 psi and Rockwell hardness of B55. Sheets were specified as CS Type B which indicate a carbon content of .02-.15%. Invar sheet with 35% nickel was also obtained of 1 mm thickness that meets ASTM F1684

standards with a yield strength of 40,000 psi and Rockwell B90 hardness.

The two meteorites shown in Figure 5.2 were obtained were from the Campo del Cielo fall in Argentina. They are considered a Group 1, polycrystalline, coarse octahedrite. The average bulk chemical makeup from meteorites from this site contain 6.68% Ni, 0.43% Co, 0.25% P, 87 ppm Ga, 407 ppm Ge, 3.6 ppm Ir with the rest composed of iron.(Buchwald 1975) While the bulk makeup contains these elements, localized regions often contain higher concentrations such as the square and rectangular inclusions known as rhabdite and schreibersite as shown in Figure 5.3. The first meteorite was obtained from the University of Tennessee's Earth and Planetary Science Department, and the second was purchased to provide additional material for initial experimentation.

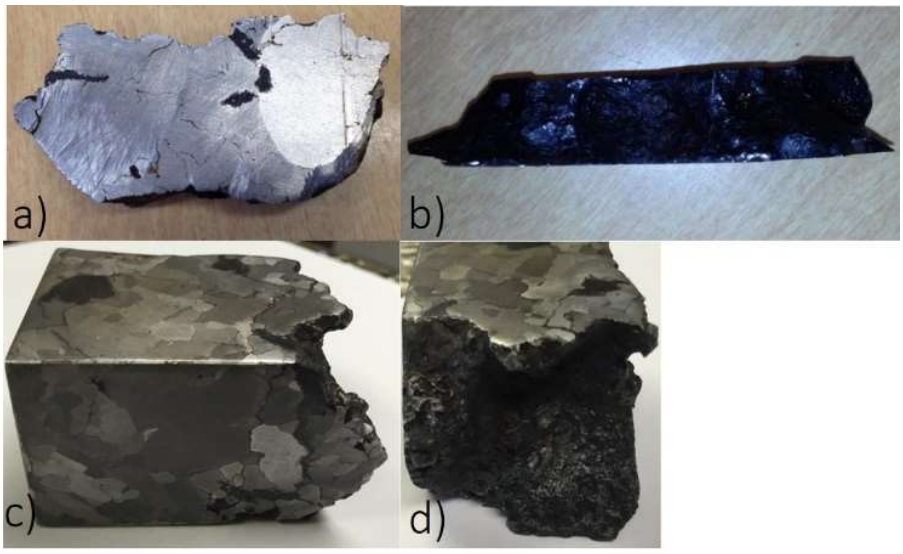

Figure 5.2- As received Campo del Cielo Meteorites. a)first meteorite surface b) fusion crust. c) second meteorite etched view showing kamacite and taenite layers. d) fusion crust

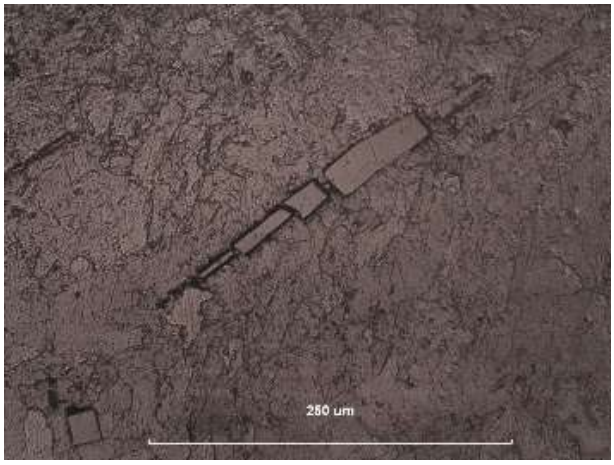

Figure 5.3- Rhabdite and Schreibersite inclusions

EDS analysis of one of the meteorite samples was obtained to compare to published bulk properties. The analysis focused on major compositional elements and other trace elements were excluded and deconvoluted. Analysis and imaging was performed in a Zeiss Merlin SEM, and EDS was performed using the Oxford AZtec software. The accelerating voltage was 20kV and the working distance was 8.5mm. Results can be seen in Figure 5.4

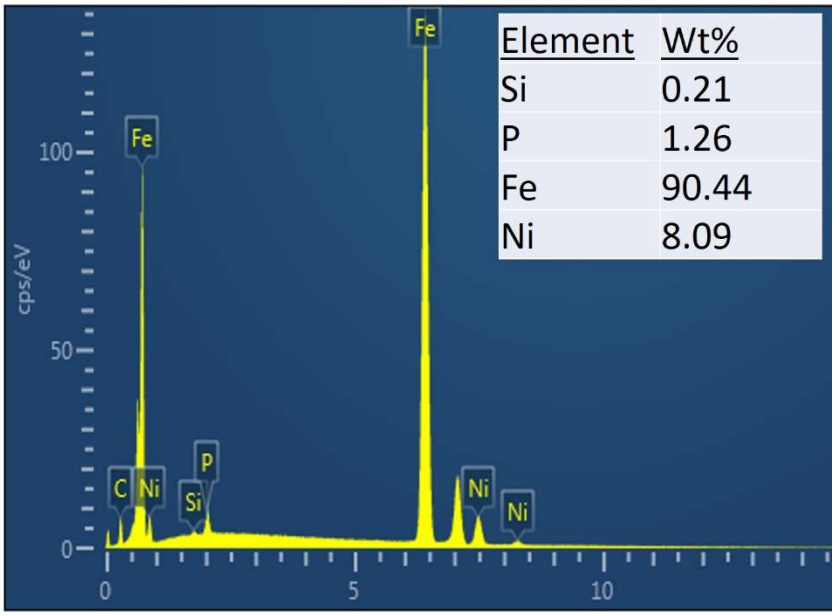

Figure 5.4- EDS Analysis of Campo Del Cielo meteorite sample

Methods

There is little publicly available research on FSSW of low carbon steel or the cutting of thin sections of meteorite. Therefore, tool selection, sample preparation, and welding parameters all had to be determined and represented a large portion of this investigation.

Tool Selection

The FSW and FSSW of steel requires special tools to withstand the heat and wear that occurs on a material as hard as steel. Most tools used for the FSW of steel use expensive materials such as Polycrystalline Cubic Boron Nitride (PCBN) since it must be strong enough to stir the steel and, ductile enough to withstand shear forces

while traversing the weld. FSSW is performed as a spot weld, so a cheaper alternative material such as tungsten carbide (WC) was chosen for the FSSW tool.

Initial tool selection, as shown in Figure 5.5a, was based on a large flat probe/shoulder design of 12.7 mm. similar to that reported by Baek.(Baek et al. 2010) This design needed over 12 kN force to weld which is near the safety limits allowable on our welding machine as pictured in Figure 5.6. Two alternative designs were chosen to allow more penetration into the bottom sheet while reducing the z-force. The second tool with a 2.38 mm WC probe and 12.7 shoulder produced a successful weld, but the probe quickly fractured, leaving a similar design to the first tool. The third tool, as shown in Figure 5c, was also made of WC with a 12.7 mm shoulder and tapered probe. The probe's base was 6.35 mm with a 20 degree taper and an overall probe depth of 1.2 mm. This tool created suitable welds only requiring 8 kN of z force. All data reported in this paper was from the use of this tool. All three tools can be seen below in Figure 5.5.

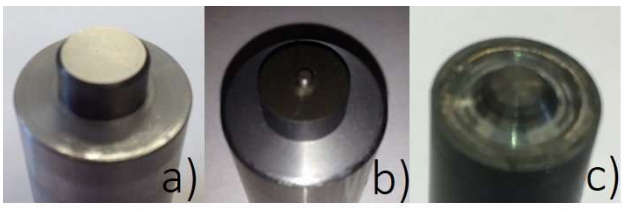

Figure 5.5- Tools used for FSSW

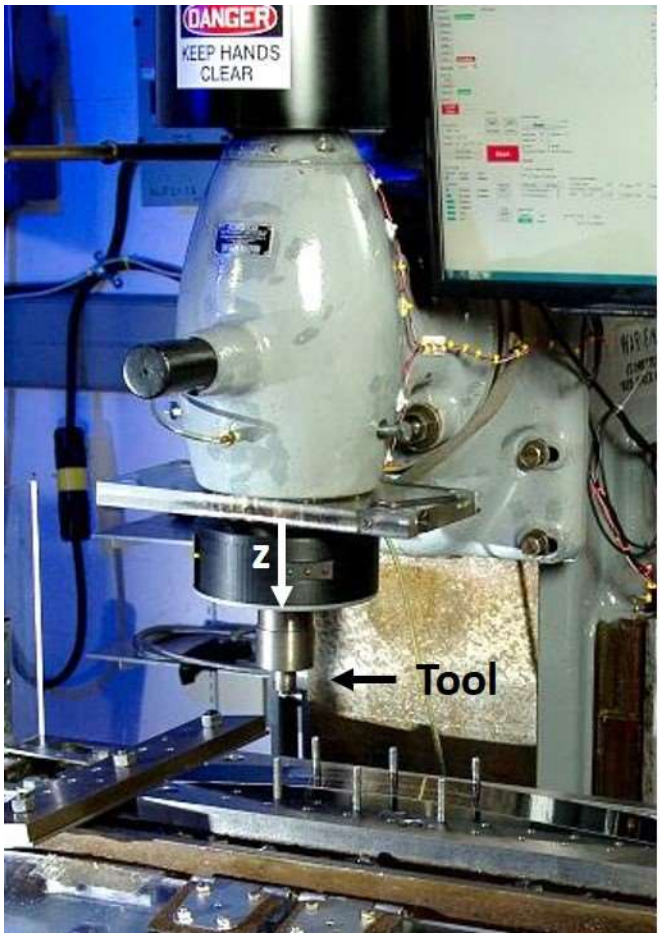

Figure 5.6- Friction Stir Spot Welding Machine

Meteorite Cutting

Due to the expense of the meteorite material, attempts were made to cut the meteorite that would prevent the loss of material and eliminate heat treatment during the cutting process. The use of water jet cutting was explored but the operator was concerned due to the thinness and the small overall size. The thin sheets could lead to curling or further cracking and there was a concern of losing the cut sheet as it was removed from the larger parent piece. The first

attempt to cut the meteorite and minimize material loss was the use of Electrical Discharge Machining(EDM). The fusion crust of the meteorite frequently broke the wire and made cutting very expensive and time consuming. The first cut took nearly eight hours to EDM cut. To eliminate this issue, the meteorite was squared down to a smaller size that removed the outer fusion crust. Removing of the fusion crust allowed for better and faster EDM cutting, but the inclusions in the meteorite still created issues with the EDM process and broke the wire often, leading to longer processing time and expenses.

Next, traditional meteorite cutting methods were employed by using a wafer, diamond embedded cut-off wheel. The wafer blade reduced the amount of material that would be lost in the cut area, but proved to also take a very long time to cut with a constant need to dress the blade. It would only be feasible for small samples.

Finally, it was determined that the tradeoff between expense of material and expense of cutting necessitated a faster cutting method even if material was lost in the process. Therefore, it was decided to use an abrasive cutoff wheel to make rough cuts to create thin sections of material close to the final dimensions and then use a surface plane grinder to achieve the final desired dimension of 1 mm thick. The cutting and grinding were done in an oil bath to keep the meteorite cool and in its native microstructural state. It should be

noted that the cracks that are present in the samples are from the parent material. Cracks often occur in meteorites and many theories have been proposed to explain their origin such as shock waves from impact with earth or other meteorites.(Sharp and Decarli 2006) Representative specimens of prepared meteorite sheets can be seen in Figure 5.7.

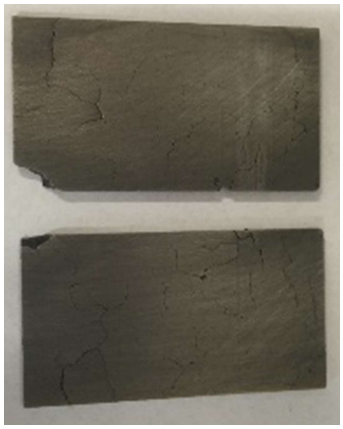

Figure 5.7- Meteorite samples cut by EDM for welding

FSSW Welding Parameter Optimization

The sheets of low carbon steel and invar are commercially available in the desired thickness and were cut into 6.35 cm by 3.8 mm coupon samples. The low carbon steel coupons were then secured to an anvil and FSSW was performed on them while varying key parameters. As shown in Table 5.1, rotation rate, plunge speed and dwell time were varied with the low carbon steel samples. Low carbon steel welds were then tensile tested to determine suitable welding

parameters that could be applied to the invar and the meteorite. Invar and meteorite FSSW welds were made at these chosen parameters.

Table 5.1- Parameters used to determine suitable welding conditions- 24 total combinations.

RPM	Plunge Rate (mm/min)	Dwell time (s)	Plunge Depth (mm)
1400	5	0.5, 1, 1.5, 2	1.27
1400	10	0.5, 1, 1.5, 2	1.27
1600	5	0.5, 1, 1.5, 2	1.27
1600	10	0.5, 1, 1.5, 2	1.27
1800	.5	0.5, 1, 1.5, 2	1.27
1800	10	0.5, 1, 1.5, 2	1.27

Testing

The low carbon steel samples were tested by traditional ASTM lap-shear tensile testing methods. The meteorite welds could not be tensile tested due to the existence of cracks throughout the material which may be a consequence of aerodynamic heating or impact with the Earth. Therefore, comparisons were made to the low carbon steel and invar samples based on the bond area, microstructural observation and hardness testing. Welded samples of all 3 materials were then cut with a diamond wire saw, polished and etched for macro and microscopic analysis. Polishing proved to be very difficult for the

meteorite due to the inclusions and large differences in hardness values of its different inclusions. Polishing was done by increasing from 180 grit up to 1,200 grit sand paper followed by fine polishing on a felt pad with jeweler's rouge. Polishing of the low carbon steel and invar were also prepared this way for experimental consistency.

Etching for all samples was performed with a solution of 6% HNO3 continuously brushed on the sample and then rinsed as detailed by HH Nininger.(Nininger 1945) Samples were then examined under a microscope to verify that joining had taken place and to study the microstructure of the material. In addition, Vickers micro hardness tests with a 100 kgf load were performed on the meteorite weld to determine the hardness of the parent material and that of the welded zone.

Results and discussion

FSSW welds were performed on the low carbon steel sheets with the 24 different combinations of parameters and then tensile tested. It was found that welds with the parameters of 1600 RPM, 5 mm/min plunge rate, and 1.5 s dwell time showed the greatest average peak tensile strength of 8,714 N which was over 1,200 N more than any other combination of parameters. The strength of the weld was a combination of two factors. First, diffusion bonding occurred on the

outer ring of the spot weld equal to the width of the shoulder. The second and larger contribution came from the center of the weld zone where the tool probe penetrated the second sheet and created a stirred zone of welded material from both sheets. As the goal was to produce a quality weld, these parameters were chosen as satisfactory and used on all welds of the meteorite and invar as well as additional low carbon steel samples for comparison. More measurements could be made to determine the optimum strength of the weld along with other parameters or tool designs, but that was beyond the objectives of this investigation.

As noted earlier, stress cracks from impact with the earth or aerodynamic heating were present in the welded samples. It was found that in some cases these cracks were further amplified by the force of the FSSW process as shown in Figure 5.8. However, 4 successful meteorite welds were completed.

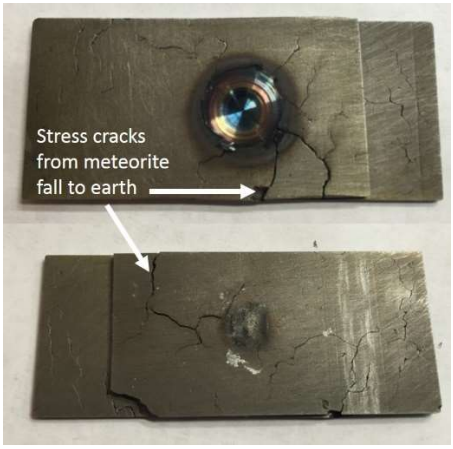

Figure 5.8- Cracks initially from earth impact, amplified by FSSW

Cracks in the meteoric material will limit the application of the FSSW process on terrestrial samples. The specimens in this research where performed on small sheets with a single weld, but larger sheets could be tacked together using FSSW in a manner similar to traditional spot welding techniques. It is also likely that the asteroid material will have fewer and smaller cracks and this should not be a major issue for in situ applications.

Due to the cracking present, only one weld was evaluated by tensile testing. As predicted, the parent material containing the cracks fractured before the weld as shown in Figure 5.9. The sample withstood a tensile load of 1,200 N. This is well below the threshold of the low carbon steel samples which had an ultimate tensile strength of 8,714. While it is difficult to provide much analysis based on this result, it is apparent that the weld is stronger than the parent material.

Figure 5.9- FSSW weld region intact with failure in the parent meteorite material

To provide further insight into the weld characteristics, welds of all three materials were cut, polished, and etched as shown in Figures 5.10 and 5.11. It can be seen that they exhibit the typical structures of FSSW welds with refined grains in the stir zone (SZ) and thermo mechanically affected zone(TMAZ). A small hooking feature can be seen in the low carbon sample on the bottom sheet in the TMAZ from the force of the penetration and stirring of the tool in the bottom sheet. The feature is still evident in the invar sample, but is much less pronounced. The meteorite sample shows a small bulge in the same area that appears to be in between the effects of the low carbon steel and the invar. The hooking feature is a known artifact of the FSSW process that reduces the overall joint strength, but current research has not found a way to eliminate this in pin-based FSSW tools.

All three samples show a successful bond in the stir zone between the two sheets predominantly on the inner edge where the sheets meet next to the tool. The area of stirring quickly falls off as it reaches the TMAZ zone as can be clearly seen in the meteorite in Figure 5.7c. In this weld the bands of individual kamacite and taenite layers are well mixed and refined in the stir zone, but still show partially stirred, recognizable bands of the layers in the TMAZ.

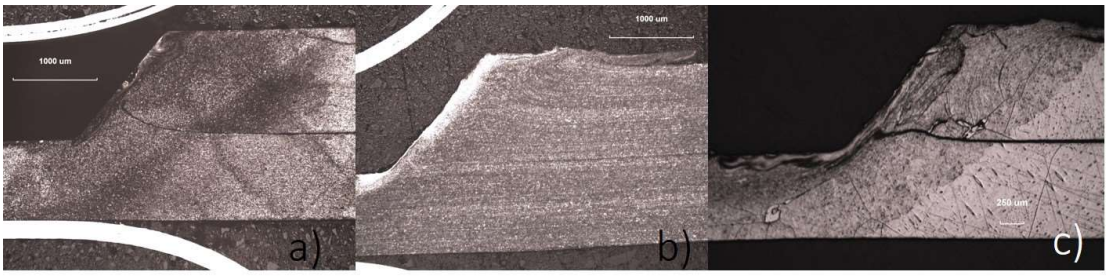

Figure 5.10- Etched FSSW weld samples 5x a) low carbon steel. b) invar. c) meteorite

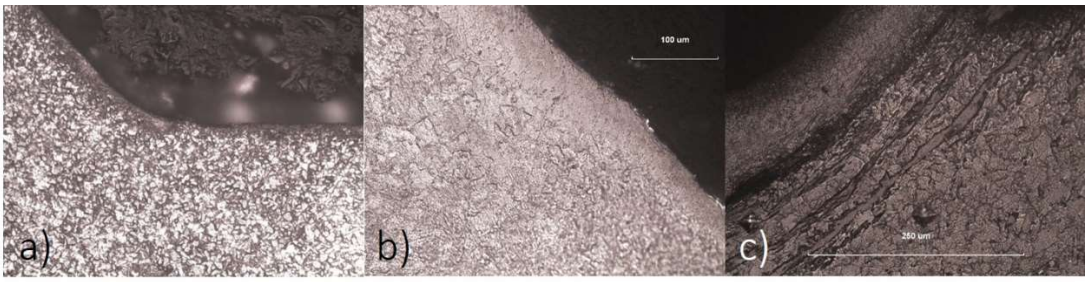

Figure 5.11- Etched FSSW weld samples 50x- a) low carbon steel. b) invar. c) meteorite

Additional imaging with the SEM shows further evidence of stirring and homogeniziation within the weld zone. Figure 5.12 shows two images at the same magnification. The image on the left is a typical size feature of schreibersite as seen throughout the parent meteorite material. The red elemental mapping shows the large presence of iron while the greenish area is a mixture of Ni and P. The figure on the right was taken from within the weld zone. This area, while still mostly homogenous, shows two clear regions of schreibersite. These regions are significantly smaller than the schreibersite regions outside of the weld zone. It can also be noted

that there is a greater distributed presence of Ni and P within the weld zone.

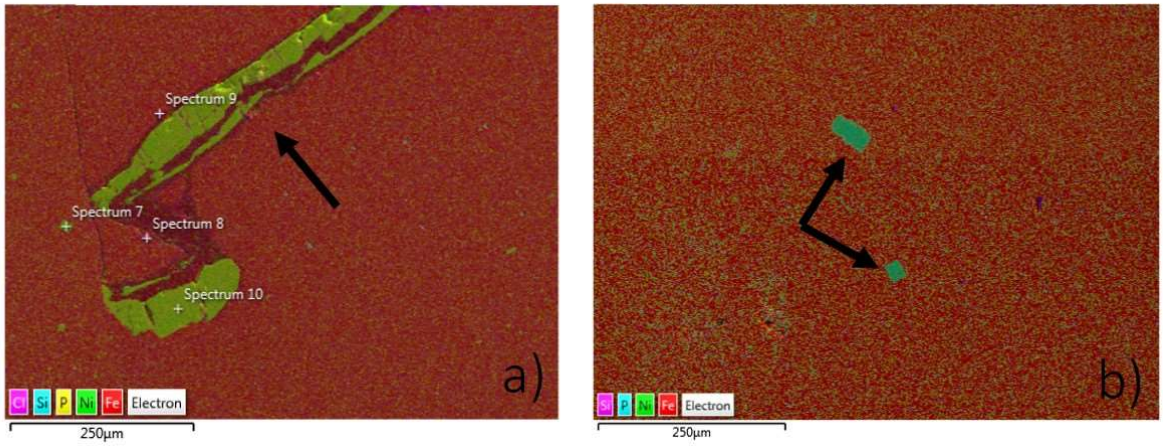

Figure 5.12- a) Parent Meteorite material showing large schriebersite feature. b) Weld zone of meteorite material showing two small schreibersite pieces.

In order to approximate the effects of mixing on the homogeneity of meteorite, the size of schreibersite features were measured in the weld zone and outside the weld zone. The features were measured using ImageJ, and the size results are summarized below in Table 5.2.

Table 5.2- Summary of Schreibersite feature measurements

	Feature 1	**Feature 2**	**Feature 3**
	(outside weld zone)	(inside weld zone)	(inside weld zone)
D1 (µm)	170	53	20
D2 (µm)	55	25	24
Area (µm2)	9066	1216	480

The area was measured by using the polygon trace of the feature, while D1 and D2 are the largest and smallest dimensions respectively. These results show a clear reduction in schreibersite feature size. There is an area reduction of 86% between feature 1 and feature 2, and an area reduction of 95% between features 1 and 3. While there weren't enough distinguishable schreibersite features within the weld zone to do a full statistical analysis, this shows a large reduction in feature size. This indicates that the heat input and physical mixing from FSSW had a large impact on homogeneity.

Both the optical analysis and SEM analysis show that mixing is occuring within the weld zone. This is a positive side effect of the FSSW and FSW process and has actually evolved into its own field known as Friction Stir Processing (FSP). These are promising results for the use of traditional FSW to process large sections of the material while it welds. It could even be applied as an FSP process on the entire top layer of the sample to create a stronger material by breaking up and mixing features and inclusions within the meteorite to create a more uniform material. This will lead stronger bonds and more resilient structures.

In addition to microscopic analysis, hardness values were obtained on the Vickers micro hardness scale with a 100 kgf. Measured values in the parent material ranged from 127-150HV. A

range like this is to be expected as the material is inhomogenous with inclusions, Neuman bands, and different phases of iron/nickel as can be seen in Figure 5.13.

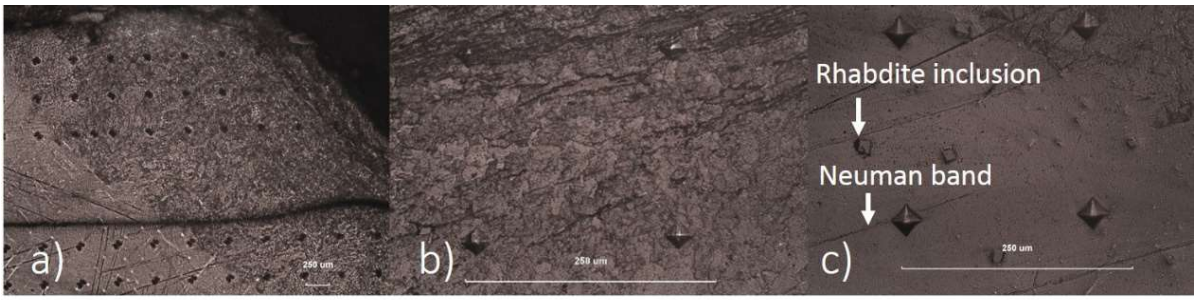

Figure 5.13- Etched meteorite sample with selected hardness indentations shown a) 5x left side of weld. b) 50x under stir zone. c) 50x parent TMAZ transition area

The heat affected and stir zones show increased hardness values ranging from 150-322 as shown in Figure 5.14. The trends matched closely with reported data from low carbon steel FSSW welds by Aota, which showed a range of hardness values from 120-220 in the TMAZ to stir zone(Aota and Ikeuchi 2009) and also those reported for the attempted meteorite weld by Elmer with values 175-408.(Elmer et al. 2014)

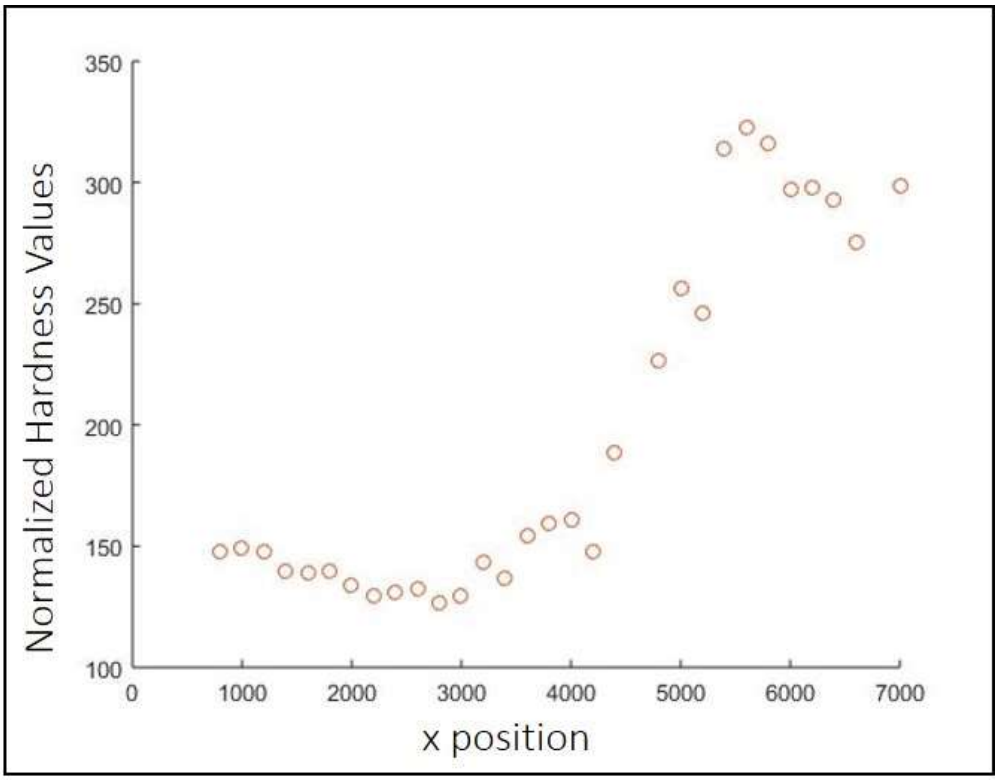

Figure 5.14- Hardness plot of meteorite weld at base of weld (-1200 y position)

Future Applications

The goal of this research was to investigate the ability to join meteorite material to itself with a Friction Stir process. FSSW was primarily chosen because of the reduced forces of the process and the ability to perform welds with a limited amount of material. Initial research into the use of FSSW for the joining of meteoric material has proven successful. FSSW could be used for thin sheet construction of in situ materials as long as there is a limited number of cracks in the asteroid. However, FSW represents a much more feasible process for larger and thicker sectioned material as would be expected in space.

Current processes are able to routinely join up to 20 mm thick steel sheets. Cracking would be less of an issue with FSW as the sheets could be thicker and most cracks would not permeate the full thickness of the material. More research is needed to apply FSW to meteoric material which will require larger samples and larger machines. The cost of obtaining large samples of meteorite might be mitigated by creating a fixture to load multiple smaller machined pieces of meteorite end to end. The success of the FSSW process indicates that the previous limitations of weld hot cracking can be avoided by using FSW processes.

FSW has not been used in space before, but it is a viable option that has the potential to be used in space once the forces can be further reduced. Progress has been made in force reduction with bobbin type tools and it is expected that the technology will continue to develop rapidly as it has become a mainstream technique used in many industries.(Prater 2015) Conceivably, a small portable FSW welder could be deployed with a ship on a venture to a large iron rich asteroid such as 16 Psyche. There, material could be roughly cut from the asteroid in sheets or bars. This material could then be used as is or it could be enhanced with an FSP process. It could then be joined in situ with the FSW welder to create larger structures.

Conclusions

This study focuses on the ability to join meteorite materials by Friction Stir processes. The findings of this study are:

1. Successful FSSW welds of low carbon steel, invar and meteoritic materials were obtained.
2. Comparison of the microstructures and hardness values indicate that meteorite material reacts in a similar way to low carbon steel FSSW welds and findings of other research on welding of low carbon steel can in general be applied to the FSSW of meteorites.
3. There are some differences between the weld properties of low carbon steel and meteorite These include more differentiated layers of the metal phases that were not fully stirred at the interface and the increased hardness range in the stir zone likely due to deposition of inclusions.
4. Based on the success of FSSW welding of the meteorite, it is recommended that further research be continued on the FSW of meteorites. The FSW process should enable the formation of stronger bonds and create better mixing of the material where the meteorite material has been friction stir processed. Most importantly, FSW welds can be tensile tested along the

longitudinal direction to give a better picture of the true strengths attainable from welded asteroids.

5. We have demonstrated that iron meteorites can be a viable and practical resource for in-space and planetary assembly and manufacturing by using Friction Stir processes.

Special thanks to

Kate Lansford, University of Tennessee Space Institute, Tullahoma, TN

Lawrence Taylor, University of Tennessee, Knoxville, TN

John Elmer, Lawrence Livermore National Labs

Tony Wirth, Skyline Manufacturing, Nashville, TN

Chapter VI

FRICTION STIR EXTRUSION: A NEW PROCESS FOR JOINING DISSIMILAR MATERIALS

As published in Manufacturing Letters, 2015.

Authors

William T. Evans, Brian T. Gibson, Jay T. Reynolds, Alvin M. Strauss, George E. Cook

Abstract

The need to join dissimilar materials such as aluminum and steel is prevalent in many industries. This paper investigates a new process called Friction Stir Extrusion(FSE) for joining aluminum and steel. The process uses Friction Stir Welding(FSW) to extrude aluminum into a premade concave groove cut into steel. FSE eliminates the concerns of intermetallic compounds and tool wear. This technique leads to a mechanically bound joint whose strength is determined by the mechanical bond between the steel and the extruded aluminum. Successful joints were created showing the FSE process has the potential for application to any combination of dissimilar materials.

Introduction

In many industries there is a need to join dissimilar materials. Joining modern alloys of aluminum and steel has been a challenge as most current welding methods do not work on these new alloys because of the disparate properties of the materials. Other joining processes such as adhesives, rivets, bolts, etc… have limitations in their use, application and/or strength.

Friction Stir Welding(FSW) has the advantage that the alloys are not melted, but efforts to use it so far have had limited success due to the creation of intermetallic bonds that weaken the weld (Liyanage, et al., 2009),and (Bozzi, et al., 2008) or severe tool wear that makes it cost prohibitive. (Gibson, et al., 2014) A good overview of the challenges associated with traditional FSW and FSSW for dissimilar welding of aluminum and steel can be found in (Haghshenas, et al., 2013). A limited amount of work has been used to extend FSW and FSSW processes to create dissimilar joints using prefabricated geometrical configurations (Evans, et al., submitted), (Nishihara, 2003), (Balakrishnan, et al., 2007) and (Lazarevic, et al., 2013). This contribution presents a new method for joining aluminum and steel by a process called Friction Stir Extrusion (FSE) which is an extension of the FSW technique.

Material and methods

In order to prove the concept, aluminum 6061 plates of 0.25 inch thickness are joined to 0.25 inch thick low carbon steel plates in a lap configuration using the Friction Stir Extrusion process. Prior to welding, a concave groove was cut along the length of a 0.25" steel plate as shown in Figure 6.1. The initial groove design was created by creating two cuts with a 1/32 inch slit saw at two perpendicular 45 degree angles. The middle section of the groove was then removed with a small end mill followed by 11/64 inch diameter end mill cutting to a depth of 0.07 inches. This particular setup proved difficult to reproduce consistently, so additional experiments were performed with an O-ring dovetail groove design. The dovetail groove had a neck diameter of 0.116 inches and a depth of 0.103 inches with an included angle of 48 degrees. A sheet of 6061 of equal length was placed on top of the steel sheet in a (FSW) lap weld configuration.

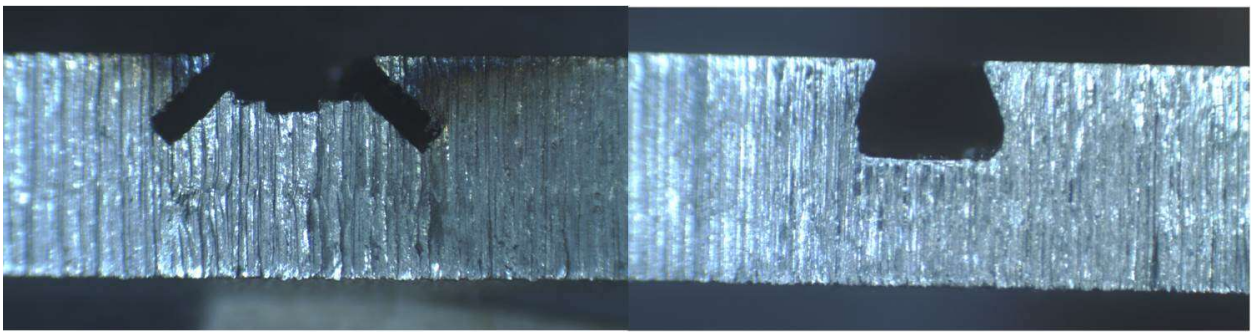

Figure 6.1 Groove patterns cut into base steel layer: slit saw and endmills(left), O-ring dovetail(right)

The tools used for FSE were the same as those used in standard FSW. In this case, tools were chosen with convex, scrolled shoulders and threaded probes to enhance the extruding process as shown in Figure 6.2. Tool A has a 0.25 inch diameter threaded probe of 0.18 inch length and a 7 degree convex shoulder with six scrolls. Tool B also has a 0.25 inch diameter threaded probe of 0.18 inch length, but the convex shoulder has a 12 degree slope and the scrolls are shorter in length.

The FSE is performed in a similar manner to a FSW. The center of the tool is placed 0.1 inches below the center of the groove on the advancing side of the weld. This location was chosen to prevent the probe from acting as a plug that would prevent the extrusion of material into the groove as was found to be the case in some FSSW welds performed by Lazarevic. (Lazarevic, et al., 2013) The tool is then plunged 0.215 inches into the aluminum and welds at a rate of 3 ipm and 1500 RPM. This ensures that the tool always remains in the aluminum and the majority of the shoulder is engaged in the weld. This mitigates one of the main issues in welding dissimilar materials which is the excessive tool wear caused by the harder material since the tool never touches the harder material. (Gibson, et al., 2014) However, instead of mixing the two lapped materials, the FSE process plasticizes the aluminum and extrudes it into the concave groove. The

scrolled shoulder and threaded pin help in this process by stirring and forcing the material down into the groove. Once the material is extruded into the groove, the materials are fixed to each other due to the concave nature of the groove. The result is a strong, dissimilar joint created from a single pass of the FSW tool.

Results

FSE with tool A created a joint that appeared very smooth with an even surface and a small amount of flash on the edges of the weld. The surface finish looked the same as a traditional FSW. The aluminum was fully extruded into the groove and a joint between the two materials was created without any visible volumetric flaws.

Tool B was then used to perform the weld at the same parameters of 3 ipm and 1500 RPM. With tool B, the aluminum was partially extruded into the groove, but the process left a large void along the length of the weld. The weld was repeated at different traverse rates, plunge depths, RPM rates, while also adjusting the center line of the tool in relation to the center of the groove with similar results. The void was finally eliminated by placing the center of the probe 0.15 inches below the center of the weld on the advancing side, but the aluminum did not fully extrude into the bottom edges of the groove and the tool removed significantly more material from the

advancing side creating a large amount of flash on the advancing side as seen in Figure 6.2.

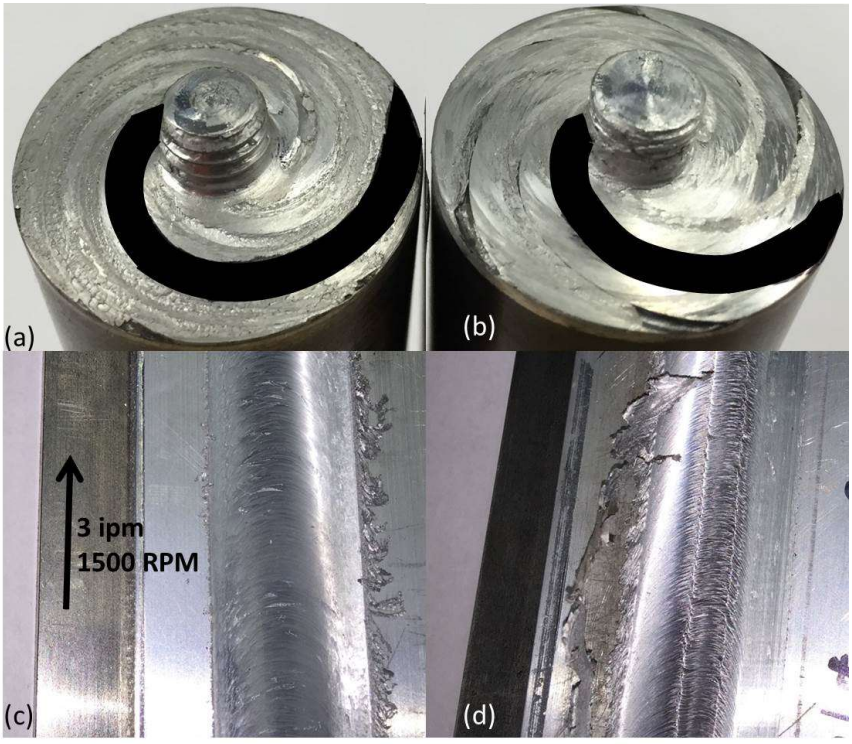

Figure 6.2 (a) Tool A with threaded probe and scroll pattern highlighted, (b) Tool B with threaded probe and scroll pattern highlighted, (c) Surface of Tool A, (d) Surface of Tool B

The welds made by tool A were cut into 1/2 inch wide samples for macrographic examination and tension-shear testing with a tensile tester as seen in Figure 6.4. The slit saw grooved joint had an average ultimate tensile shear load of 608 kgf for the three ½" samples tested. Failure of the joint occurred in the section of the joint on the side in tension(B) at about a 45 degree angle to the surface of the steel. The O-ring dovetail groove had an average ultimate tensile

load of 488 kgf for the three ½" samples tested. Failure of the joint occurred across the neck of the groove parallel to the surface of the steel.

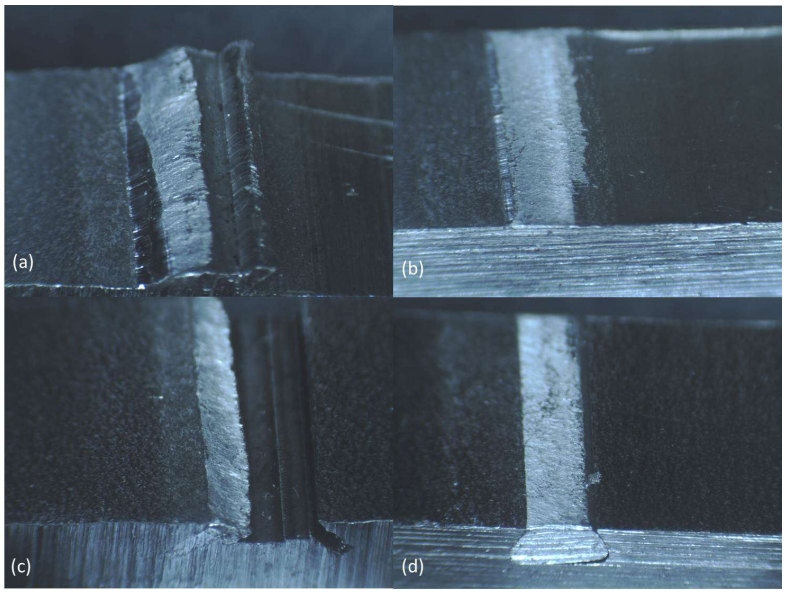

Figure 6.3 (a),(c) Fracture pattern of slit saw groove (b), (d) Fracture pattern of O-ring dovetail groove

Figure 6.4 Experimental results of FSE for two groove types

Discussion

FSE created strong joints between the aluminum and steel and offers a new way of joining dissimilar materials. The two tools tested were very similar in design, but the resulting joints differed greatly in their surface appearance and in the amount of extrusion. The larger shoulder angle of tool B necessitated making a deeper plunge to fully engage the shoulder which placed the probe closer to the surface of the groove. It is likely that this inhibited the flow of aluminum into the groove. As the probe was moved further away from the groove, it allowed the space for the aluminum to extrude, but also moved the most active part of the stir zone further from the groove, thus leading to only partial extrusion into the groove. Additional experimentation will be needed to determine the optimum tool for industrial applications, but tool A seems to be an excellent starting point.

The major contribution of strength of the FSE joint comes from the cross section of aluminum that is extruded into the groove. The two types of grooves in this experiment had different geometries, but the cross section of the fractured area was very similar. The higher ultimate tensile strength of the slit saw cut can be attributed to the extra contribution from the opposed slit saw groove that acted as an anchor on the back side of the joint (Figure 6.4, point A). The slit on the back side of the joint kept the larger neck diameter in line with the

shear force of the tester until it pulled out and the resulting failure happened on a section of lesser width than the neck. Other groove shapes such as slit saw cuts without the use of an endmill in the middle, circular shaped grooves, or other geometries will likely improve joint strength. Also, a cutter that would allow for a larger radius on the top surface of the steel would be preferred as it would reduce the stress concentration of the sharp angle present at the neck.

Conclusions

FSE provides an effective way to join dissimilar materials such as aluminum and steel. It eliminates the need for costly tools and tool replacement since traditional FSW tools used for welding aluminum can be used in the FSE process and the tool never touches the steel plate. Initial experimentation showed a large difference in the quality of the joint based on tool selection. Tool A performed very well, but would likely need to be optimized for the intended application. FSE also creates a strong mechanically bound joint that eliminates many of the concerns of intermetallic bonding that occur in traditional FSW of aluminum and steel. Since the process creates a mechanical joint, it could potentially be extended to other materials from plastics to super alloys.

Chapter VII

JOINING AEROSPACE ALUMINUM 2024-T4 TO TITANIUM BY FRICTION STIR EXTRUSION

As published in Friction Stir Welding and Processing IV, 2017.

Authors

William Todd Evans, George E. Cook, Alvin M. Strauss

Abstract

The welding of titanium and aluminum is difficult due to differences in their material properties and the formation of intermetallic compounds(IMCs) which can weaken the weld. A new process, Friction Stir Extrusion (FSE), has been used to join dissimilar materials by using Friction Stir Processing to extrude a top sheet of material into a pre-made, concave groove in the bottom sheet of material. FSE has been used to create a strong, mechanically interlocking joint between aluminum 6061 and steel that eliminates IMCs. However, FSE hasn't been applied to any other material combinations. This current research applies the FSE process to join aluminum 2024-T4 to commercially pure titanium. The process was optimized by adjusting the RPM, traverse rate, and groove geometry. The Al-Ti joints are evaluated based on shear strength and ultimate

tensile strength. The groove geometry proved to be the most important parameter as different geometries can enhance the strength by mechanical means and by optimizing the volume and shape of the material extruded. Successful joints were created by the FSE process and can be used as a viable alternative for joining aluminum to titanium.

Introduction

High strength aluminum alloys are used extensively in the aerospace, automotive and ship building industries due to their strong mechanical properties and low weight compared to other materials such as steel. Titanium also has a high strength to weight ratio in addition to corrosion resistance which makes it another widely used material in these fields. With the increasing use of these materials, there is a need to find more effective and innovative ways of joining these two dissimilar materials.

The welding of titanium and aluminum is difficult due to differences in their material properties and the formation of intermetallic compounds(IMCs) which can weaken the weld. Numerous joining techniques have been proposed such as diffusion bonding(Jiangwei, Yajiang, and Tao 2002)(Miyagawa et al. 2009)(Wilden and Bergmann 2004), laser welding(Anawa, Olabi, and

Elshukri 2009), friction welding(Fuji 2002)(Fuji, Ameyama, and North 1995), friction stir welding(Chen and Nakata 2009)(Aonuma and Nakata 2011), and ultrasonic welding(Zhang, Robson, and Prangnell 2016) to name a few. Each of these methods provides a way to join aluminum and titanium and can be used for different geometries and material thicknesses. Previous research introduced a new technique called Friction Stir Extrusion(Evans et al. 2015) that showed a new way to join aluminum 6061 to steel. This process relies on the Friction Stir Welding (FSW) process to extrude material into a preformed concave groove. The process eliminates the issues of IMCs by creating a mechanical joint of dissimilar materials. The formation of intermetallic compounds has limited the strength of most aluminum to titanium friction stir welds and therefore is a prime candidate to test the feasibility of an aluminum/titanium joint formed by FSE. This research seeks to prove the ability to use the fundamentals of the FSE process to join aluminum 2024-T4 to commercially pure titanium.

Materials and Methods

The materials used in this research are commercially available 2024-T4 Aluminum and Grade 2, 99% pure titanium bars. The 2024 material was rated at 324 Mpa yield strength and the titanium was 275 Mpa. The bars of each material were cut into 155 mm by 52 mm by

6.35 mm thick sections. The titanium bar was prepared for Friction Stir Extrusion(FSE) by creating a concave groove 15 mm from the edge of the material. The initial size of the groove was chosen based on the previous research in FSE of 6061 to steel and was an o-ring groove of 3 mm depth, 48 degree included angle and a neck diameter of 3 mm. As will be discussed later, this groove setup did not create successful FSE joints and additional groove geometries were implemented.

The 2024-T4 aluminum was positioned in a lap joint configuration over the titanium with 35 mm of overlap. This positioning kept the entire width of the FSW tool on the titanium and allowed enough overhang for tensile shear testing. The tool was chosen to maximize the flow of material. The tool was made of 25.4 mm O1 hardened tool steel with a 7 degree convex shoulder with six scrolls and a 6.35 mm diameter threaded probe of 4.6 mm length. The setup can be seen in Figure 7.1.

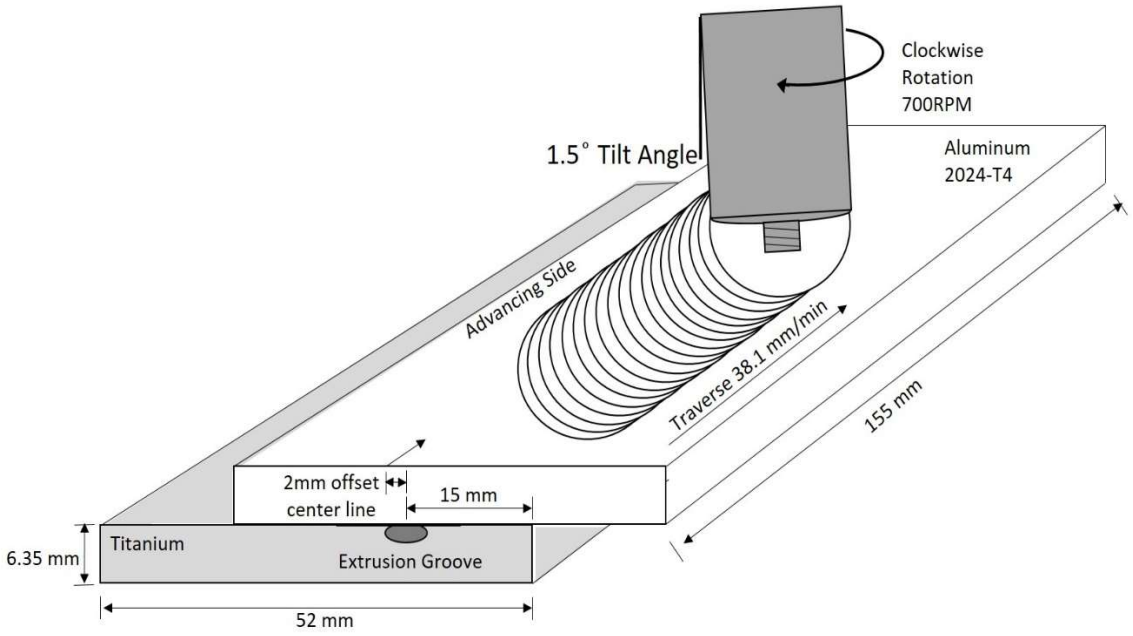

Figure 7.1 Friction Stir Extrusion setup for joining aluminum to titanium

FSE is, essentially, a bead on plate FSW that extrudes the material into the groove. Therefore, similar FSW welding parameters from successful 2024-T4 welds were chosen. The best tensile properties obtained by Mohammed of FSW welded 2024-T4 were found at an RPM of 710 RPM and 20 mm/min traverse rate.(Kassim Mohammed 2011) This was used as an initial starting point and FSE joints were performed at 500, 700, and 900 RPM with traverse rates of 38, 50.8, 76.2, and 101.6 mm/min. The tool was positioned at both a 0 and 1.5 degree tilt angle. The tool was plunged 5.3 mm into the aluminum to allow maximum engagement of the tool shoulder. This

also kept the probe just above the aluminum titanium interface to prevent tool wear by only engaging the 2024 with the probe. The tool was offset from the center of the groove by 2mm to the advancing side. This both prevents the probe from inhibiting the flow of aluminum into the groove, as was noted in FSSW welds by Lazaveric(Lazarevic et al. 2013) and maximizes material flow into the groove.

Results and Discussion

Groove Shapes

Figure 7.2 shows the surface features of the FSE joint with a full o-ring groove as was presented in the previous research on FSE joining of 6061 to steel.(Evans et al. 2015) While the process was successful with the 6061 and a smooth, classic onion ring pattern was formed, this extruded volume proved to be too large to allow proper consolidation of the 2024. The extra volume of aluminum extruded into the groove left extra space in the weld zone. Some material from the advancing side was extruded down into the groove and additional material flowed behind the pin in rough chips/clumps. Since there was less material behind the tool, this material accumulated at the bottom of the nugget zone at a level below the back edge of the tool. The tool shoulder could not fully engage the aluminum in the nugget area and

therefore could not stir and consolidate the aluminum into a smooth surface as evidenced in Fig. 7.2b and c. This convex tool was designed to operate at a 0 degree tilt angle to compensate for any thermal expansion or uneven surface features. To improve the performance of the tool, the tilt angle was changed to 1.5 degree lead angle. This improved the ability to consolidate the material since the back edge of the shoulder was engaged deeper in the material, but it still could not overcome the volumetric void issue.

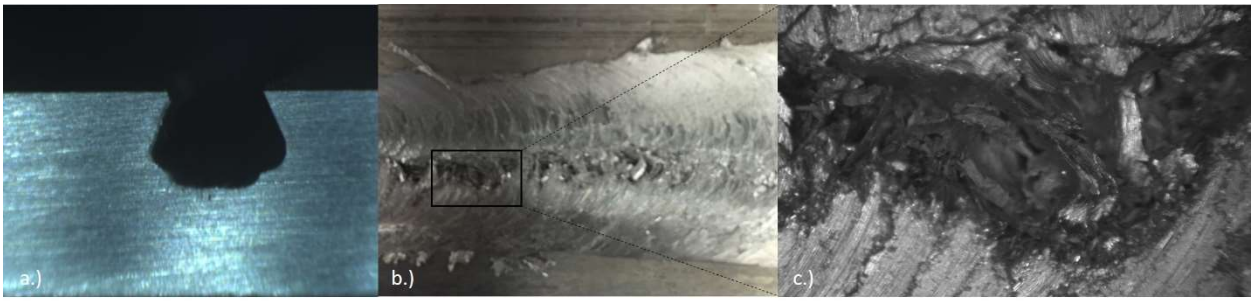

Figure 7.2 O-ring groove results
a.) Full O-ring groove shape. b.) Surface finish of FSE joint with non consolidated material. c.) Magnified image of voids showing chunks of aluminum that have not been consolidated by the shoulder.

To address this problem, 3 new groove shapes that required less volume were created, as pictured in Figure 7.3. For the first groove, a slit saw was used to create two opposing slits, 2 mm deep at 45 degree angle to the surface. This left behind a triangular wedge of titanium to help direct the extruded aluminum into both slits. The second groove shape created a modified dovetail by widening the cross-sectional area at the surface of the slot to 3 mm and milling out

the triangular wedge of material. This groove left a small section of the slit intact while allowing for more material to flow into the groove. The third adjusted groove shape was created by raising the o-ring cutter depth from 3 mm to 2 mm. This reduced the volume of the full o-ring cut by about 30% but still allowed a slightly concave region in the groove to hold the 2024. These changes allowed for successful FSE joints with a good surface finish to be achieved.

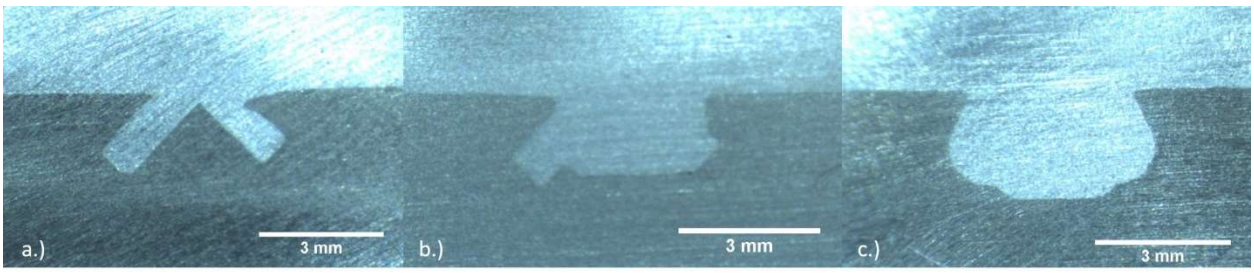

Figure 7.3 Friction Stir Extrusion Groove Shapes
a.) Slit saw groove. b.) Modified slit saw groove. c.) Modified o-ring groove.

RPM and Traverse

Figures 7.4, 7.5, and 7.6 show the effects of RPM and traverse rate on the surface of the joints. Fig. 7.5 shows the full depth of the top plate of aluminum with the surface shape of the joint and the extruded region. Successful joints were formed at both 500 and 700 RPM at 50.8 mm/min. However, the surface of the joint was more evenly distributed across the width of the weld and better consolidated at 700 RPM as can be seen in Fig. 7.6 represented by the solid orange

line with square markers. At 900 RPM and 50.8 mm/min visible voids/worm holes were formed in the weld as noted on Fig. 7.4 and 7.6. At 900 RPM the tool creates coarser onion rings and deposits more of the aluminum on the retreating side. This deposit of material on the retreating side does not leave enough material to be fully consolidated back into the FSE joint in the nugget region on the advancing side which leads to void formation.

Figure 7.4 Surface Finish of FSE joints at 50.8 mm/min. a.) 500 RPM. b.) 700 RPM. c.) 900 RPM.

700 RPM was set as successful parameter for consolidated joints and three additional traverse rates were tried to see their impact on the joint. Successful FSE joints were produced at 700 RPM and 38.1 mm/min, 50.8 mm/min, 76.2 mm/min, and 101.6 mm/min. The slower rate of 38.1 mm/min produced a very smooth finish that covered almost the entire width of the joint. At the higher traverse rates, the onion rings were not as consistent and smooth and did not

cover the entire width of the joint as seen in Fig. 7.6 where the right side of the joint has more material built up on it. This shows that the shoulder did not engage as evenly with the material on the advancing and retreating side. These results indicate that as the tool traverses more quickly, there is less time to stir the material and less heat input into the joint for the material to be sufficiently plasticized and stirred evenly across the width of the weld. In addition, the faster traverse rates led to higher axial forces in the x and y directions that started to approach the safety limits of the dynamometer. Given these results 700 RPM and 38.1 mm/min were chosen as parameters that led to the best joints.

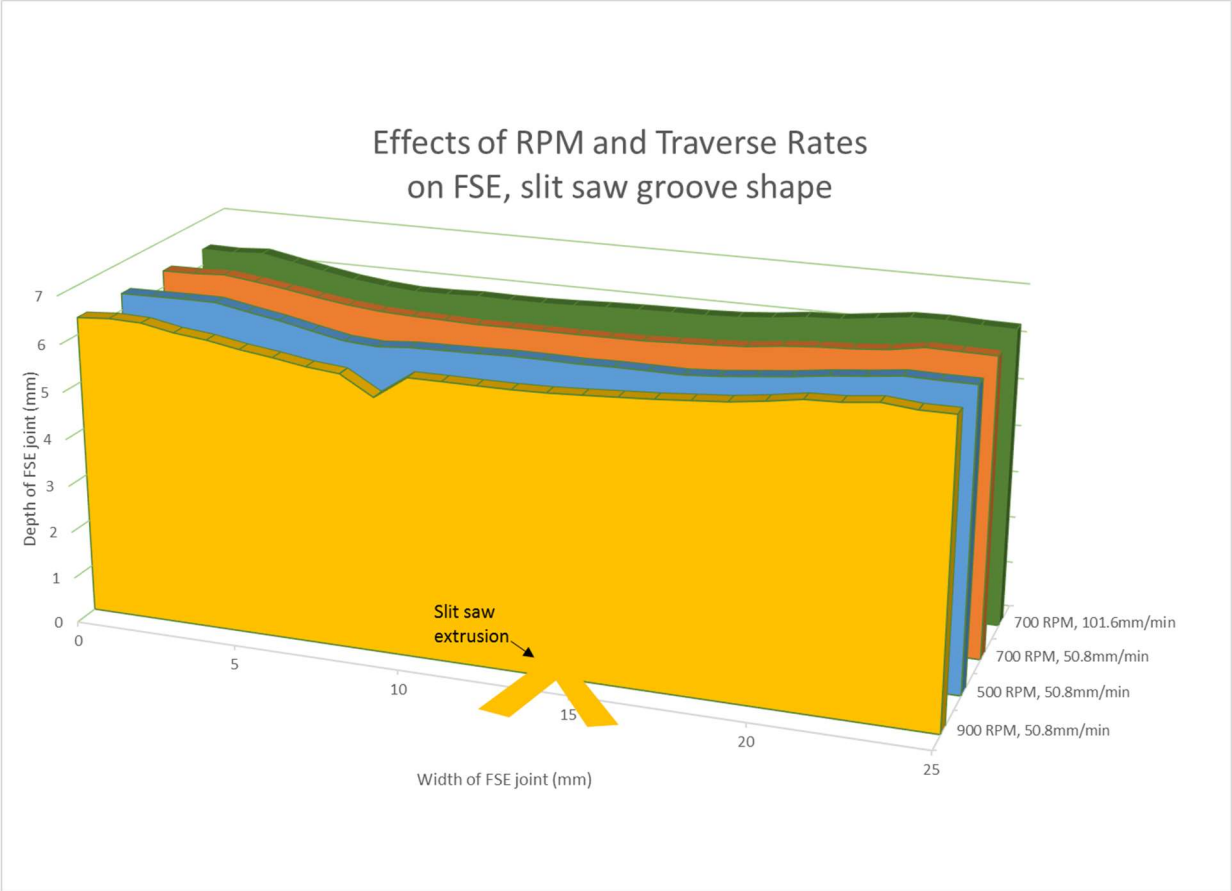

Figure 7.5 Surface finish of FSE joints at different RPMs and traverse rates

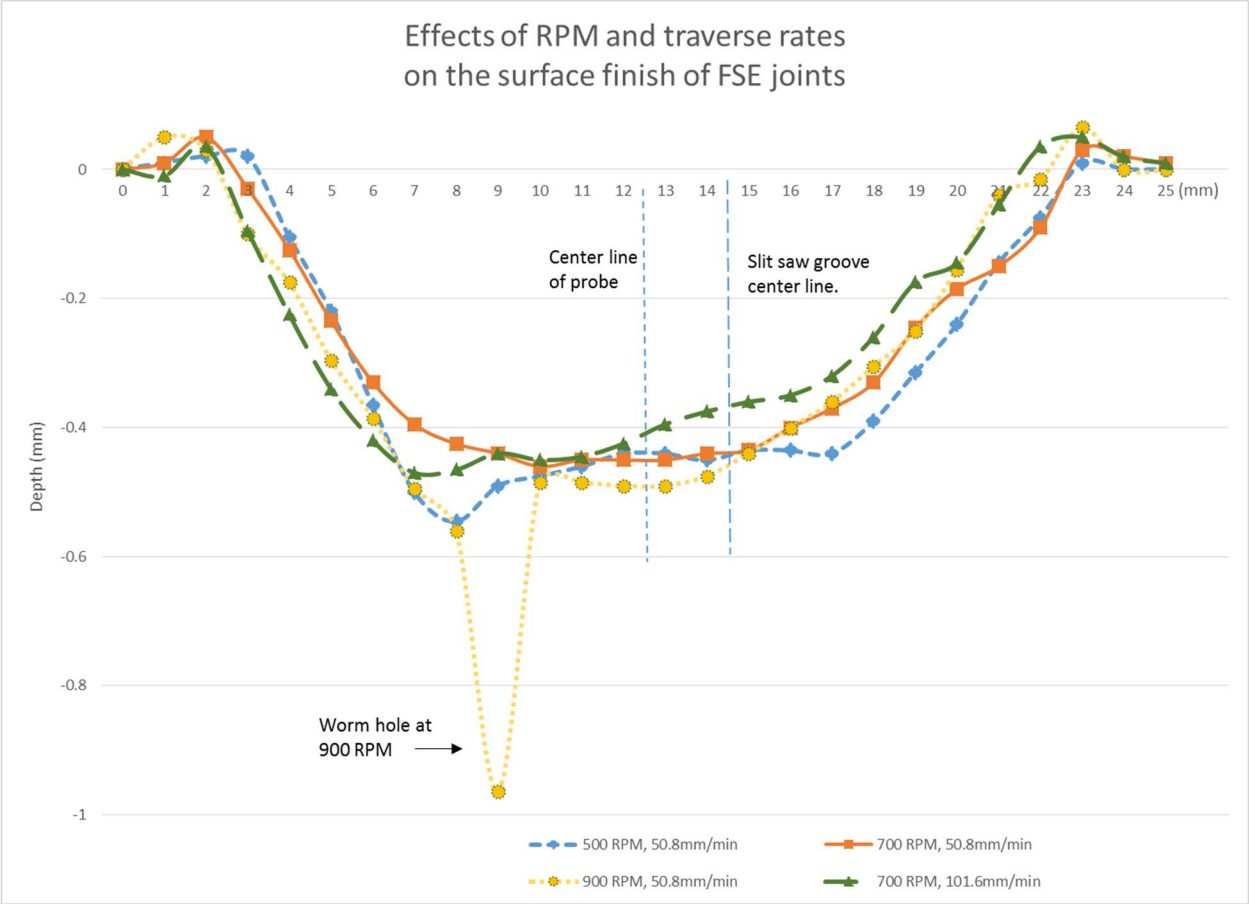

Figure 7.6 Surface plot of effects of RPM and traverse rates for FSE joints

Tensile Results

Samples of the three modified grooves were cut into smaller samples for tensile testing. Tensile shear testing was completed on an Instru-met Model TTC-102MC tensile testing machine with a 5,000 kg capacity. The samples were tested at a rate of 5mm/min and sampled at 10 Hz.

The cross-sectional area of the material in shear dictates the shear strength of the joint. For consistency across the groove shapes, the widest area of the neck at the surface of the steel plate was used

to calculate the cross-sectional area used to determine the shear strength. For the first modified groove with the slit saw cuts and the triangular section of titanium, the average shear strength was 198.9 Mpa, which is 70% of the parent material. For the second modified dovetail groove with the widened opening and the triangular feature milled out, the average shear strength of the material was 164 Mpa, which is 58% of the parent material. The third modified groove created with a shallower o-ring cut had an average shear strength of 170.5 Mpa, which is 60% of the parent material. These results can be seen and compared in Fig. 7.7.

The shear strength gives a good way to compare the strength of the cross-sectional area of the extruded material to that of the parent material, but load bearing applications will also need to know the peak load strength of the joint. Therefore, the peak load strength for a 6.35 mm wide specimen was used to evaluate the overall strength of the joint. All peak load strength values were normalized to this value of 6.35 mm to account for small variations in actual sample width. The highest average peak load obtained was 386 kgf for the modified o-ring. The modified slit saw groove had a peak load of 319 kgf and the slit saw groove was 193 kgf. So, while the slit saw groove had the best shear properties at 70% of the parent material, the average peak load was 50% less than that of the modified o-ring groove. This

makes sense physically given that the distance across the neck of the modified o-ring groove is just over twice that of slit saw groove and this extra cross-sectional area contributes to the much higher peak load of the joint.

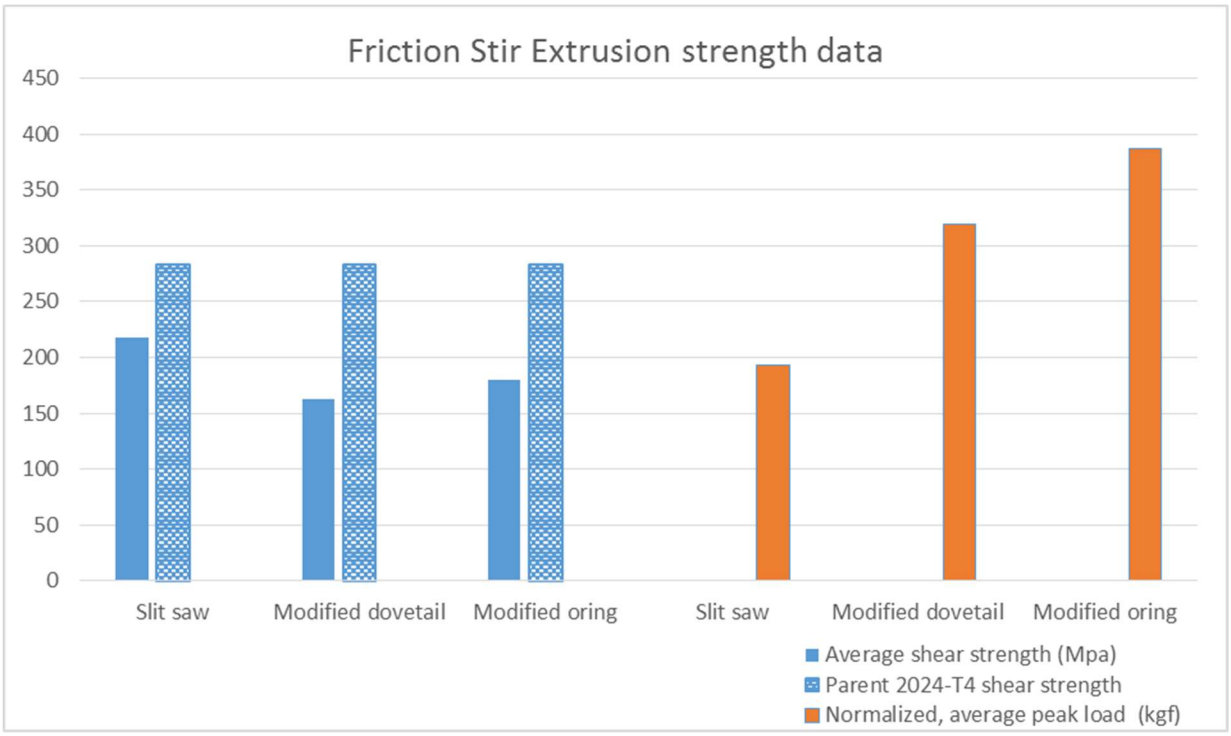

Figure 7.7 Friction Stir Extrusion shear strength and peak loads for different groove geometries.

Discussion

Examination of the joints after fracture reveals that no intermixing or bonding occurred between the aluminum and titanium. This eliminates the concern over IMCs at the interface weakening the joint and provides a good way to join the materials. These results also

show that the strength of the FSE joint for this particular setup is determined only by the physical properties of the joint. The main contributions to the strength based on the physical setup in this research are frictional forces, clinching, volume of material, and cross-sectional area of the smallest region.

The two basic types of geometries of the shaped slit saw versus the extruded volume of the modified dovetail/o-ring give further insight into the optimization of the FSE process. The slit saw groove represents a groove geometry that leads to better overall strength per volume of material extruded. It does this by adding other mechanical elements that contribute to the strength of the joint. First, the opposing slit saw angles act as anchors that increase the surface area in contact between the two materials. This adds to the overall strength both by keeping the material in true shear with no bending until close to failure, and by increasing the frictional and mechanical resistance. Secondly, it can be seen in the polished groove section in Fig. 7.3a that the titanium at the lip of the joint has been deformed downward by the z force of the FSE machine. This acts as a clinching force that also helps keep the joint in line while in tension and thus, increases the overall strength. This result is both a limiting factor and an opportunity to increase the strength. It is limiting because materials must be chosen that can withstand the strong zforce of the

FSE process, as well as, dictating limits on how much overhang can be designed into the groove edge geometry. However, it also provides an opportunity to use the natural deflection, clinching or other mechanical deformation features to enhance the strength of the weld.

In contrast to the slit saw, the o-ring groove uses more volume and increases the cross-sectional area. It resembles a solid chunk of material and its strength is almost entirely dependent on the cross-sectional area of the material. Figure 7.8b and 7.8c show that before joint failure, the aluminum is elongated and a space forms at the back side of the groove. This space eventually negates the ability of the concave shape to hold the material. This creates a rotation of the extruded material that adds stress to the material and quickly leads to failure.

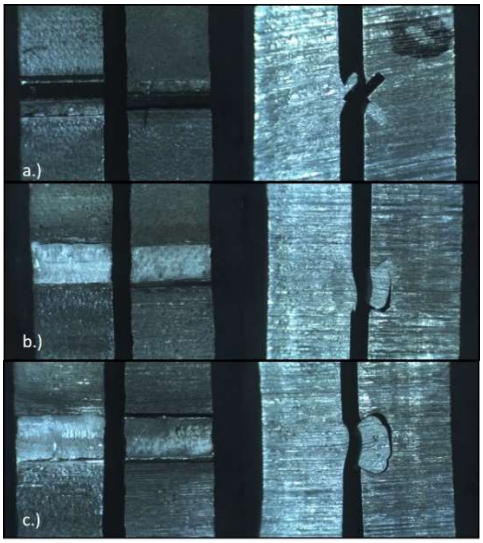

Figure 7.8 Failure Surfaces and profiles of 3 FSE groove shapes. a.) Slit saw groove. b.) Modified slit saw groove. c.) Modified o-ring groove.

These results show that the ultimate tensile strength of the joint can be increased by increasing the cross-sectional area. However, increasing the cross-sectional area can necessitate a larger volume, unless the volume of the groove is decreased by other means such as making a shallower cut. Shallower cuts can lead to less depth and less ability to create a concave region to extrude in to. Therefore, each of these considerations must be assessed for the individual application. In this research the plates were thick to allow for more volume of material to be available for extrusion into the weld. Therefore, the geometry that could form a successful joint and create the largest cross-sectional area will be the most successful as can be seen is the case for the modified o-ring in this paper. However, many applications such as the aerospace industry use thinner sheet material. Thinner sheets have less material available for extrusion into the groove and groove geometry will become a key design component. Geometries like the slit saw groove that add mechanical properties to the joint and enhance the overall strength will likely prove more effective for most applications. In addition, other materials could be used as an interlayer between the materials in order to add additional strength. This could be achieved by using a material that can be brazed during the process to provide a better locking or adding a sealant that can increase the rigidity of the joint.

Conclusions

The Friction Stir Extrusion process was used to join aluminum 2024-T4 to commercially pure titanium. It has been shown that:

- Successful Friction Stir Extrusion joints were formed at 700 RPM and 38.1 mm/min.
- Joints exhibited a shear strength of up to 70% of the parent material.
- No intermixing of aluminum and titanium occurred, minimizing concerns of IMCs.
- Three different groove geometries were successfully used while one was unsuccessful. The groove geometry is the most significant factor in both the success and strength of FSE joints.
- FSE joint strength is a combination of cross-sectional area of the extruded material and mechanical attributes that contribute to the overall strength.
- The process was applied to thick sheet material to allow for more material extrusion, but optimized joint geometries should allow for application to thin sheet materials and increases in overall strength.

Chapter VIII

TWO-SIDED FRICTION STIR RIVETING BY EXTRUSION: A NEW PROCESS FOR JOINING DISSIMILAR METALS

As published in Journal of Manufacturing Processes, 2016.

Authors

William T Evans, Chase D Cox, Brian T Gibson, Alvin M Strauss and George E Cook

Abstract

Two-Sided Friction Stir Riveting(FSR) by Extrusion is an innovative process developed to rapidly, efficiently, and securely join dissimilar materials. This process extends a previously developed one-sided friction stir extrusion process to create a strong and robust joint by producing a continuous, rivet-like structure through a preformed hole in one of the materials with a simultaneous, two-sided Friction Stir Spot Weld. The Two-Sided FSR by Extrusion process securely joins the dissimilar materials together and effectively locks them in place without the use of any separate materials or fasteners. In this paper we demonstrate the process by joining aluminum to steel and illustrate its potential application to automotive and aerospace manufacturing processes.

Introduction

With the development of new and lightweight materials to satisfy the demand for lighter and stronger structures and systems, there is a need for new joining methods. These new materials are being integrated into current systems, but they must interface and connect with other parts that are of a dissimilar material such as steel to aluminum. Their dissimilar nature makes joining with traditional welding methods costly or ineffective.

Background and Challenges of Joining Dissimilar Materials

FSW of aluminum and steel has been used in the manufacture of certain vehicle components such as the trunk hinge on the Mazda MX-5(Mishra and Mahoney 2007) and the hybrid steel/aluminum sub frame introduced by Honda on the 2013 Accord.(HondaWorldwide 2012) While these examples are promising, there are still three major difficulties that arise in the application of the FSW of aluminum to steel: 1.) the rate of wear of the FSW tool, 2.) the formation of an intermetallic compound(IMC) layer at the weld interface, and 3.) the difficulty of reliably creating a bond between the two metals.

Significant wear of the FSW tool can occur because of the hardness of the steel. Common tool materials used for joining

aluminum wear out very quickly when in operational contact with a wide variety of steels and harder, more robust tool materials are expensive and much more difficult to machine. One way of avoiding wear is through the use of pinless tools that contact only the aluminum, or tools with short pins along with position control that keep the pin within the aluminum only.(Watanabe et al. 2011)(Chen and Nakata 2008)(Lee et al. 2009)

The second issue that must be considered in joining aluminum to steel is the formation of IMC layers which can weaken the joint. Bozzi has shown that some IMC layer is necessary in traditional FSW to create a bond, but that it will weaken the joint if it is too thick.(Bozzi et al. 2010) Another study has shown a significant increase in strength when the IMC layer is less than 1.5 μm.(Qiu, Iwamoto, and Satonaka 2009) Watanabe has shown that the thickness of the IMC is proportional to the square root of the dwell time, so it becomes important to limit the amount of dwell time.(Watanabe et al. 2011)

The third and greatest challenge in welding steel and aluminum is the great difference in their material properties which makes it very difficult to create a bond between the surfaces. In fact, most of the current studies attribute the majority of the strength of the weld to factors other than welding of steel to aluminum. In the FSSW study by Lee where the probe only entered the aluminum, the conclusion

was that the strength of the bond was entirely attributed to the formation of IMCs and that no mixing of the aluminum and steel occurred.(Lee et al. 2009) In another study of FSSW that penetrated into the steel layer, it was concluded that the strength of the joint was due mainly to a mechanical interlocking produced by a "hanging" section of displaced steel similar to a hook and the greatest tensile strength reached was 407 kgf.(Bozzi et al. 2008) Other experiments in FSW have found that the use of a zinc coated steel helps to form a stronger bond because of the better bonding between the Zinc and Al due to a brazing effect of the melted Zinc.(Miyagawa et al. 2009)(Choi et al. 2010)(Chen and Nakata 2008)

Other authors seeking to join dissimilar materials have attempted to bypass the material properties issue by creating preformed mechanical features such as Lazarevic for an aluminum and steel joint, Balakrishnan for joining nylon to aluminum, Nishihara with aluminum and steel, and Evans with aluminum to steel.(Lazarevic et al. 2013)(Balakrishnan, Kang, and Mallick 2007)(Nishihara 2003)(Evans et al. 2015) Yet another alternative has been proposed of introducing a third material by using a combination of Friction Stir Welding(FSW) and riveting. Two main processes following this research have emerged called Friction Stir Blind Riveting (FSBR) as proposed by Gao(Gao et al. 2009), Min(Min et al. 2015), and

Lathabai(Lathabai et al. 2011) and Friction-Stir Riveting as presented by Ma and Durbin(Ma and Durbin 2012) These processes use Friction Stir Welding to plasticize the material to be joined so that an actual rivet made of a different material can be driven into and left behind in the materials to be joined.

These three issues make the welding of aluminum directly to steel difficult and the complexity of the problems increase with the introduction of high strength alloys.

The Two-Sided Friction Stir Riveting by Extrusion process

This paper presents a new method of joining dissimilar materials such as aluminum and steel by applying the Friction Stir Spot Welding process to a new setup that creates a bond between multiple layers of dissimilar materials while creating a solid riveted pin at the same time. This process has been termed Two-Sided Friction Stir Riveting by Extrusion to help differentiate it from other processes with similar names. The result is a combination of three sheets that are joined and strengthened by a solid, rivet-like feature that joins the materials together with no additional processing needed, no weight added, no bulges, and no chance for crevice corrosion as must be dealt with when using traditional rivets.

Two-Sided FSR by Extrusion is here presented as an innovative method of quickly and effectively joining dissimilar materials while creating strong joints in a process that is easily implemented at minimal cost. Also, unlike other joining processes, a strong bond is achieved at every location with no missed or defective spots. Two-Sided FSR by Extrusion has broad applications to a variety of materials, but this study has been focused on one particularly challenging problem of joining high strength aluminum alloys and steel as these materials are widely used in many industrial and manufacturing processes.

Two-sided FSR by Extrusion combines elements of Friction Stir Extrusion(FSE)(Evans et al. 2015) and Rotating Anvil Friction Stir Spot Welding (RAFSSW).(Cox, Gibson, Delapp, et al. 2014) The FSE process is a single-sided, linear friction stir weld that extrudes material into a preformed cavity to create a mechanical interlock. Two-Sided FSR by Extrusion uses this idea of extruding material by Friction Stirring, but does so at a single spot using the two sided RAFSSW process. The setup, as shown in Figure 8.1, is unique because it creates a triple lap configuration of Al/steel/Al with a predrilled hole in the steel which serves to create an area where the aluminum can be extruded and joined together. The aluminum is joined to the steel by diffusion bonding, while at the same time the process plastically deforms the

aluminum within the stir zone of the top and bottom aluminum sheets and extrudes the aluminum into the preformed through hole. As it is extruded, it joins together at the junction of the two channels of extruded aluminum. This creates a solid-state aluminum joint that effectively locks the aluminum plates into the steel via the through hole. The resulting joint will join the three sheets (Al-Steel-Al) in a manner similar to a mechanical fastener such as a rivet. The final friction stir extrusion rivet is a solid, joined connection between the sheets that also prevents crevice corrosion and creates a hermetic seal.

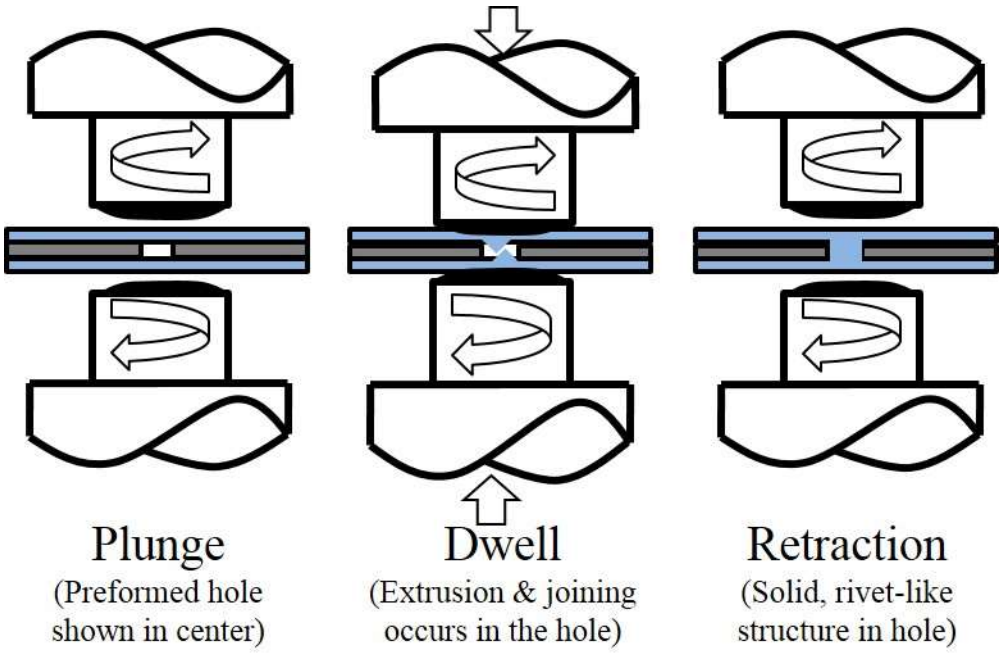

Figure 8.1 Two-Sided Friction Stir Riveting by Extrusion Process

Joining tools

The Two-Sided FSR by Extrusion process uses two pinless FSSW tools which feature a convex taper with scroll-like features that are cut into O1 tool steel and then hardened. The extrusion tool has a maximum overall diameter of 25.4 mm and features a scrolled, spherically tapered (convex) shoulder and a 10.2 mm flat as pictured in Figure 8.2.

Figure 8.2. Pinless FSSW tool with a spherically tapered shoulder.

Sample preparation

For all experiments, 1mm Al 6061 was used for the top and bottom aluminum plates and 1.5mm low-carbon steel for the middle steel plate. The aluminum was in the T6 heat treated condition exhibiting a yield strength of 276 MPa, Rockwell hardness B60 and the low-carbon steel had a yield strength of 413 MPa and Rockwell

hardness B80. Initial samples were prepared without a through hole to determine the baseline strength of the aluminum/steel bond. For the rest of the samples, the center of the extrusion/welding zone was marked and a through hole was punched into the steel plate. The effect of dwell time, hole size, and number of holes was explored by varying these parameters. The diameters of the hole sizes chosen for the single hole samples were 2.38 mm, 3.18 mm, 3.97 mm, 5.56 mm. For the two and three-hole samples, a hole size of 3.18 mm was chosen. There was a concern that the extruded material might cause too much top and bottom sheet thinning and reduce the strength of the joint, so hole sizes were chosen to keep the volume of extruded material from the extrusion zone below 25% of the available volume of aluminum in the extrusion zone. Prior to joining, all three of the sheets for the work piece were scrubbed to remove any surface oxide layers or any other possible contaminant. The sheets were then cleaned with a 50/50 solution of MEK (methyl ethyl ketone) and toluene to remove any oils or other contaminants. These configurations can be seen in Figure 8.3.

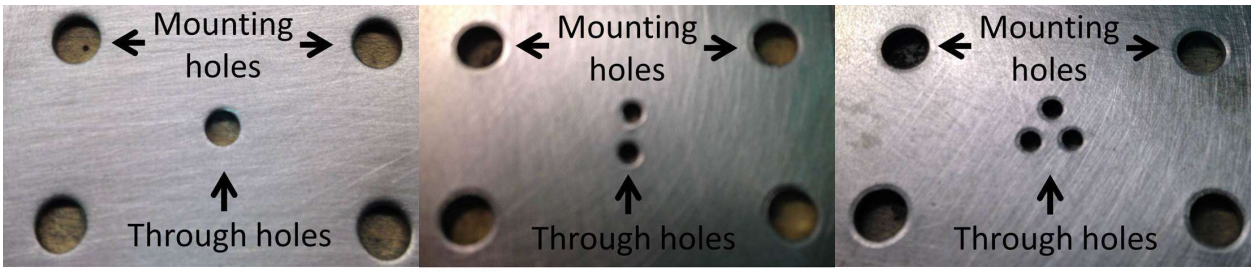

Figure 8.3. Single, double and triple through hole steel plates.

Joining parameters

For the friction stir extruded rivets in this experiment an open-loop force control system was used. Force control limits were set at 4250 N, 7200 N, and 8000 N. Both the extrusion tool and rotating anvil had a rotation rate of 1200 rpm with a plunge rate of 12.7mm per minute. Dwell times were varied from one to five seconds.

Experimental Design

The primary goal of the investigation was designed to create a stronger bond between the dissimilar metals of aluminum and steel than that made by diffusion only bonding. Baseline RAFSSW welds were made on an aluminum-steel-aluminum sample to determine the strength of the bonding between the aluminum and steel. Next, samples with holes in the steel were welded with the same setup to find suitable parameters that would allow the aluminum sheets to be extruded and joined together to create a successful joint. Plunge and

rotation rates were set at 10.16 mm/min and 1200 RPM and the process was performed with an axial force control of 4250 N and 8000 N at various dwell times. Once the Two-Sided FSR by Extrusion concept was proven successful, a second series of investigations sought to optimize the overall joint strength by adjusting the dwell time, the size of the holes and the number of holes while keeping all other parameters the same.

Four hole sizes ranging from 2.38-5.56 mm diameter were chosen and three dwell times of 2, 3, and 4 seconds were used. For each dwell time and hole size, four samples were prepared with an axial control force of 7200 N for a total of 48 extrusions. This allowed one sample at each dwell time and hole size to be cross sectioned to determine the integrity of the extrusion and three samples were then tensile tested to provide an average ultimate tensile load.

An additional 8 samples were prepared at a control force of 7200 N and a dwell time of 3 seconds to explore the effects of multiple through holes. Four samples were prepared with two through holes of 2.38 mm diameter centered on a radius of 2.5mm. Four samples were prepared with three through holes of 2.38 mm centered on a radius of 2.5 mm.

Testing

Tensile shear testing was completed on an Instru-met Model TTC-102MC tensile testing machine with a 5,000 kg capacity. All samples were loaded with a shim placed between the two aluminum sheets to ensure shear along the center line of the sample. Samples were tested at a rate of 5mm/min and sampled at 10 Hz. All results are reported as ultimate tensile load which represents the actual force needed to cause failure of the joined area as opposed to the peak stress which reports the ultimate load divided by the cross sectional area. As is common in reporting the strength of spot welds and rivets, the ultimate tensile load presented here is only a measure of the peak force required to cause a failure of the joint.

In addition, samples were cross-sectioned and examined in more detail to identify key contributions to the strength of the joints. Macrosection analysis was performed by taking a cross-section at the center of the rivet and polishing the sample to reveal the amount of material extruded into the through hole. Selected samples were polished to 1 μm and then etched with Keller's reagent and examined under a microscope to reveal the grain structure or other cracks, joint lines or voids within the extrusion zone.

Results

Ultimate tensile strength

The baseline aluminum/steel/aluminum samples with no hole were found to have an average ultimate tensile load of 324 kgf for 4250 axial force control and 449 kgf for 8000 N. Initial testing of the Two-Sided FSR by Extrusion samples at 4250 N of axial force control showed a decrease in ultimate tensile strength of 230 kgf. Macrosection analysis revealed that in these samples, the aluminum was extruded into the through hole, but it did not form a viable joint in the through hole as shown in Figure 8.4a.

The cutoff control force was increased to 8000 N in an attempt to better fill the void of the through hole and create a solid-state bond between the aluminum plates. The resulting joint had an ultimate tensile load was 739.24 kgf, which was over 3 times stronger than the first extrusion joint at 4250 N and 1.6 times the strength of the baseline configuration at 8000 N. The macrosection of this sample revealed that, again, the volume of the through hole was not completely filled as volumetric voids can be seen on both sides of the through hole near the outer edge of the hole. However, the material extruded by the top and bottom plates did converge within the through hole resulting in a bonded aluminum joint as seen in Figure 8.4b. The length of the joined section was approximately 1 mm long.

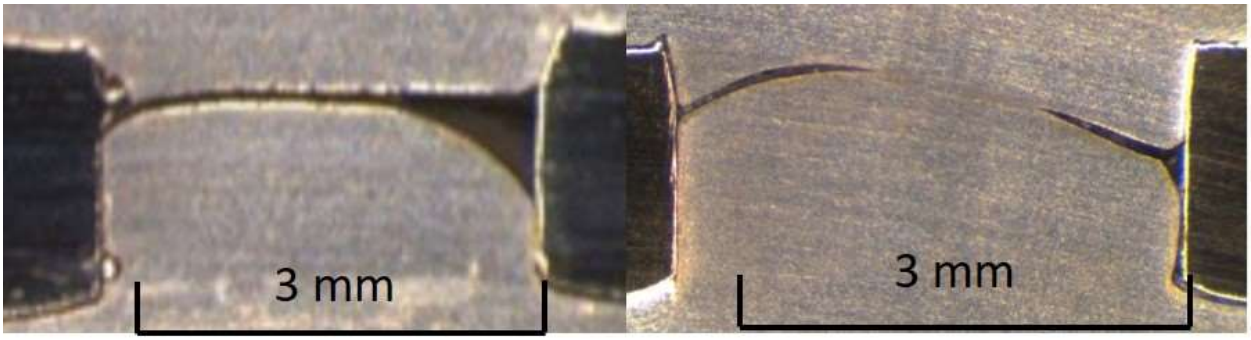

Figure 8.4. Al-Steel-Al Two-Sided FSR by Extrusion process at 1200 rpm and 1 sec a) 4250 N control force. The extruded material partially fills the volume of the through hole but does not create a joint. b) 8000 N control force. The extruded material partially fills the volume of the through hole with a small joined section.

Once it was shown that the process produced a strong and reliable bond, a more detailed study was performed to better understand the contributions of dwell time, hole size, and the number of holes as detailed in Table 8.1. Results of the study at 7200 N axial control force show that strong joints were created by the process whose average ultimate tensile strength ranged from 629.66 kgf to 767.38 kgf with individual samples ranging from 530 kgf to 958 kgf. For single hole samples, the lowest average ultimate tensile load of 629.66 kgf was found at the lowest dwell time of two seconds. The highest average load of 715.25 kgf was found in the longest dwell time of four seconds. The two and three-hole samples showed a stronger peak load of about 11-12% greater than the single holes at the same parameters.

Table 8.1. Parameters and Results

Hole Size Diameter	Dwell	RPM	Plunge Rate (mm/min)	Force Control	Num. of Samples	Average Ultimate Tensile Load (kgf)
"2.38 mm"	2	1200	10.16	7200	3	629.66
"3.18 mm"	2	1200	10.16	7200	3	632.62
"3.97 mm"	2	1200	10.16	7200	3	656.17
"5.56 mm"	2	1200	10.16	7200	3	650.66
"2.38 mm"	3	1200	10.16	7200	3	680.05
"3.18 mm"	3	1200	10.16	7200	3	677.53
"3.97 mm"	3	1200	10.16	7200	3	688.11
"5.56 mm"	3	1200	10.16	7200	3	685.25
"2.38 mm"	4	1200	10.16	7200	3	702.52
"3.18 mm"	4	1200	10.16	7200	3	715.25
"3.97 mm"	4	1200	10.16	7200	4[a]	713.78
"5.56 mm"	4	1200	10.16	7200	3	697.56
2 * 2.38 mm"	3	1200	10.16	7200	3	755.72
3 * 2.38 mm"	3	1200	10.16	7200	5[a]	767.38
[a]The number of samples for the 3.97 mm" hole and the 3 * 2.38 mm" was increased due to a large variance in measured ultimate tensile load.						

Failure Modes

The major failure mode for the Two-Sided FSR by Extrusion joints was shearing of the aluminum extrusion at both edges of the steel along with a breaking of the aluminum/steel bond. The aluminum shearing in most samples occurred at both the top and bottom of the steel hole leaving a deformed, cylindrical section of aluminum in the hole as seen in Figure 8.5. The setup of the "rivet" in a perpendicular orientation to the tensile direction helped increased

the ultimate tensile strength of the joint by doubling the surface area since the rivet was in double shear. Other samples fractured only along one edge of the steel, leaving the aluminum rivet attached to the opposite aluminum sheet. The failure in the aluminum/steel region is a shear fracture between the interface of the materials and was similar to results found by Uematsu in their study of dissimilar FSSW of A6061 and low carbon steel.(Uematsu et al. 2011) The lighter colored region in Figure 8.5b is aluminum that has been left behind on the steel from the fracture.

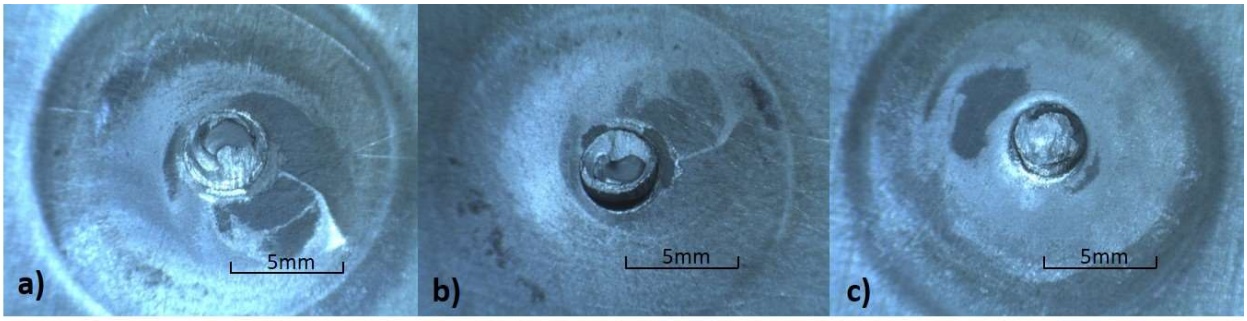

Figure 8.5. Failure Mode of samples. a) Rivet has been sheared off of the top aluminum plate. b) Steel sheet with deformed cylindrical puck of aluminum left behind. c) Rivet has been sheared off of the bottom plate.

An additional failure mode was noted in some of the larger hole samples with a 5.56 mm hole or three 3.18 mm holes. These samples showed partial nugget pull out as shown in Figure 8.6.

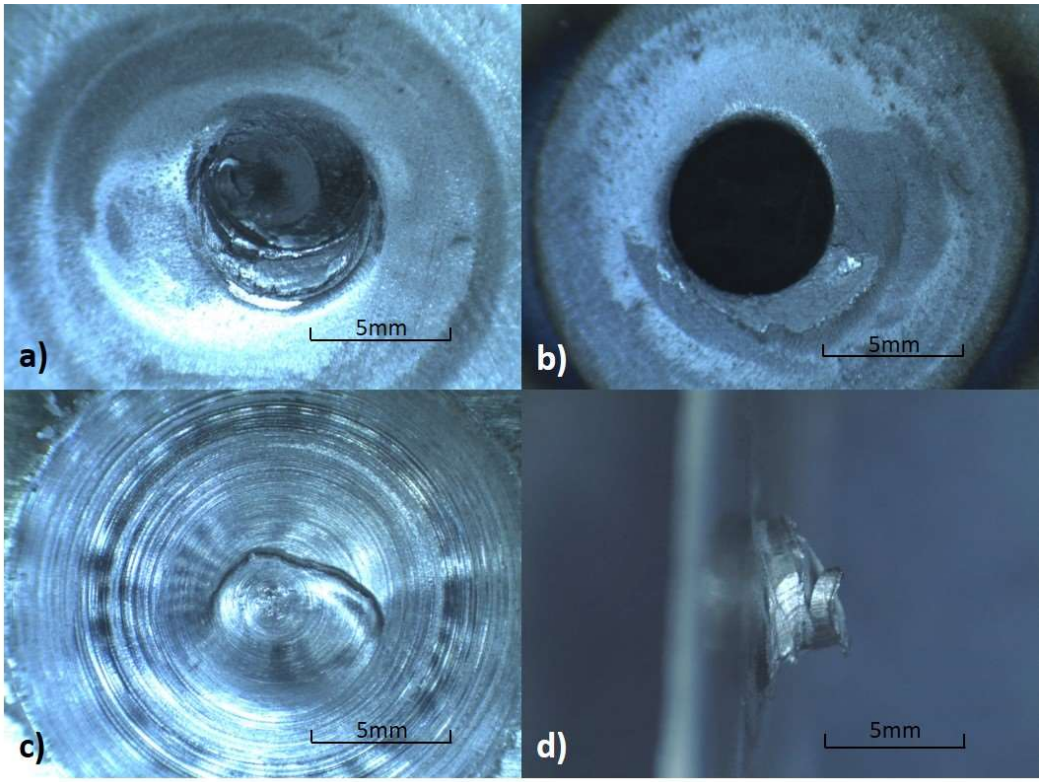

Figure 8.6. Failure of Two-Sided FSR by Extrusion joints with partial nugget pullout. a) Bottom sheet of aluminum with rivet sheared off. b) Empty hole left in the steel sheet. c) Outer surface of the top sheet showing fracture due to top sheet thinning. d) Extrusion rivet left attached to top sheet.

Macro and micro structural results

Microscopic analysis of the grain structure showed that the aluminum created a solid-state joint in the through hole to form a rivet-like structure. The percent of joined area varied from <10% up to 100%. In some samples, joint lines were visible on the edges and some cracks were noted at the edge of the hole in the steel. Figure 8.7 shows two etched samples that exhibit these characteristics.

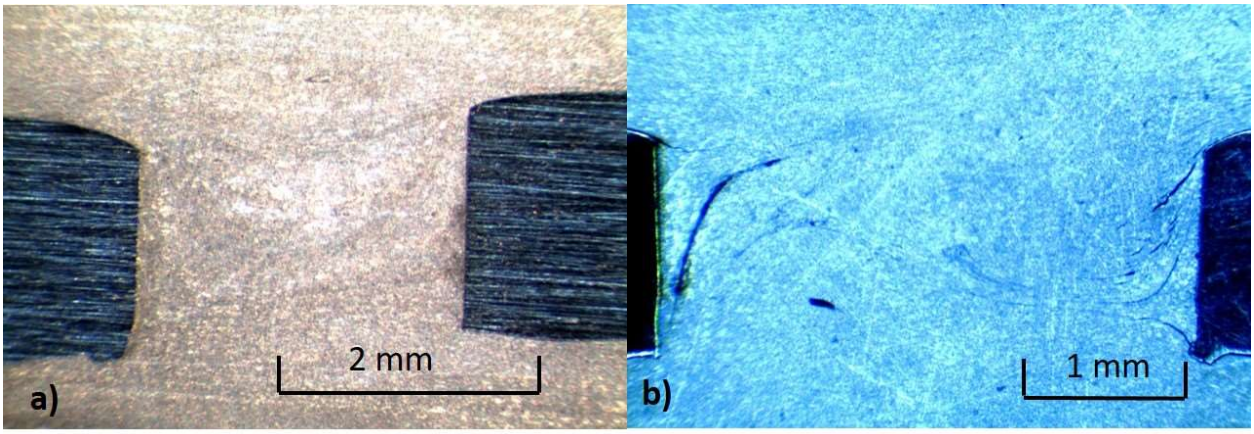

Figure 8.7. Al-Steel-Al with a through hole, polished and etched. 1200 rpm, 7200 N control force. a) The extruded material from the top and bottom sheet has completely filled the volume of the through hole and a fully joined rivet has been formed. b) The extruded material from the top and bottom sheet has filled the volume of the through hole and a partially formed rivet was formed with small joint lines and a crack present at the edges.

Discussion

Initial evaluation of the Two-Sided FSR by Extrusion process showed a significant difference in the strength of the joint based on whether the two aluminum sections joined in the hole or not. When the aluminum was extruded into the through hole, but did not join, the overall strength of the joint went down by 29% from 324 kgf to 230kgf. This can be understood because the overall area of the joint was reduced by the area of the through hole and the aluminum extrusions added little strength to the joint. This center region is also the area where the greatest interaction between steel and aluminum occurs because it is the area that experiences the greatest force from

the tool. Effectively removing this section weakens the joint as expected.

When the aluminum was extruded into the through hole and it formed a joint between the upper and lower plates, the ultimate tensile load increased by more than three times that of the samples that did not join in the through hole from 230 kgf to 739 kgf. These results indicate that the addition of this solid "rivet" like section of the weld significantly impacts the overall strength of the joint. So, to achieve maximum strength with the process, it is critical that the top and bottom sheet join to one another in the through hole. This "riveted" structure provides additional clinching or normal force that helps hold the weld together similar to how a bolt holds sheets of metal together. This is likely due to expansion of the aluminum from heat during the process and its subsequent cooling and contraction. Additional research is needed to more fully understand the bonding characteristics of this joint.

All extrusion rivets tested in Table 8.1 showed this characteristic joining in the through hole upon macrosection analysis. For the single hole samples, the average ultimate tensile load was found to correlate linearly with dwell time with longer dwell times leading to stronger joints as seen in Figure 8.8. This will reach some physical maximum when all of the extruded material is joined across the entire area of

the hole. A 10% increase in strength was noted as the dwell time was increased from 2 to 4 seconds. As time is critical in a manufacturing setting, the tradeoff in strength for a shorter joining time will be an important consideration. Test samples at 8000 N and 1 sec dwell time in the initial part of the experiment showed similar strengths to those at 7200 N thus indicating that a larger axial control force will be able to shorten the dwell time needed for the process and make it better suited for manufacturing processes.

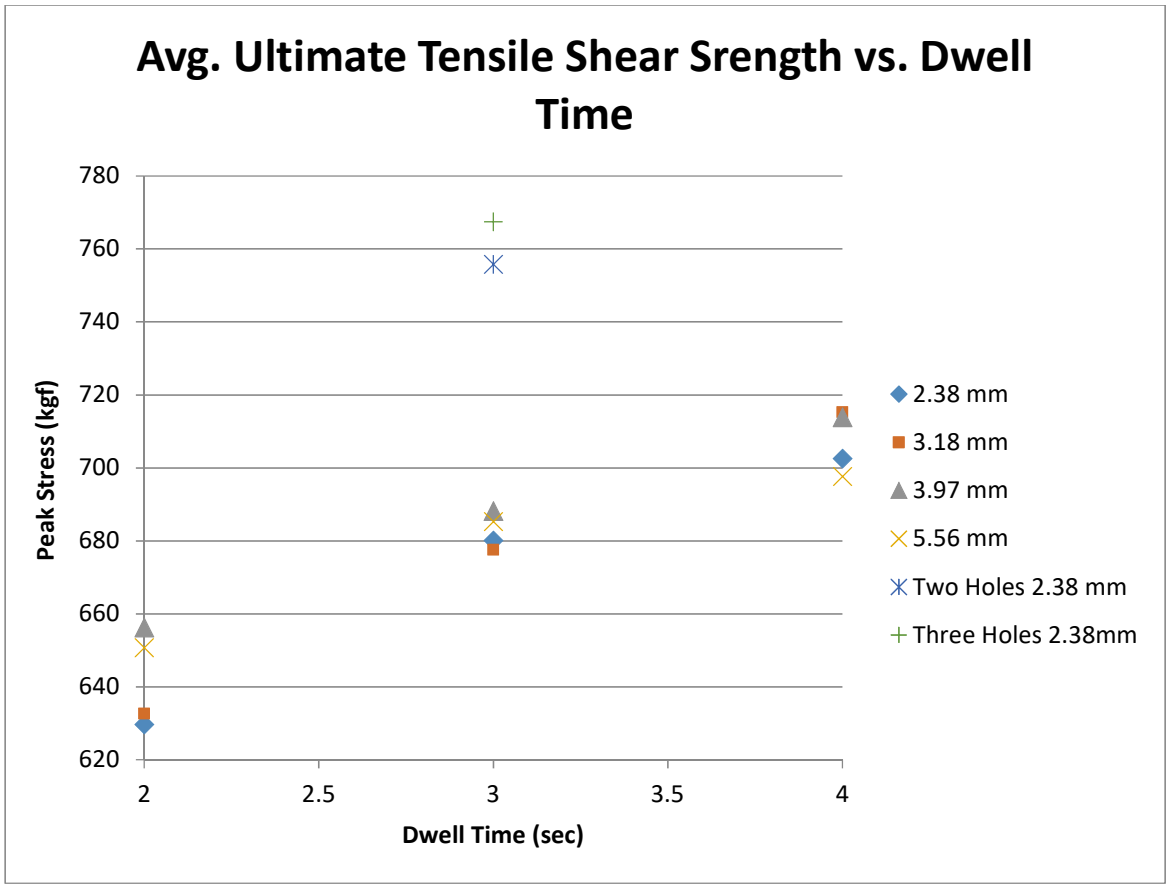

Figure 8.8 Average ultimate tensile load vs. dwell time for aluminum/steel rivet extrusions

At each dwell time the average ultimate tensile loads are clustered within a window of 10-26 kgf with no particular order based on hole size noted. Therefore, at these parameters there does not appear to be a strong relationship between the hole size and the ultimate tensile load within these extrusion parameters. (Figure 8.8) This is likely because there was sufficient time and space for a partial or full joint to form in the through hole in all joints. Shorter dwell times, lower axial forces or smaller holes will likely impact the strength of the extrusion rivets as each of these play a part in the process of allowing the aluminum to quickly extrude and join together.

Two and three-hole samples showed an 11% and 12% increase respectively in joint strength compared to the average ultimate strength of similar 3 second dwell time samples. This shows an additional way to create stronger joints by distributing the load between multiple pins without increasing dwell time. Additional configurations and geometries such as hole shape, hole location, inclusion of threads in the hole, tapers, etc… may also lead to additional increases in strength.

Analyzing the fracture patterns reveals that the fracture lines of most samples are similar to what would be expected from a solid rivet placed in a hole that fractures along the plane of greatest stress at the

top and/or bottom of the hole during a tensile test. Samples that exhibited partial nugget pullout exhibited the same fracture lines, but the difference in type of fracture resulted from top and bottom sheet thinning since a larger percentage of volume of the aluminum sheets was needed to fill the hole. So, while increasing the overall volume of the rivet(s) increases the ultimate shear strength, it must be balanced with potential losses from top and bottom sheet thinning.

Initial ultimate tensile loads at first glance seem higher than the base material of Aluminum 6061 which has yield strength of 276 MPa. This is due to the fact that the overall strength of the Two-sided FSR by extrusion joint is a complex combination of forces and interactions of both a mechanical and chemical nature and not just the strength of the aluminum. This is one of the unique features of this process as it derives its strength from at least 3 main sources: the strength of the aluminum, the strength of the diffusion bonds between aluminum and steel, and the clinching/normal force of the rivet holding all three sheets together. More research needs to be done to characterize and optimize these interactions to achieve higher tensile strengths, but initial results show a new way of joining dissimilar metals that is significantly stronger than other processes to date. This continuous rod/rivet of joined aluminum within the preformed through hole greatly increases the strength of the joint and is what differentiates

the Two-Sided FSR by Extrusion process from other mechanical joining processes.

Future Applications

This process was performed on aluminum and steel, but a large portion of the strength of the joint is based on the extruded material. Therefore, the process will work with other combinations of materials as long as one of the materials can be extruded and joined to itself or to another material used on the opposite sheet. This opens the possibilities to combinations of materials that were previously thought unweldable or difficult to join such as plastics to metal, metals to organic materials, metals to metal matrix composites and many more.

The process also lends itself to the automotive industry and other applications that involve robotic resistance spot welding applications. A typical automotive welding robot could conceivably be fitted with a pneumatic two-sided attachment and used in a very similar way for large scale production. The opposing forces of the two simultaneous welding tools help balance the process and eliminate the need for a bulky machine or anvil to absorb the strong axial force. The Two-Sided FSR by Extrusion joints can be made in as little as 1 second and probably faster upon optimization, which would make it feasible to

implement them on an industrial line to join dissimilar parts that could not previously be joined in a cost effective or efficient way.

Conclusions

Two-sided Friction Stir Riveting by Extrusion is a novel process that introduces a new way of joining dissimilar materials. Initial findings show that the process creates a strong joint between aluminum and steel sheets by forming an extruded rivet-like structure within a preformed through-hole placed in the steel. If the top and bottom layers do not join in the through hole, the overall strength is reduced. However, as the process is better optimized and the top and bottom sheets are joined, the overall strength of the joint goes up significantly. The strength of a successful joint can be increased by increasing the dwell time or by increasing the number of pre-made holes in the extrusion zone. Compared with a baseline joint of aluminum/steel/aluminum with no through hole (324 kgf ultimate tensile strength), this new process was able to triple the strength with individual samples reaching an ultimate tensile load of 958 kgf.

Two-Sided FSR by Extrusion works well with thin sheet sections of aluminum and steel and the process can be extended to thicker or thinner sheets and a variety of materials such as metal matrix composites, carbon fiber reinforced thermoplastics, high strength

alloys, etc… Applications of the Two-Sided FSR by Extrusion process lend themselves to many manufacturing applications, especially where dissimilar materials are used and composite structures are needed such as a joining a corrosion layer and a strength layer, or in the automotive industry where dissimilar, lightweight materials are joined in numerous places.

Chapter IX

CONCLUSIONS AND FUTURE WORK

Conclusions

Friction Stir Welding has progressed significantly since its official inception in 1991. Initial research within the field largely focused on aluminum and how to best weld the different Al alloys. Investigation continued on how to make a weld, but researchers also began to explore the fundamental properties and processes that were involved in FSW. Models were introduced to try and explain what was going on within the weld so that the process could be optimized. The last twenty years have seen an explosion of research in the field to use aspects of the Friction Stir Welding Process for unique applications and to broaden the ability to use more and more materials. The research contained in this dissertation continues in this tradition by applying the Friction Stir Welding process to new applications and to extend our understanding and use of new materials that can be Friction Stir Welded.

Chapter IV was focused on using the FSW process to join Additively Manufactured (AM) materials. AM materials are being used

extensively in design and manufacturing as they allow custom built parts and features that are difficult to make or can't be created by traditional milling or joining processes. The AM field shows tremendous promise, but almost all AM printers have a limited build volume. This necessitates that these smaller AM parts will need to be joined and integrated into larger designs.

This research began the process of examining the feasibility of joining AM parts by FSW by focusing on Ultrasonic Additively Manufactured (UAM) 6061 Aluminum Alloy. This 3D material is relatively new and no research has been published to examine its ability to be joined by Friction Stir Welding. This study showed that it is possible to join UAM 6061 by FSW and showed that optimized parameters from stock 6061 Al worked well with this material. It was shown that FSW significantly improved the properties of the UAM material. The stirring effect of FSW eliminated any gaps within the material and consolidated the tape layers of the UAM material. Gains of 50% increase in tensile strength were achieved in the longitudinal direction.

Chapter V focused on a similar issue of examining the feasibility of using an FSW process to join a unique material. The material chosen for this research was a Campo del Cielo iron meteorite. This meteorite material was collected from a meteorite that struck earth

over four millennia ago and represents similar material to that of other metal meteorites and asteroids in space. These iron meteorites and asteroids represent an amazing opportunity to acquire raw materials for in-space construction. This can save considerably on the cost of building in space as scientists would not have to send the material in to space, and resources could be utilized as encountered during long distance space travel.

The main challenge in using this material is the impurities that are inherent in their composition. These impurities lead to cracking and poor weld quality when the welds are created by traditional welding methods that melt the iron. This research showed that Friction Stir Spot Welding can be successfully used to join the material without cracking or defects within the weld zone as seen in other welding techniques. This opens the possibility of using this or other FSW processes for in-space construction.

Chapters VI, VII, and VIII focused on joining new material combinations by innovative Friction Stir Welding process variants. The focus on fuel efficiency and strength to weight ratio in the transportation and other industries has given rise to the need for systems made of dissimilar materials. One common scenario is the need to join lightweight aluminum alloys from one part of the design to a rigid material such as steel which provides rigidity and strength in

another part of the design. The material properties of these dissimilar materials make it difficult to weld them together as one material melts before the other one or brittle intermetallic compound (IMC) layers are created that lead to failure. Other joining techniques such as bolting or rivets add extra weight and can lead to additional issues such as crevice corrosion or weaker joints.

Traditional FSW has struggled to provide strong welds of these dissimilar materials due to the disparate melting temperatures, IMCs and tool wear. To join dissimilar materials and avoid these issues, two new processes were developed. Friction Stir Extrusion was developed as a variant on the FSW process by using an FSW weld to force one material to flow into a pre-made geometrical groove. This configuration allowed the two materials to be joined due to mechanical interlocking. This allows the materials to be joined without adding any weight to the design and allows a solid joint that is not subject to crevice corrosion. This setup can be used for cladding, such as to provide chemical corrosion protection on armored vehicles, or for any other application were a rigid joint is needed between dissimilar materials.

Friction Stir Extrusion creates a linear weld, but the process can also be used in a Friction Stir Spot Welding setup to create a joint similar to a rivet. This second process, as presented in Chapter VIII, is

known as Two-sided Friction Stir Riveting by Extrusion. This Friction Stir Riveting process applies two simultaneous FSSW welds to a sandwiched, composite material of at least three layers. The middle layer has a pre-formed hole in it. As the top and bottom sheets are subjected to the two FSSW welds, the material is forced into this preformed hole, where it joins to form a solid connection similar to a rivet. This process shows great promise for joining thin sheet materials in applications such as door panels on cars.

The research has advanced the field of Friction Stir Welding by successfully welding new materials. It also developed innovative ways of joining dissimilar materials that can be used in future manufacturing applications.

Future Work

The research presented here has laid the foundational work for many areas of further investigation. UAM Al 6061 was chosen to explore the ability to join AM materials, but there are numerous other AM materials that are limited by the same build volume constraints and need to be joined to larger structures. Research must continue to determine the feasibility of friction stir welding other AM materials as

each one is unique and has its own characteristics that must be taken in to account to develop welding parameters for that material.

Friction Stir Spot Welding of the meteorite has shown that FSW processes can be used to weld meteoric materials. The next step would be to build on this to do a full linear weld of a meteorite. The main challenges of doing this are obtaining a large enough specimen of material and gaining access to a larger machine that can handle the large forces required to weld iron nickel alloys. FSW can also be used to process and enhance the raw material by stirring it to eliminate natural defects and create a more homogenous material. Friction Stir Processing can provide an effective way to create uniform, in-space building materials without having to refine and process the raw iron alloy from the meteorite or asteroid.

The final area of investigation into the joining of dissimilar materials can also be expanded to include different combinations of metals. This process is not necessarily just confined to metallic elements, but could also be used with plastics, wood or other hard materials. Optimizing these methods was begun by choosing three different groove shapes for the Friction Stir Extrusion, and with a variety of hole sizes and number of holes for Two-sided Friction Stir Riveting by Extrusion, but many other combinations need to be explored. The size of the groove and the size of the holes made a

large impact on the quality of the weld and further investigations into different geometries need to be undertaken. In addition, different thicknesses of material need to be explored as the volume of material can be a limiting factor of these processes. The fundamental aspects of these processes are similar to FSW, but they are not exactly the same. The two extrusion processes must move a large volume of material without thinning the area around the weld too much. New tool designs specific to this application need to be developed. This would involve the integration of new features and enhancing current ones to increase material flow. It would also benefit from larger tool shoulder diameters that could stir a larger surface area of material into the weld and thus allow the use of thinner sheet material.

REFERENCES

Anawa, E M, A G Olabi, and F A Elshukri. 2009. "Modeling and Optimization of Tensile Shear Strength of Titanium/Aluminum Dissimilar Welded Component." *Journal of Physics: Conference Series* 181 (August): 12033.

Aonuma, Masayuki, and Kazuhiro Nakata. 2011. "Dissimilar Metal Joining of 2024 and 7075 Aluminium Alloys to Titanium Alloys by Friction Stir Welding." *MATERIALS TRANSACTIONS* 52 (5): 948–52.

Aota, Kinya, and Kenji Ikeuchi. 2009. "Development of Friction Stir Spot Welding Using Rotating Tool without Probe and Its Application to Low-Carbon Steel Plates." *Welding International* 23 (8). Taylor & Francis Group.

Baek, Seung-Wook, Don-Hyun Choi, Chang-Yong Lee, Byung-Wook Ahn, Yun-Mo Yeon, Keun Song, and Seung-Boo Jung. 2010. "Structure–Properties Relations in Friction Stir Spot Welded Low Carbon Steel Sheets for Light Weight Automobile Body." *Materials Transactions* 51 (No. 2): 399–403.

Balakrishnan, Karthik N., H. T. Kang, and P. K. Mallick. 2007. "Joining Aluminum to Nylon Using Frictional Heat." In . SAE World Congress & Exhibition.

Balasubramanian, N., Rajiv Mishra, and K. Krishnamurthy. 2009. "Friction Stir Channeling: Characterization of the Channels." *Journal of Materials Processing Technology* 209 (8). Elsevier: 3696–3704.

Bozzi, S., a. L. Etter, T. Baudin, a. Robineau, and J. C. Goussain. 2008. "Mechanical Behaviour and Microstructure of Aluminum-Steel Sheets Joined by FSSW." *Texture, Stress, and Microstructure* 2008 (Figure 1): 1–8.

Bozzi, S., a. L. Helbert-Etter, T. Baudin, B. Criqui, and J. G. Kerbiguet. 2010. "Intermetallic Compounds in Al 6016/IF-Steel Friction Stir Spot Welds." *Materials Science and Engineering A* 527 (16–17). Elsevier B.V.: 4505–9.

Buchwald, VF. 1975. *Handbook of Iron Meteorites: Their History, Distribution, Composition, and Structure. Volume 2*. Berkeley: University of California Press.

Chen, Y.C., and K. Nakata. 2008. "Effect of the Surface State of Steel on the Microstructure and Mechanical Properties of Dissimilar Metal Lap Joints of Aluminum and Steel by Friction Stir Welding." *Metallurgical and Materials Transactions A* 39 (8): 1985–92.

Chen, Y C, and K Nakata. 2009. "Microstructural Characterization and Mechanical Properties in Friction Stir Welding of Aluminum and Titanium Dissimilar Alloys." *Materials & Design* 30: 469–74.

Choi, C. Y., D. C. Kim, D. G. Nam, Y. D. Kim, and Y. D. Park. 2010. "A Hybrid Joining Technology for Aluminum/Zinc Coated Steels in Vehicles." *Journal of Materials Science and Technology* 26 (9). Journal of Materials Science & Technology: 858–64.

Colegrove, P. A., and Hugh R. Shercliff. 2005. "3-Dimensional CFD Modelling of Flow Round a Threaded Friction Stir Welding Tool Profile." *Journal of Materials Processing Technology* 169 (2): 320–27.

Colegrove, P A, and H R Shercliff. 2013. "Science and Technology of Welding and Joining Experimental and Numerical Analysis of Aluminium Alloy 7075-T7351 Friction Stir Welds Experimental and Numerical Analysis of Aluminium Alloy 7075-T7351 Friction Stir Welds."

Cox, Chase D., Brian T. Gibson, David R. Delapp, Alvin M. Strauss, and George E. Cook. 2014. "A Method for Double-Sided Friction Stir Spot Welding." *Journal of Manufacturing Processes* 16 (2). The Society of Manufacturing Engineers: 241–47.

Cox, Chase D., Brian T. Gibson, Alvin M. Strauss, and George E. Cook. 2012. "Effect of Pin Length and Rotation Rate on the Tensile Strength of a Friction Stir Spot-Welded Al Alloy: A Contribution to Automated Production." *Materials and Manufacturing Processes* 27 (4). Taylor & Francis Group : 472–78.

Cox, Chase D, Brian T Gibson, Alvin M Strauss, and George E Cook. 2014. "Energy Input during Friction Stir Spot Welding." *Journal of Manufacturing Processes* 16: 479–84.

DeepSpaceIndustries. 2017. "Asteroid Mining: An Unlimited Future for All Mankind." 2017. https://deepspaceindustries.com/mining/

Elangovan, K, and V Balasubramanian. 2007. "Influences of Pin Profile and Rotational Speed of the Tool on the Formation of Friction Stir Processing Zone in AA2219 Aluminium Alloy." *Materials Science*

and Engineering A 459: 7–18.

Elmer, J. W., C. L. Evans, J. J. Embree, G. F. Gallegos, and L. T. Summers. 2014. "Electron Beam Weldability of a Group IAB Iron Meteorite." *Science and Technology of Welding and Joining* 19 (4).

Evans, William T., Brian T. Gibson, Jay T. Reynolds, Alvin M. Strauss, and George E. Cook. 2015. "Friction Stir Extrusion: A New Process for Joining Dissimilar Materials." *Manufacturing Letters* 5: 25–28.

Fuji, Akiyoshi. 2002. "In Situ Observation of Interlayer Growth during Heat Treatment of Friction Weld Joint between Pure Titanium and Pure Aluminium." *Science and Technology of Welding & Joining* 7 (6). Taylor & Francis: 413–16.

Fuji, Akiyoshi, K. Ameyama, and T. H. North. 1995. "Influence of Silicon in Aluminium on the Mechanical Properties of Titanium/aluminium Friction Joints." *Journal of Materials Science* 30 (20). Kluwer Academic Publishers: 5185–91.

Gao, Dalong, Ugur Ersoy, Robin Stevenson, and Pei-Chung Wang. 2009. "A New One-Sided Joining Process for Aluminum Alloys: Friction Stir Blind Riveting." *Journal of Manufacturing Science and Engineering* 131 (6). American Society of Mechanical Engineers: 61002.

Gibson, Brian T., D.H. Lammlein, T.J. Prater, W.R. Longhurst, C.D. Cox, M.C. Ballun, K.J. Dharmaraj, G.E. Cook, and A.M. Strauss. 2014. "Friction Stir Welding: Process, Automation, and Control." *Journal of Manufacturing Processes* 16 (1): 56–73.

Gibson, Ian, David Rosen, and Brent Stucker. 2015. "Additive Manufacturing Technologies: 3D Printing, Rapid Prototyping, and Direct Digital Manufacturing." In , Second Edi. New York: Springer.

Gould, Jerry E., and Zhili Feng. 1998. "Heat Flow Model for Friction Stir Welding of Aluminum Alloys." *Journal of Materials Processing & Manufacturing Science* 7 (2): 185–94.

Graff, K F, M Short, and M Norfolk. 2010. "Very High Power Ultrasonic Additive Manufacturing (VHP UAM) for Advanced Materials."

Greicius, Tony. 2015. "Curiosity Finds Iron Meteorite on Mars." https://www.nasa.gov/jpl/msl/pia18387

Haghshenas, M. Sahraeinejad, S., A. Abdel-Gwad, B. Gocke, and A.P. Gerlich. 2013. "Disssimilar Joining of Automotive Sheet Materials

by Friction Stir Welding." In . Niagra Falls: CanWeld Conference 2013.

HondaWorldwide. 2012. "'Honda Develops New Technology to Weld Together Steel and Aluminum and Achieves World's First Application to the Frame of a Mass-Production Vehicle.'" 2012. http://world.honda.com/news/2012/4120906Weld-Together-Steel-Aluminum/

Hovanski, Y., M.L. Santella, and G.J. Grant. 2007. "Friction Stir Spot Welding of Hot-Stamped Boron Steel." *Scripta Materialia* 57 (9). Pergamon: 873–76.

Jiangwei, Ren, Li Yajiang, and Feng Tao. 2002. "Microstructure Characteristics in the Interface Zone of Ti/Al Diffusion Bonding." *Materials Letters* 56 (5): 647–52.

Kassim Mohammed, Haitham. 2011. "A Comparative Study between Friction Stir Welding and Metal Inert Gas Welding of 2024-T4 Aluminum Alloy." *APRN Journal of Engineering and Applied Sciences* 6 (11).

Landis, Geoffrey. 2009. "Meteoritic Steel as a Construction Resource on Mars." *Acta Astronautica* 64 (2): 183–87.

Landis, Geoffrey A. 2007. "Materials Refining on the Moon." *Acta Astronautica* 60 (10): 906–15.

Lathabai, Sri, Vinay Tyagi, David Ritchie, Trevor Kearney, Barrie Finnin, Shane Christian, Andrew Sansome, and Gary White. 2011. "Friction Stir Blind Riveting: A Novel Joining Process for Automotive Light Alloys." *SAE International Journal of Materials and Manufacturing* 4 (1): 589–601.

Lazarevic, Sladjan, Scott F. Miller, Jingjing Li, and Blair E. Carlson. 2013. "Experimental Analysis of Friction Stir Forming for Dissimilar Material Joining Application." *Journal of Manufacturing Processes* 15. The Society of Manufacturing Engineers: 616–24.

Lee, C.-Y., D.-H. Choi, Y.-M. Yeon, and S.-B. Jung. 2009. "Dissimilar Friction Stir Spot Welding of Low Carbon Steel and Al–Mg Alloy by Formation of IMCs." *Science and Technology of Welding and Joining* 14 (3): 216–20.

Liyanage, T., J. Kilbourne, A. P. Gerlich, and T. H. North. 2009. "Joint Formation in Dissimilar Al Alloy/steel and Mg Alloy/steel Friction Stir Spot Welds." *Science and Technology of Welding and Joining* 14 (6): 500–508.

Longhurst, William R, Alvin M Strauss, George E Cook, Paul A Fleming, W R Longhurst, A M Strauss, G E Cook, P A Fleming, Int J Adv, and Manuf Technol. 2010. "Torque Control of Friction Stir Welding for Manufacturing and Automation." *International Journal of Advanced Manufacturing Technologies*.

Ma, Genze, and Samuel Durbin. 2012. "Friction-Stir Riveting: Characteristics of Friction-Stir Riveted Joints." Master Thesis, University of Toledo.

Miler, Miloš, and Mateja Gosar. 2011. "Mineral and Chemical Composition of the New Iron Meteorite Javorje from Slovenia." *Meteoritics & Planetary Science* 46 (12): 1939–46.

Min, Junying, Jingjing Li, Yongqiang Li, Blair E. Carlson, Jianping Lin, and Wei-Ming Wang. 2015. "Friction Stir Blind Riveting for Aluminum Alloy Sheets." *Journal of Materials Processing Technology* 215 (January): 20–29.

Misak, H. E., C. A. Widener, D. A. Burford, and R. Asmatulu. 2014. "Fabrication and Characterization of Carbon Nanotube Nanocomposites Into 2024-T3 Al Substrates Via Friction Stir Welding Process." *Journal of Engineering Materials and Technology* 136 (2). American Society of Mechanical Engineers: 24501.

Mishra, Rajiv, and Z.Y. Ma. 2005. "Friction Stir Welding and Processing." *Materials Science and Engineering: R: Reports* 50 (1–2). Elsevier: 1–78.

Mishra, Rajiv, and Murray W. Mahoney, eds. 2007. *Friction Stir Welding and Processing*. ASM International.

Miyagawa, Katashi, Masami Tsubaki, Toshiaki Yasui, and Masahiro Fukumoto. 2009. "Spot Welding between Aluminium Alloy and Zn-Coated Steel by Friction Stirring." *Welding International* 23 (9). Taylor & Francis Group: 648–53.

Nininger, HH. 1945. "Directions for the Etching and Preservation of Metallic Meteorites." *Contributions of the Society for Research on Meteorites* 3 (11).

Nishihara, T. 2003. "Development of Friction Stir Forming." *Materials Science Forum* 426–432 (Aug.). Trans Tech Publications:2971–78.

Norfolk, Mark. 2016. "Lasers Today – Ultrasonic Additive Manufacturing a Solid Choice for 3D Metal Printing." 2016. https://www.laserstoday.com/2016/08/ultrasonic-additive-manufacturing-a-solid-choice-for-3d-metal-printing/

Northon, Karen. 2017. "NASA Selects Two Missions to Explore the Early Solar System." https://www.nasa.gov/press-release/nasa-selects-two-missions-to-explore-the-early-solar-system

Nunes, A.C., E.L. Bernstein, and J.C McClure. 2000. "A Rotating Plug Model for Fricion Stir Welding." In . Proceedings of the 81st American Welding Society Annual Convention.

PlanetaryResources. 2017. "Our Technology Today Enables the Vision of Tomorrow." 2017. http://www.planetaryresources.com/technology/#technology-value-statement

Prater, Tracie. 2015. "Welding in Space: A Comparative Evaluation of Candidate Welding Technologies and Lessons Learned from On-Orbit Experiments." *Journal of the British Interplanetary Society's Space Chronicle* 68.

Qiu, Ranfeng, Chihiro Iwamoto, and Shinobu Satonaka. 2009. "Interfacial Microstructure and Strength of Steel/aluminum Alloy Joints Welded by Resistance Spot Welding with Cover Plate." *Journal of Materials Processing Technology* 209 (8). Elsevier Inc.: 4186–93.

Schick, D. E., Sudarsanam Suresh Babu, John C Lippold, R.M. Hahnlen, M.J. Dapino, Ryan R Dehoff, and P. Collins. 2010. "Microstructural Characterization of Bonding Interfaces in Aluminum 3003 Blocks Fabricated by Ultrasonic Additive Manufacturing." *Welding Research Council* 89 (5).

Schmidt, H, J Hattel, and J Wert. 2004. "An Analytical Model for the Heat Generation in Friction Stir Welding." *Modelling and Simulation in Materials Science and Engineering* 12 (1): 143–57.

Sharp, Thomas G, and Paul S Decarli. 2006. "Sharp and DeCarli: Shock Effects in Meteorites Shock Effects in Meteorites." In *Meteorites and the Early Solar System II*, 653–77.

Sridharan, Niyanth, Maxim Gussev, Rachel Seibert, Chad Parish, Mark Norfolk, Kurt Terrani, and Sudarsanam Suresh Babu. 2016. "Rationalization of Anisotropic Mechanical Properties of Al-6061 Fabricated Using Ultrasonic Additive Manufacturing." *Acta Materialia* 117 (September): 228–37.

Thomas, Wayne. 1995. Improvements Related to Friction Welding. EPO Patent EPO0615480, issued 1995.

Thomas, Wayne, and ED Nicholas. 1997. "Friction Stir Welding for the Transportation Industries." *Materials & Design* 18 (4–6). Elsevier: 269–73.

Threadgill, P. L. 2007. "Terminology in Friction Stir Welding." *Science and Technology of Welding and Joining* 12 (4): 357–60.

Uematsu, Y., K. Tokaji, Y. Tozaki, Y. Nakashima, and T. Shimizu. 2011. "Fatigue Behaviour of Dissimilar Friction Stir Spot Welds between A6061-T6 and Low Carbon Steel Sheets Welded by a Scroll Grooved Tool without Probe." *Fatigue & Fracture of Engineering Materials & Structures* 34 (8): 581–91.

Watanabe, Mitsuhiro, Keyan Feng, Yoshio Nakamura, and Shinji Kumai. 2011. "Growth Manner of Intermetallic Compound Layer Produced at Welding Interface of Friction Stir Spot Welded Aluminum/Steel Lap Joint." *Materials Transactions* 52 (5): 953–59.

White, Dawn. 2002. Object consolidation employing friction joining. US Patent # 6457629, issued 2002.

Wilden, J., and J.P. Bergmann. 2004. "Manufacturing of Titanium/aluminium and Titanium/steel Joints by Means of Diffusion Welding." *Weld Cutting* 3 (5): 285–90.

Wilson, Jim. 2015. "What Is NASA's Asteroid Redirect Mission?" 2015. https://www.nasa.gov/content/what-is-nasa-s-asteroid-redirect-mission

Wolcott, Paul J., Adam Hehr, and Marcelo J. Dapino. 2014. "Optimal Welding Parameters for Very High Power Ultrasonic Additive Manufacturing of Smart Structures with Aluminum 6061 Matrix." In . International Society for Optics and Photonics.

Wolcott, Paul J., Adam Hehr, Marcelo J. Dapino, C.Y. Kong, R.C. Soar, C.Y Kong, R.C Soar, et al. 2014. "Optimized Welding Parameters for Al 6061 Ultrasonic Additive Manufactured Structures." *Journal of Materials Research* 29 (17). Cambridge Univ. Press: 2055–65.

Xu, S, X Deng, A P Reynolds, and T U Seidel. 2001. "Finite Element Simulation of Material Flow in Friction Stir Welding Finite Element Simulation of Material Flow in Friction Stir Welding." *Science and Technology of Welding and Joining*, 191–93.

Zhang, C.Q., J.D. Robson, and P.B. Prangnell. 2016. "Dissimilar Ultrasonic Spot Welding of Aerospace Aluminum Alloy AA2139 to Titanium Alloy TiAl6V4." *Journal of Materials Processing Technology* 231: 382–88.